

University of Montana

ScholarWorks at University of Montana

Graduate Student Theses, Dissertations, &
Professional Papers

Graduate School

2007

Elucidation of the Specificity of Neuroactive Steroids and Related Compounds at the at the Vesicular Glutamate Transporter

Wesley Edward Smith
The University of Montana

Follow this and additional works at: <https://scholarworks.umt.edu/etd>

Let us know how access to this document benefits you.

Recommended Citation

Smith, Wesley Edward, "Elucidation of the Specificity of Neuroactive Steroids and Related Compounds at the at the Vesicular Glutamate Transporter" (2007). *Graduate Student Theses, Dissertations, & Professional Papers*. 370.
<https://scholarworks.umt.edu/etd/370>

This Dissertation is brought to you for free and open access by the Graduate School at ScholarWorks at University of Montana. It has been accepted for inclusion in Graduate Student Theses, Dissertations, & Professional Papers by an authorized administrator of ScholarWorks at University of Montana. For more information, please contact scholarworks@mso.umt.edu.

ELUCIDATION OF THE SPECIFICITY
OF NEUROACTIVE STEROIDS AND RELATED COMPOUNDS
AT THE VESICULAR GLUTAMATE TRANSPORTER

By

Wesley Edward Smith

Bachelor of Science, Bridgewater State College, Bridgewater, MA, 2000

Dissertation

presented in partial fulfillment of the requirements
for the degree of

Doctor of Philosophy
Biomedical Sciences

The University of Montana
Missoula, MT

Spring 2007

Approved by:

Dr. David A. Strobel, Dean
Graduate School

Dr. Richard J. Bridges, Co-chair
Department of Biomedical and Pharmaceutical Sciences

Dr. John M. Gerdes, Co-chair
Department of Biomedical and Pharmaceutical Sciences

Dr. Keith K. Parker
Department of Biomedical and Pharmaceutical Sciences

Dr. David J. Poulsen
Department of Biomedical and Pharmaceutical Sciences

Dr. Charles M. Thompson
Department of Biomedical and Pharmaceutical Sciences

Dr. Kent Sugden
Department of Chemistry

Elucidation of the Specificity of Neuroactive Steroids and Related Compounds at the Vesicular Glutamate Transporter

Chairperson: Dr. Richard J. Bridges

As the primary excitatory amino acid, glutamate is essential to proper functioning of the mammalian CNS. Proper regulation of the synaptic release of glutamate, potentially regulated by synaptic vesicle content, is one of many critical aspects to normal excitatory functioning. In particular, the vesicular glutamate transporters (VGLUTs), which load synaptic vesicles with glutamate prior to presynaptic release of neurotransmitter, are distinct from that of the plasma membrane excitatory amino acid transporters (EAAT). The development of a library of compounds which selectively inhibit the uptake of [³H]-L-glutamate into the VGLUTs, has revealed importance of particular structural motifs. Among these structural motifs, one of the most important is that of the “embedded glutamate” which mimics the endogenous substrate of the transporter. With respect to potency, the substitution of a lipophilic moiety at the C6 position seems to be the most important to date, as illustrated by 5,6-naphthyl quinoline dicarboxylic acid (5,6-QDC). The structure of this compound strongly resembles that of a steroid molecule. In light of recent research suggesting steroids act within the CNS in a non-genomic manner, this observation prompted the testing of a panel of steroid molecules at VGLUT. These compounds, known as “neuroactive steroids” have been shown to be synthesized, modified, and/or active within the brain. Research from our lab, as well as from the Thompson lab, shows that certain sulfated neuroactive steroids are potent inhibitors of [³H]-L-glutamate uptake into synaptic vesicles. This work identifies pregnenolone sulfate, along with 5,6-QDC, as competitive inhibitors of VGLUT (K_i values of 107 and 228 μ M, respectively). These two molecules display specificity for VGLUT, with respect to other sites on the synaptic vesicle (i.e., electrochemical gradient), and among other vesicular neurotransmitter transporters (i.e., VGAT, VMAT). Two molecules, 5,6-QDC and Congo Red Fragment (CRF) were aligned to the VGLUT Pharmacophore to illustrate the SAR of these compounds. Biochemical studies have also been conducted to delineate substrate activity of neuroactive steroids and related compounds at VGLUT. The specificity of certain sulfated neuroactive steroids suggest that they could be endogenous regulators of vesicular glutamate uptake.

ACKNOWLEDGEMENTS

This work would not have been possible without the help of some very patient folks. I would like to acknowledge all of those people who helped bring this work to its final form. First and foremost, I would like to thank my research advisor Dr. Richard Bridges who served as both an advocate and inspiration on my behalf. Secondly, none of this would have come to fruition without the generosity of Dr. Vernon Grund, who gave me the opportunity to start this work. Thanks to Dr. John Gerdes, Dr. Charles Thompson, Dr. Keith Parker, Dr. David Poulsen, and Dr. Kent Sugden for advice regarding the development and culmination of this project. I also give special acknowledgement to those who helped in generating experimental data: Dr. Holly Cox, Dr. Kim Cybulski, and Dr. Erin Bolstad. To the members of the Bridges Lab, past and present, who never let a single moment be dull, I give special thanks: Shailesh Agarwal, Dr. Sarj Patel, Fred Rhoderick, Todd Seib, Dr. Brady Warren, and Ran Ye. I would like to thank my fellow graduate students, faculty, and staff of the Department of Biomedical and Pharmaceutical Sciences for the support and opportunities which were provided to me. I would also like to thank friends outside of the lab: JC Schneider, Rob and Jana Greenwell, and Glen Sundberg. I would especially like to thank my parents, Gary and Jane Smith, for supporting me throughout my academic career. Also, I extend my gratitude to my surrogate family in Missoula: Natalie, Dave, and Rose. Lastly, I give my utmost appreciation to the members of my personal lab: my wife, Tara, who was instrumental in keeping me focused, but also encouraging me to take a day off when necessary, and also, our two dogs, Hank and Quinn, for their enthusiasm when I just wanted one last run.

TABLE OF CONTENTS

ABSTRACT.....	ii
ACKNOWLEDGEMENTS.....	iii
LIST OF TABLES.....	v
LIST OF FIGURES.....	vi
CHAPTER 1: BACKGROUND AND SIGNIFICANCE.....	1
CHAPTER 2: MATERIALS AND METHODS.....	21
CHAPTER 3: RESULTS	
<u>Section I: Specificity of inhibition elicited by Sulfated neuroactive steroids, substituted QDCs, and derivatives of naphthalene disulfonic acids at VLGUT.....</u>	27
<u>Section II: Development of a VLGUT pharmacophore model and alignments with identified, competitive inhibitors.....</u>	37
<u>Section III: Influence of neuroactive steroids and related compounds on ³H-L-glutamate efflux from synaptic vesicles.....</u>	58
<u>Section IV: Specificity of sulfated neuroactive steroids and related compounds at other sites on the synaptic vesicle.....</u>	69
<u>Section V: Specificity of sulfated neuroactive steroids and related compounds at other vesicular transporters (i.e. VMAT, VGAT).....</u>	79
CHAPTER 4: DISCUSSION.....	88

LIST OF TABLES

Table 3.I.1. Inhibition of VGLUT by sulfated neuroactive steroids.....	31
Table 3.II.1. Ligands used in the generation and testing of the VGLUT Pharmacophore	45
Table 3.V.1. Pharmacological specificity of neuroactive steroids.....	83
Table 3.V.2. Pharmacological specificity of sulfated-neuroactive steroids as inhibitors of VGLUT, VMAT, and VGAT.....	86

LIST OF FIGURES

Figure 1.1.	Excitatory amino acid synapse.....	2
Figure 1.2.	Previously identified VGLUT inhibitors.....	11
Figure 1.3.	Commonalities of various VGLUT inhibitors.....	15
Figure 1.4	Depiction of a steroid nucleus.....	17
Figure 1.5.	Structures of inhibitory and excitatory neuroactive steroids.....	18
Figure 3.I.1.	Concentration-response analysis of potent sulfated-neuroactive steroids at VGLUT.....	30
Figure 3.I.2.	Demonstration of the competitive inhibition by PREGS on ³ H-L-Glutamate uptake into synaptic vesicles.....	34
Figure 3.I.3.	Demonstration of the competitive inhibition by 5,6-QDC on ³ H-L-Glutamate uptake into synaptic vesicles.....	35
Figure 3.I.4.	Structures of identified competitive inhibitors.....	36
Figure 3.II.1.	Illustration of the superposition of CSB, BCT, and 6-(4')-QDC.....	40
Figure 3.II.2.	Identified regions and measures of the VGLUT Pharmacophore.....	41
Figure 3.II.3.	Alignment of VGLUT Pharmacophore with PREGS.....	43
Figure 3.II.4.	Diagram of CRF alignment with the VGLUT Pharmacophore (A1).....	48
Figure 3.II.5.	Demonstration of pharmacophore alignment (A1) <i>versus</i> conformer number	49
Figure 3.II.6.	Alignment (A1) of VGLUT pharmacophore with CRF.....	50

Figure 3.II.7.	Diagram of CRF alignment with the VGLUT Pharmacophore (A2)	51
Figure 3.II.8.	Demonstration of pharmacophore alignment (A2) <i>versus</i> Conformer number	53
Figure 3.II.9.	Alignment (A2) of VGLUT pharmacophore with CRF.....	54
Figure 3.II.10.	Diagram of 5,6-QDC alignment with the Pharmacophore model.....	55
Figure 3.II.11.	Alignment of VGLUT pharmacophore with 5,6-QDC.....	56
Figure 3.III.1	Effect of nonsubstrate inhibitor and demonstration of <i>trans</i> -stimulation on vesicular ³ H-L-glutamate.....	61
Figure 3.III.2	Demonstration of the effect of VGLUT inhibitors on ³ H-L-glutamate from synaptic vesicles.....	64
Figure 3.III.3	Effect of a partial substrate on vesicular ³ H-L-Glutamate efflux.....	65
Figure 3.III.4	Mathematical simulation of L-glutamate efflux from synaptic vesicles.....	66
Figure 3.IV.1.	Effect of 5,6-QDC on the proton gradient generated by a V-ATPase in synaptic vesicles.....	72
Figure 3.IV.2.	Effect of PREGS on the proton gradient generated by a V-ATPase in synaptic vesicles.....	73
Figure 3.IV.3.	Effect of 5,6-QDC on the membrane potential generated by a V-ATPase in synaptic vesicles.....	75
Figure 3.IV.4.	Effect of PREGS on the membrane potential generated by a V-ATPase in synaptic vesicles.....	76
Figure 3.IV.5.	Absorbance spectrum of Oxonol V.....	77

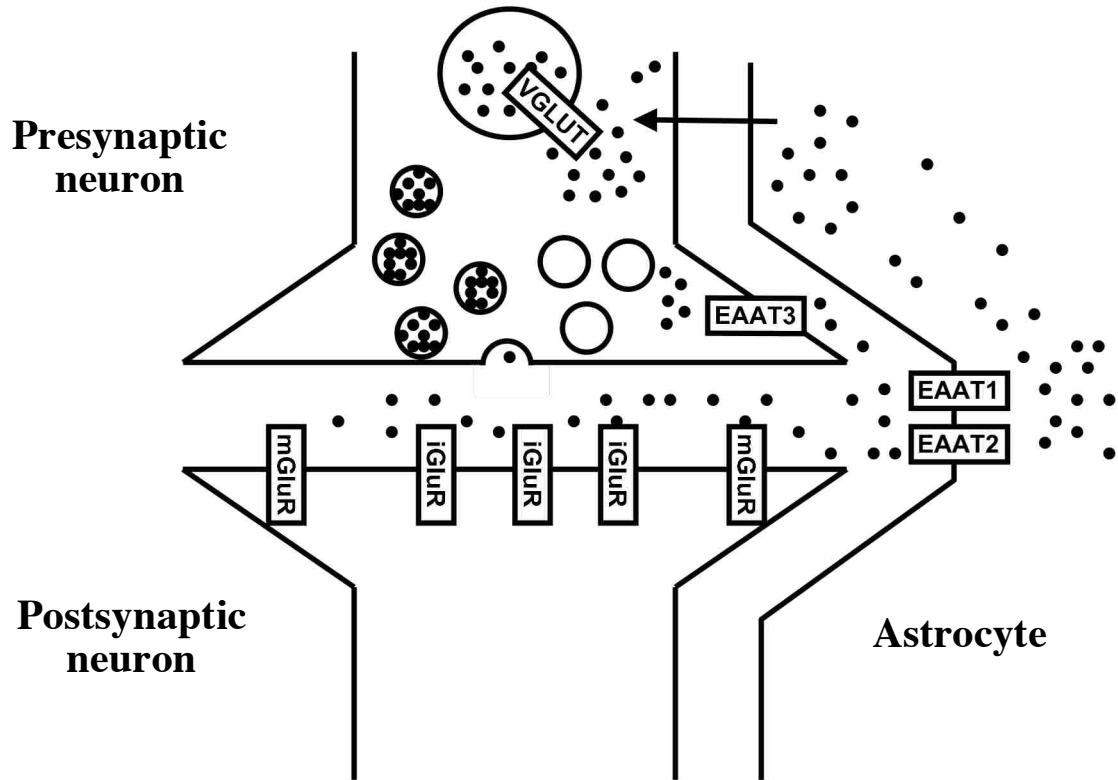
Figure 3.V.1.	Concentration-response analysis of PREGS, DHEAS, 3 α ,5 β THPROGS, and 3 α ,5 α THPROGS against vesicular ³ H-5HT uptake.....	84
Figure 3.V.2.	Concentration-response analysis of PREGS, DHEAS, 3 α ,5 β THPROGS, and 3 α ,5 α THPROGS against vesicular ³ H-GABA uptake.....	85
Figure 4.1.	Development of the QDC template.....	96
Figure 4.2.	Model of transport via VGLUT: <i>trans</i> -stimulation.....	104

CHAPTER 1: BACKGROUND AND SIGNIFICANCE

Glutamate is widely accepted as the primary excitatory neurotransmitter in the mammalian central nervous system (CNS). As such, the maintenance of correct extracellular concentrations of glutamate is essential to the appropriate functioning of the brain and spinal cord. When properly regulated, glutamate contributes to a wide array of processes that range from fast excitatory signaling to higher-order processing (e.g., memory, learning, plasticity) (Balazas et al., 2005). In contrast to its physiological roles, excessive extracellular levels of L-glutamate can also contribute to the pathological damage observed in a variety of neurological insults and diseases, including acute trauma (i.e., seizures, stroke, traumatic brain injury, etc.), as well as chronic neurodegenerative diseases, such as ALS, Alzheimer's, and Huntington's disease (Mattson, 2003; Olney, 2003).

Multiple proteins, located at distinct subcellular locations, are important for glutamatergic signaling (Fig. 1.1). Receptors, present both pre- and postsynaptically, are necessary for transmission of the chemical signal across the synapse. Glutamate transporters present on the plasma membrane are involved with the regulation of extracellular glutamate. Additionally, vesicular glutamate transporters, present in the axon terminal of the presynaptic neuron, aid in sequestering the neurotransmitter into synaptic vesicles in preparation for release from the terminal.

Figure 1.1. Excitatory amino acid synapse



This image depicts a stereotypical excitatory synapse. After L-glutamate is released into the synapse, it binds to ionotropic (iGluR) and metabotropic (mGluR) glutamate receptors. The glutamate is then removed from the synapse into astrocytes by the excitatory amino acid transporters (EAATs). Glutamine synthetase, present in astrocytes, converts L-glutamate to glutamine. The glutamine is then transported back to the presynaptic neuron, where it is converted to L-glutamate via glutaminase. The vesicular glutamate transporter (VGLUT) sequesters glutamate into synaptic vesicles prior to release.

Glutamate Receptors

Historically, the characterization of glutamate receptors was an important component in the establishment of glutamate as a CNS neurotransmitter. Glutamatergic receptors are divided into two groups, ionotropic (iGluR), which are directly associated with ion channels, and metabotropic (mGluR), which are linked to second messenger systems. The iGluRs are composed of three subtypes: N-methyl-D-aspartate (NMDA), α -amino-3-hydroxy-5-methyl-4-isoxazole propionate (AMPA), and kainic acid (KA), while the metabotropic receptor classes are classified as Group I, II, and III receptors (Balazas et al., 2005). Glutamate ionotropic receptors, which were initially named after selective agonists, gate various ionic currents (Na^+ , K^+ , and Ca^{2+}), and share approximately 20-30% homology. AMPA receptors (AMPA) are composed of GluR1-GluR4 subunits that are presumed to be functional in a tetrameric form (Rosenmund et al., 1998). Similar to AMPAR, the KA receptors (KAR) most likely form tetramers composed of GluR5-GluR7 and KA1-KA2 subunits, with the requirement that a GluR5-GluR7 subunit is present for a functional ion channel. Both AMPAR and KAR are involved in fast synaptic signaling.

Certain factors, unique to the NMDAR, confer the ability of being both ligand- and voltage-gated, which in turn, underlies its role in long-term potentiation (LTP) (Balazas et al., 2005). Functioning of the NMDA receptor requires the binding of glutamate and membrane depolarization, typically mediated by AMPAR and KAR, to remove the ion channel block created by Mg^{2+} . With the release of the Mg^{2+} block, Ca^{2+} can enter via

the channel into the cell, activating downstream effectors involved in LTP. In addition to the binding of glutamate, the NMDA receptor also requires glycine as a coagonist. The NMDA receptors are composed of three subunit types; all receptors contain the NR1 subunit, which includes the primary glycine-binding site. The NR2A-NR2D combine with NR1 to form the majority of NMDA receptors found in the human brain. Additional glycine binding-sites are presumed to be present on NR3A and NR3B subunits.

The mGluRs make up the second major group of the glutamatergic receptors in the mammalian brain (Balazas et al., 2005). These receptors are coupled to different forms of the guanosine nucleotide-binding protein (G-protein) and belong to the seven transmembrane (7-TMS) superfamily of receptors. The mGluRs share approximately 70% homology within groups and about 40% homology between groups (Schoepp, 2001). Three subtypes make up this class: Group I receptors, comprised of mGluR1 and mGluR5, are ultimately coupled to the downstream effector phospholipase C via G_q. The Group II receptor class includes mGlu2 and mGlu3, while Group III consists of mGlu4, mGlu5, and mGlu6. Both Group II and III inhibit stimulated 3'-5'-cyclic adenosine monophosphate (cAMP) formation through G_i (Conn and Pin, 1997; Schoepp et al., 1998).

Excitatory Amino Acid Transporters (EAATs)

The glutamatergic synapse, unlike cholinergic synapses, lacks a degradative enzyme, to remove neurotransmitter from the synaptic cleft. To account for this, glutamate plasma

membrane transporters are present to aid in the regulation of extracellular glutamate levels. Five transporters have been identified within the high-affinity, sodium-dependent transporter class: the excitatory amino acid transporters (EAATs1-5). The EAATs are primarily found in the CNS, with additional expression in the heart, liver, kidney and intestine (Gegelashvili and Schousboe, 1998). EAAT3 and 4 are generally considered the neuronal transporters, whereas EAAT1 and 2 are primarily located on glial cells (Chen et al., 2002; Furuta et al., 1997; Schmitt et al., 2002). EAAT2 is thought to be the primary transporter involved in clearing glutamate from the synaptic cleft (Koch et al., 1999). The localization of EAAT3 to GABAergic neurons suggests that it may also serve as the manner by which glutamate is transported into GABAergic neurons as a precursor of GABA (Sepkuty et al., 2002). EAAT4 is primarily localized to the cerebellum (Lin et al., 1998). EAAT5 expression is limited to neurons and Muller cells in the retina (Eliasof et al., 1998).

Vesicular Glutamate Transporters (VGLUTs)

In addition to EAATs, which aid in the regulation of extracellular glutamate concentrations, transporters present on synaptic vesicles within the presynaptic axon are necessary to load vesicles with L-glutamate prior to its release during excitatory transmission. The VGLUTs are classified within the SLC-17/type I class of phosphate transporters, which were initially characterized as phosphate carriers. In fact, these proteins, which are involved in processes ranging from degradation of glycoproteins to the sequestration of neurotransmitters into synaptic vesicles, are broadly defined as

organic anion transporters. Proteins from the SLC-17 family are typically found on synaptic vesicles, lysosomes, and plasma membranes and are predicted to contain 6-12 membrane-spanning domains (Reimer and Edwards, 2004). VGLUT1 was originally classified as the brain-specific Na⁺-dependent phosphate transporter (BNPI), which was discovered in a screen for cDNAs upregulated in response to subtoxic levels of NMDA in cerebellar granule cells (Ni et al., 1994). The nucleotide sequence of BNPI predicts a protein with 6-8 putative transmembrane loops with approximately 32 percent sequence identity to the rabbit kidney Na⁺-dependent, P₁-transporter. Similarly, VGLUT2 was previously classified as the differentiation-associated, Na⁺-dependent phosphate transporter (DNPI). DNPI was identified in an experiment screening for cDNAs upregulated during differentiation of rat pancreatic AR42J cells to a neuroendocrine phenotype (Aihara et al., 2000). Additionally, a third vesicular glutamate transporter, which localizes to cholinergic and serotonergic neurons, has also been identified (Fremeau Jr. et al., 2002; Gras et al., 2002; Schafer et al., 2002). The membrane spanning domains of the three isoforms of VGLUT are highly homologous (~90% homology); however, N- and C- terminal domains differ from one another.

VGLUT1 and VGLUT2 have a complementary distribution in the brain, with VGLUT1 enriched in areas that have a low probability of release, such as the cerebral cortex, cerebellar cortex, and hippocampus; while VGLUT2 localizes to areas of higher probability of release, such as the diencephalon and rhombencephalon (Fremeau Jr. et al., 2004; Fremeau Jr. et al., 2001; Varoqui et al., 2002). In contrast to VGLUT1 and VGLUT2, VGLUT3 colocalizes with other phenotypic markers, such as tryptophan

hydroxylase, glutamic acid decarboxylase (GAD), and choline acetyl transferase (ChAT) (Fremeau Jr. et al., 2002; Herzog et al., 2004; Schafer et al., 2002). This colocalization suggests that these neurons may be capable of co-releasing glutamate and the respective neurotransmitter, as has been shown by Takamori and coworkers (Takamori et al., 2000).

Two important characteristics describe the chemical signal that is transferred across the synapse: (1) quantal content and (2) quantal size. The number of synaptic vesicles released from the presynaptic terminal determines quantal content. Evidence suggests that the amount of vesicular neurotransmitter transporter expression may influence quantal content. For example, overexpression of VAcHT (Song et al., 1997), VMAT (Colliver et al., 2000; Gong et al., 2003), and VGLUT1 (Wojcik et al., 2004) has been shown to increase quantal content in various cell culture systems. It is generally presumed that the amount of neurotransmitter in each synaptic vesicle is at steady-state conditions; and hence, altering these steady-state conditions with the overexpression of vesicular transporters may increase quantal content. On the other hand, quantal size is a functional measure of postsynaptic signal. The wide diversity of glutamate receptor subtype organization allows for an extensive range of function.

Although, the VGLUTs are hypothesized to function primarily as glutamate transporters, it is possible that they may also serve as phosphate transporters (Takamori, 2006). If the VGLUTs transport phosphate (as has been shown in *Xenopus* oocytes *in vivo* (Ni et al., 1994), then it is possible that they may play an additional role in synaptic functioning. The transport of phosphate into the presynaptic terminal could increase the activity of

phosphate-activated glutaminase (PAG). The increased activity of PAG could increase the amount of glutamate available for uptake into synaptic vesicles. Recent evidence has shown that VGLUT proteins are present on the presynaptic membrane (Hagiwara et al., 2005). Additionally, ammonia, which is a byproduct of glutamate synthesis via PAG, could cause a shift of the electrochemical gradient. In turn, this shift would cause an increase in glutamate sequestration via VGLUT.

In contrast to the EAATs, which rely on sodium and potassium gradients, the VGLUTs rely on a proton gradient to transport glutamate from the cytosolic space to the vesicular lumen. Vesicular glutamate sequestration in the brain is facilitated by an electrochemical gradient ($\Delta\mu$), generated by a vacuolar-type Mg^{2+} -dependent ATPase. Recent evidence suggests that ATP, supplied by a membrane-bound complex of glyceraldehyde phosphate dehydrogenase (GAPDH) and 3-phosphoglycerate kinase (3-PGK), is sufficient to supply enough energy for vesicular glutamate uptake (Ikemoto et al., 2003). The transport of protons into the vesicular lumen by the ATPase serves to establish a pH gradient (ΔpH) between the vesicle lumen ($\sim pH$ 6.8) and the cytosolic space ($\sim pH$ 7.4). The increased concentration of positive charges due to the uptake of protons also creates an electrical gradient ($\Delta\Psi$) in the vesicle lumen as compared to the slightly more negative charge character of the cytosolic space. The majority of evidence suggests that $\Delta\Psi$ is the primary driving force for glutamate sequestration (Maycox et al., 1988). However, there is evidence to suggest that ΔpH may play a role under certain conditions (Tabb et al., 1992). While there is some debate as to the specific extent to which glutamate

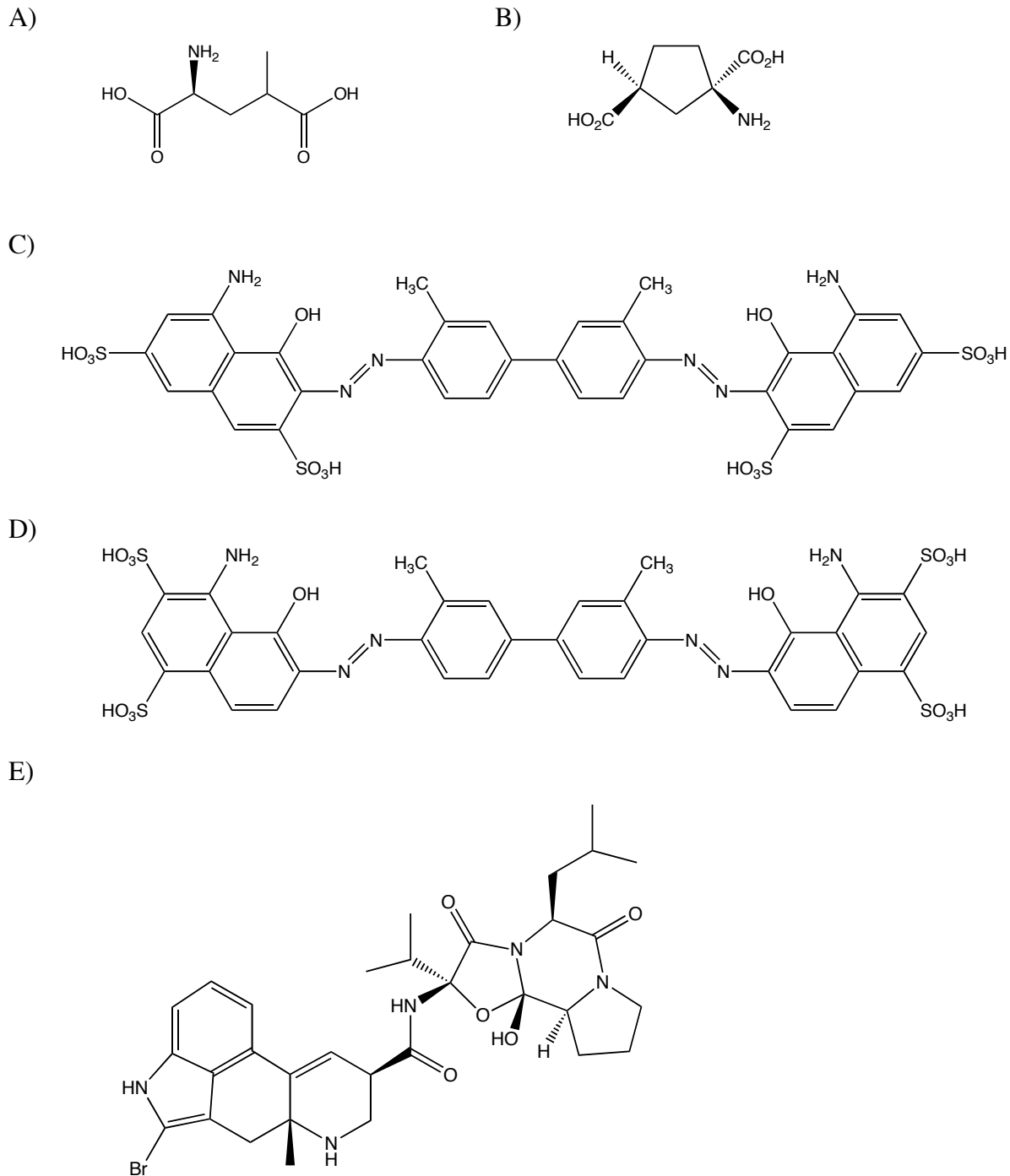
sequestration is dependent upon $\Delta\Psi$ and/or ΔpH , it is widely agreed upon that Cl^- also plays a role in glutamate uptake.

The chloride-dependence of vesicular glutamate uptake shows a biphasic curve, with the optimal concentration found at about 4 mM. The rate of glutamate sequestration decreases with either higher or lower concentrations. Glutamate transport is thought to involve an anion-binding site, which is distinct from the substrate-binding site. While the exact location of the anion binding-site is not yet clear, evidence suggests that an anion binding-site must be accessible to the cytosolic space. The potent anion channel inhibitor 4,4'-diisothiocyanostilbene-2,2'-disulfonic acid (DIDS) has been used to inhibit glutamate uptake with an IC_{50} of 0.7 μM or less. High concentrations of Cl^- (100 mM), but not glutamate or other anions, were able to restore ATP-dependent levels of L-glutamate uptake. While it is possible that chloride could be co-transported with glutamate, it would not be electrochemically favorable to do so due to the energy barrier (Hartinger and Jahn, 1993). The chloride dependence has been shown to be regulated by the α_2 subunit of the trimeric G-protein ($\text{G}\alpha_2$). In turn, $\text{G}\alpha_2$ indirectly lowers glutamate uptake by interacting with the putative Cl^- binding site (Winter et al., 2005).

Our understanding of VGLUT pharmacology has developed substantially over the past two decades from the first characterization of glutamate uptake into synaptic vesicles (Maycox et al., 1988; Naito and Ueda, 1983; Naito and Ueda, 1985) to the development of a preliminary VGLUT pharmacophore model (Thomspon et al., 2005). Unlike the EAATs, VGLUT has a relatively low affinity for glutamate ($K_M = 1\text{-}3$ mM).

Accordingly, the majority of potent inhibitors of this system exhibit affinities in the μM range, with the most potent in the mid nM range. Since the original characterization of the presence of glutamate in synaptic vesicles, a variety of competitive inhibitor classes have emerged: (1) glutamate derivatives, (2) naphthalene sulfonic acids (3) ergots, and (4) inhibitory protein factors. Classic inhibitors and substrates of the EAATs, such as D- and L-aspartate, show little or no inhibition of vesicular glutamate uptake (Fykse and Fonnum, 1991; Tabb and Ueda, 1991). Accordingly, few glutamate derivatives, which are active at the EAATs, are also active at VGLUT. *Trans*-1-aminocyclopentane-1,3-dicarboxylic acid (*trans*-ACPD) and *erythro*-4-methyl-L-glutamic acid (MGlut) are among the more potent glutamate derivatives with K_i values of 0.44 mM and 0.73 mM, respectively, while 4-methylene-L-glutamate had moderate activity with a K_i value of approximately 3mM (Winter and Ueda, 1993). EAAT substrates and inhibitors, which are also active at the VGLUTs, contain a carbon backbone at least as long as that of glutamate. While the glutamate derivatives enjoy modest potency, the most potent competitive inhibitors are derivatives of 1,3-naphthalenedisulfonic acid (also classified as naphthalene disulfonic acids), which have K_i values in the nanomolar range. Evans blue (EB) and Chicago sky blue (CSB) were the first dyes to be characterized with K_i values of 40 and 190 nM, respectively (Roseth et al., 1995). A larger number of 1,3-naphthalene disulfonic acid derivatives were further characterized; however, with the exception of trypan blue and naphthol blue black, most inhibitors were not as potent as the previously characterized dyes, EB and CSB. Trypan blue and naphthol blue black were shown to have K_i values of 50 nM and 200 nM, respectively (Roseth et al., 1998). Bromocriptine is another competitive, inhibitor considered atypical, due to its lack of an

Figure 1.2. Previously identified VGLUT inhibitors

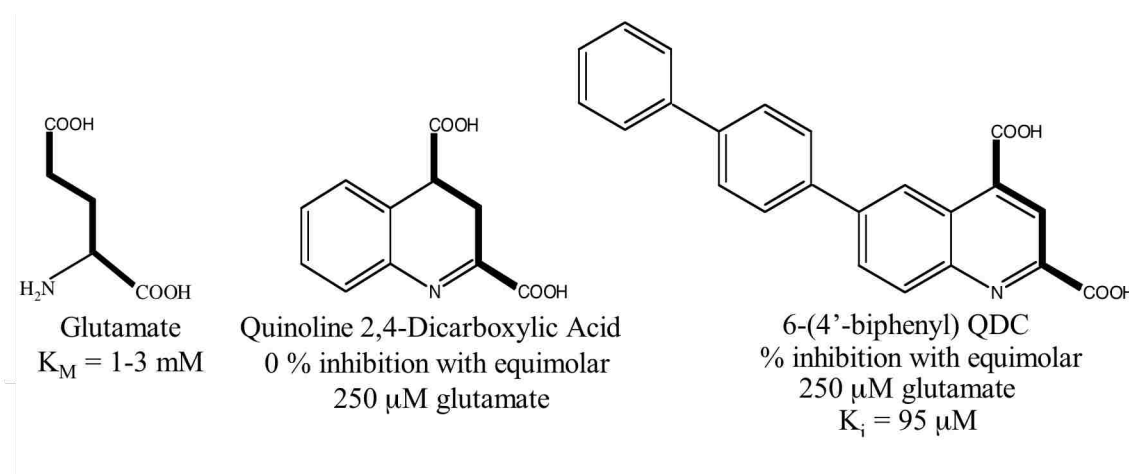


Molecules are depicted with equal bond lengths to illustrate the relative size differences of various VGLUT inhibitor classes. Molecules depicted are as follows: A) 4-methyl-L-glutamate, B) *trans*-ACPD, C) trypan blue, D) Evans blue, and E) bromocriptine.

obvious glutamate motif. With an IC_{50} of 22 μ M, it is one of the more potent competitive inhibitors to date (Carlson et al., 1989). Lastly, a structurally diverse class of inhibitors, the inhibitory protein factors (IPFs) proved to be exceptionally potent, relative to other VGLUT inhibitors, with an IC_{50} value of 26 nM (Ozkan et al., 1997).

Kynurenate, also known to be an antagonist at the iGluRs, has been shown to be active at the VGLUTs as a competitive inhibitor (Fykse et al., 1992). Two kynurenate derivatives, xanthurenate and 7-chloro-kynurenate, have been shown to possess K_i values of 0.19 mM and 0.59 mM, respectively (Bartlett et al., 1998). The lack of inhibitory activity with various monocyclic pyridine derivatives suggests the importance of the bicyclic structure of xanthurenate and 7-chloro-kynurenate, both quinoline-based molecules. The bicyclic core, along with the electronegative regions corresponding with the carboxylates of glutamate, prompted further development of a novel class of inhibitors: the quinoline dicarboxylic acids (QDC). The potential development of the QDCs as a template for inhibitors was supported by: (1) the structural resemblance to the quinoline 2-carboxylic acids, (2) the obvious embedded glutamate backbone, and (3) potential for selectivity at the VGLUTs (Fig. 1.3). The most potent VGLUT inhibitor to emerge from this synthetic effort was that of 6-[4'-biphenyl] QDC with a K_i value of 41 μ M (Carrigan et al., 2002; Carrigan et al., 1999). As will be discussed below, the structural motif of the QDC led to the hypothesis that the steroids might also act as inhibitors of VGLUT.

Figure 1.3. Commonalities of various VGLUT inhibitors



Development of the QDCs. The “embedded” glutamate is the most obvious common structural feature between these molecules. The addition of a bicyclic core, evident in QDC and 6-(4’)-QDC, increases potency. The largest increase in potency has been due to lipophilic additions, such as the biphenyl group in the 6- position of the basic QDC structure.

Neuroactive steroids

Hans Selye first reported the anesthetic effects of steroids in 1941 (Selye, 1941).

The word, “neurosteroid,” was first used by Baulieu to describe the actions of the DHEAS, found in the brain after gonadectomy and adrenalectomy (Baulieu, 1981). More recently, the term, “neuroactive steroid,” has been introduced to account for two classes of steroids active in the CNS: those (1) steroids synthesized in the brain, and those (2) steroids (or precursors) produced peripherally and then modified in the brain (Paul, 1992). For this work, the term “neuroactive steroid” will be used to refer to any steroid molecule active in the CNS in a nongenomic manner. Currently, there is a great deal of interest in this area; however, conflicting reports still exist in the literature. Evidence of neuroactive steroids began with two observations: first, studies demonstrated that certain steroids could modulate GABA_A receptor function, and secondly, Baulieu’s group showed that steroids remained in the brain after gonadectomy or adrenalectomy (Corpechot et al., 1981; Corpechot et al., 1983; Harrison and Simmonds, 1984).

As previously mentioned, while some neuroactive steroids, such as pregnenolone (PREG), are produced in the brain, the endocrine system can provide additional precursors that are modified in the brain. Therefore, there are a number of issues regarding neuroactive steroid concentrations that need to be resolved in order to better understand their potential roles in neurophysiology. First, the origin of neuroactive steroid precursors may aid in elucidating whether a specific effect is humoral or local. The quantitation of neuroactive steroids has been difficult due to environmental and

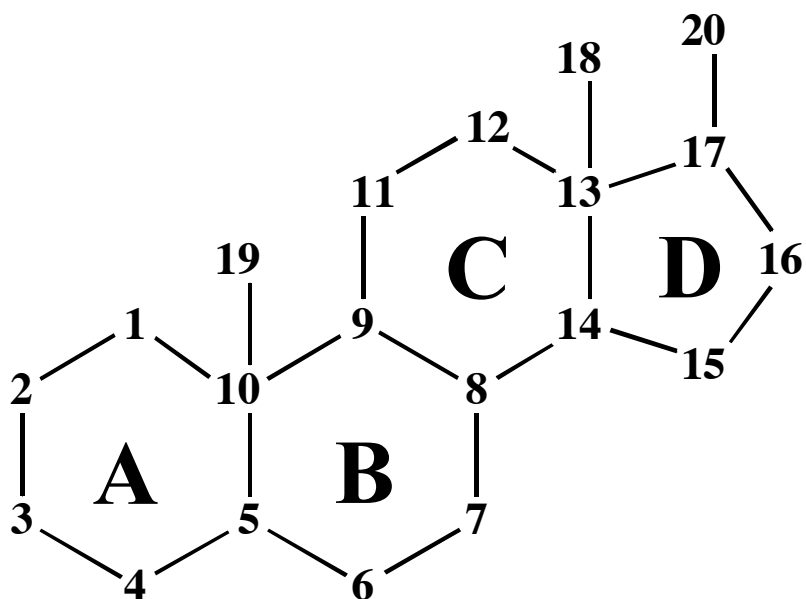
methodological issues. To overcome the environmental issues, pharmacological and physiological experiments have been performed under strictly defined conditions. Methodological issues have prevented a robust quantitation of neuroactive steroid levels in various brain regions. This makes it problematic to understand the relative contribution of neuroactive steroid effects in and between different areas (Baulieu et al., 1999). Nevertheless, steroid concentrations measured from cadavers have been shown to be in the low nanomolar range (Corpechot et al., 1981; Corpechot et al., 1983; Harrison and Simmonds, 1984; Lacroix et al., 1987; Lanthier and Patwardhan, 1986). DHEA (conjugated and unconjugated) was shown to be present in the adult male rat brain at about 2.5 ng (10 pmol)/g, while in the human brain, it was present at about 5.6 ng/g. Similarly, PREG levels (conjugated and unconjugated forms) were present in the rat brain at 35 ng (100 pmol)/g, and 38.2 ng/g in the human brain (Baulieu et al., 1999). The establishment of allopregnanolone ($3\alpha,5\alpha$ -TH PROG) concentrations has been more difficult. Estimations of $3\alpha,5\alpha$ -TH PROG levels range from undetectable to 1.3 ng/g (Cheney et al., 1995; Corpechot et al., 1993; Leblhuber et al., 1990; Purdy et al., 1991). While the concentrations of neuroactive steroids are generally in the nM range, previous evaluation of these amounts are limited in the respect that they do not assess concentrations at the level of cellular microenvironment.

Despite some of the difficulties with quantitating neuroactive steroid levels, there is an evolving body of literature describing both the involvement of these molecules in neuropathology and neurophysiology on a systemic level, as well as a biochemical level.

Research regarding neuroactive steroids has not progressed to the point to which a coherent mechanistic understanding exists. Studies which describe the effects of neuroactive steroids, tend to be at isolated levels of investigation (physiological, biochemical, etc.). Despite the current state of the literature, there appear to be two distinct patterns of neurological modulation being elicited by two different groups of neuroactive steroids. These two distinct patterns are produced by compounds which have a large degree of structural similarity. Steroid molecules, neuroactive steroids included, are composed of four fused rings as shown in Figure 1.2. The steroid nucleus is derived from cholesterol molecules. Neuroactive steroids are typically substituted at the 3-, 18-, and 20- positions. One particular group of neuroactive steroids that appear to be involved with these distinct actions are the pregnenolone derivatives, DHEAS and PREGS, also known as the excitatory neuroactive steroids (Fig. 1.3). These neuroactive steroids appear to be responsible for a positive modulation of excitatory transmission (i.e. glutamate stimulation, GABA inhibition). In contrast, the 3α -hydroxy ring A-reduced pregnane neuroactive steroids, $3\alpha,5\alpha$ -TH PROGS and $3\alpha,5\beta$ -TH PROGS (inhibitory neuroactive steroids) result in a negative modulation of the inhibitory neurotransmission (i.e. glutamate inhibition, GABA stimulation) (Monnet and Maurice, 2006). It is notable that these are generalized patterns and may not occur in all areas of the brain.

The systemic effects of DHEAS and PREGS are dependent on the concentration at their local sites of action in the brain. Although data in humans is somewhat contradictory, PREGS has been shown to enhance memory in rodent models (Vallee et al., 2001). As

Figure 1.4. Depiction of a steroid nucleus



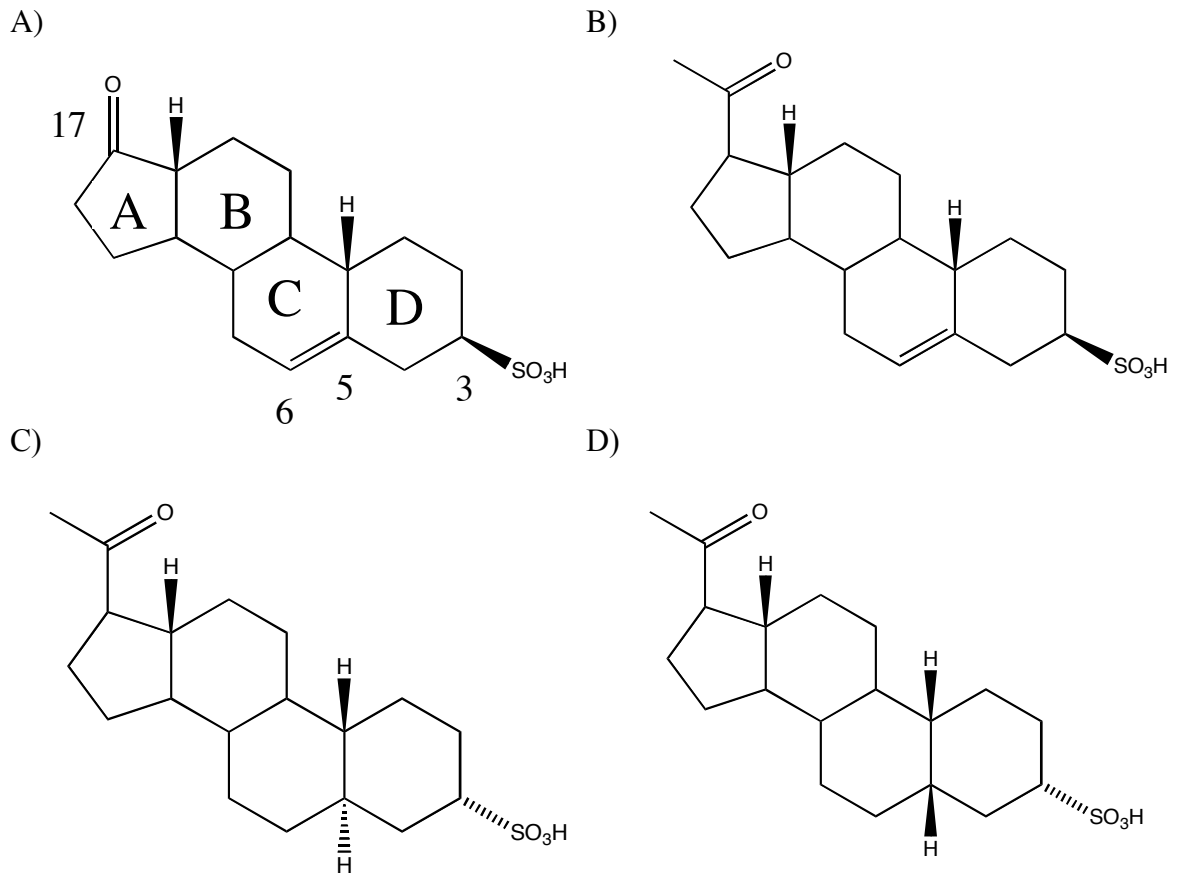
Neuroactive steroids share the basic structure pictured above. The majority of neuroactive steroids discussed in this work are substituted at the 3, 18, and 20 positions.

one of the main components of certain types of synaptic plasticity processes related to memory, NMDA receptors are involved in some forms of long-term potentiation (Collingridge, 1987). PREGS has also been shown to enhance NMDA receptor function, while not affecting GABA_A field potentials (fEPSPs) (Park-Chung et al., 1994; Park-Chung et al., 1997; Sliwinski et al., 2004)

While this evidence suggests that PREGS does not affect GABA_A fEPSPs, other studies indicate direct effect of PREGS acting as an allosteric inhibitor at GABA_A (Majewska et al., 1988). Under certain circumstances, however, PREGS has been shown to potentiate GABA_A, as well as induce cell toxicity in retinal cells (Guarneri et al., 1998). In contrast, the same study showed that DHEAS (25 μM) reduces the degree of PREGS stimulated cell death.

DHEAS, which is synthesized from pregnenolone, is much less active at the NMDA receptor than PREGS, but it is more strongly correlated with memory enhancement than PREGS. DHEAS plays a role in memory enhancement of the developing and adult rodent brains (Baulieu, 1998). In humans, a correlation has been noted between cognitive performance and circulating levels of DHEAS (Barrett-Conner and Edelstein, 1994). Moreover, patients with Alzheimer's disease tend to have lower levels of DHEAS (Leblhuber et al., 1990; Nasman et al., 1991). In mice, DHEAS reduces alternation behavior deficits in memory and learning, which is a measure of spatial working memory (Urani et al., 1998). Along with a positive correlation with memory enhancement, DHEAS is also a neuroprotectant under certain circumstances

Figure 1.5. Structures of inhibitory and excitatory neuroactive steroids



These images depict the two dimensional structures of excitatory (A) DHEAS and B) PREGS) and inhibitory (C) 3 α , 5 α -TH PROGS, and D) 3 α , 5 β -TH PROGS) neuroactive steroids

(Lapchak and Araujo, 2001). A separate pair of neuroactive steroids, pregnanolone sulfate and allopregnanolone, have been shown to potentiate inhibitory mechanisms within the CNS. For example, both pregnanolone sulfate and allopregnanolone have been shown to inhibit NMDA receptor response (Park-Chung et al., 1997). Allopregnanolone has also been shown to prolong GABA-mediated inhibitory postsynaptic currents in cultured rat hippocampal neurons (Harrison et al., 1987).

During the course of these studies, we found certain sulfated neuroactive steroids inhibited vesicular glutamate uptake, whereas the non-sulfated varieties did not. Of the neuroactive steroids tested, four showed the greatest activity against VGLUT: PREGS, DHEAS, $3\alpha,5\beta$ -TH PROGS, and $3\alpha,5\alpha$ TH PROGS. To further characterize the specificity of potent neuroactive steroids, a detailed kinetic analysis was performed on PREGS. The potent sulfated neuroactive steroids and related compounds were also assayed for activity as alternative substrates at VGLUT. In addition, PREGS was assayed for its effect on the electrical and chemical components of the ATPase-dependent gradients. The sulfated neuroactive steroids, shown to be potent inhibitors of vesicular glutamate uptake, were also tested for their cross-reactivity with additional vesicular transporters (i.e. VMAT, VGAT) to determine the specificity with respect to other vesicular neurotransmitter systems.

CHAPTER 2: MATERIALS AND METHODS

Materials

Male Sprague-Dawley Rats (200-220 g) were used in all studies. L-[³H]-Glutamic acid (42.90 Ci/mmol) and γ -[2,3-³H(N)]-aminobutyric acid (GABA) (33.70 Ci/mmol) were purchased from NEN (USA). 5-Hydroxy-[³H]-tryptamine trifluoroacetate (108 Ci/mmol) was purchased from GE Healthcare/Life Sciences. Millipore filters (0.45 μ m) were purchased from Sigma-Aldrich. All other reagents were purchased from Sigma-Aldrich.

Preparation of Synaptic Vesicles

Synaptic vesicles were isolated according to the method described by Kish and Ueda (Kish and Ueda, 1989) and modified accordingly (Bartlett, 1999). Sprague-Dawley rats (200-220 g) were sacrificed by decapitation. After which, the brains were removed and minced in ice cold buffer containing 0.32 M sucrose, 1.0 mM NaHCO₃, 1.0 mM magnesium acetate, and 0.5 mM calcium acetate (pH 7.2). The minced cerebrums were homogenized (motorized Potter-Elvehjem, Teflon/glass; Wheaton) and centrifuged for 15 min at 12,000 g (4°C, Sorvall SS-34 rotor, Du Pont, Newton, CT). The resulting pellets were resuspended in an ice-cold lysing solution (6 mM Tris-maleate, pH 8.1) for 45 min; and subsequently, centrifuged at 43,000 g for 15 min. Supernatants were then centrifuged for 55 min at 222,000 g (Beckman Ti 70 rotor; Beckman Instrumentation, Fullerton, CA). The final pellets were resuspended by homogenization in 0.32 M

sucrose, 1.0 mM NaHCO₃, and 1.0 mM dithiothreitol (pH 7.2). The final synaptic vesicles were stored at -80°C. When assayed as described below, the stored vesicles retained activity for at least 8 weeks.

Assay for Vesicular Uptake of Neurotransmitters

Vesicular uptake of L-glutamate was performed as described previously ((Bartlett et al., 1998). Synaptic vesicles were suspended in a buffer containing 5.0 mM MgCl₂, 375 mM sucrose, and 5.0 mM N-[2-hydroxyethyl]piperazine-N'-[ethanesulfonic acid] (HEPES; pH 7.4) and maintained at 4°C. Duplicate aliquots (1.0 mg protein/mL) of vesicles were preincubated for 5 min at 30°C. The uptake was initiated with the addition of a concentrated stock solution (20 µL, 30°C) which yielded a final assay mixture of 0.250 mM glutamate, 2.0 mM ATP, 4.0 mM MgCl₂, 4.0 mM KCl, 300 mM sucrose, and 5.0 mM HEPES (pH 7.4). The final mixtures (100 µL) were incubated for 1.5 min and terminated by the addition of 3.0 mL of ice cold 150 mM KCl. Termination of uptake was followed by filtration through Millipore Hawp (25 mm diameter; 0.45 µm pore size). The filters were washed twice more with 3.0 mL of the 150 mM KCl. The filters were transferred to 5 mL glass scintillation fluids. Liquiscint scintillation fluid (3.5 mL; National Diagnostics) was added to the vials. Radioactivity was quantified using a liquid scintillation counter (LSC, Beckman LS6500). Residual radioactivity (filters without ATP) was subtracted to account for non-specific binding. Kinetic analysis was done with glutamate concentrations of 0.25 - 8.0 mM, and inhibitor concentrations were typically 3x-5x above and below the calculated K_i. Nonspecific signal was quantified and

accounted for by measuring ^3H -L-glutamate signal in the absence of ATP, and subtracted from all vials. Nonspecific values were generally less than 20% of the signal, except in the case of ^3H -GABA binding (typically 30-50%). This high level of background was also noted by R. Jahn's group (Hell and Jahn, 1998). Initial experiments of ^3H -GABA and ^3H -serotonin uptake determined that uptake was linear with respect to time and protein under assay conditions employed (data not shown). The linearity of uptake with respect to time and protein was previously established for ^3H -L-glutamate uptake. Sigmoidal dose-response analysis and IC_{50} values were determined from nonlinear regression analysis of a one-site competition model (PRISM, GraphPad Software, Inc.). Estimated K_i values were calculated in accordance with the Cheng-Prusoff relationship from IC_{50} values (Cheng-Prusoff, 1973). Lineweaver-Burke analyses were completed by computer analysis utilizing Michaelis-Menten kinetics (PRISM, GraphPad Software, Inc). Protein concentrations of the assays were quantified via the Pierce BCA assay (bicinchonic acid; (Smith et al., 1985)).

Assay for Measurement of L-Glutamate Efflux

Vesicular glutamate efflux was measured as described by Bartlett (Bartlett et al., 1998). Synaptic vesicles were first incubated in the presence of ^3H -L-glutamate as previously described. After 5 min of incubation, 100 μl of suspended vesicles were diluted 20-fold with incubation buffer with L-glutamate and/or inhibitor at an indicated concentration, in the absence of ATP. The samples were then allowed to incubate for the specified times and efflux was terminated by the addition of 150 mM KCl (0°C) three times, with

vacuum filtration between rinses. Radioactivity present in the vesicle and collected on the filters was quantified by LSC.

Assay for Measurement of ΔpH and $\Delta\Psi$ by Fluorescence Quenching

The quenching of the fluorescent signal generated by either acridine orange or oxonol V was used to monitor changes in pH or electrical gradient in the isolated synaptic vesicles, respectively (Tabb, 1992; Maycox, 1988). Experiments were carried out in sucrose buffer containing (0.320 mM Sucrose, 10 mM HEPES/KOH (pH 7.4), 4 mM KCl, 4 mM MgSO_4) or a KCl buffer (10 mM HEPES/KOH (pH 7.4), 4 mM KCl, 4 mM MgSO_4). Approximately 100-150 μg of protein was included in each assay. After initiating the experiment at 0 sec, ATP was added at 180 sec. Drugs were added at either 60 sec (pretreatment) or 480 sec (treatment). The protonophore, carbonyl cyanide 3-chlorophenylhydrazone (CCCP) was added to each assay at 480 sec to terminate the experiment. Fluorescence quenching experiments were measured with an excitation of 492 nm and an emission of 520 nm for acridine orange (2 μM) on a Hitachi F2000 Spectrofluorimeter. Similarly, fluorescence quenching experiments with oxonol V (10 μM) were run with an excitation of 617 nm and an emission of 643 nm. Interactions between inhibitors and fluorescent dyes were assessed with absorbance, excitation, and emission scans.

Molecular modeling

In silico modeling was done on Silicon Graphics, Inc. (SGI) Octane workstations with R12000 processors coupled to an SGI Origin 2000server. The Sybyl software suite (versions 6.8-7.0) with the Advanced Computation Module (Tripos: St. Louis, MO), was utilized for conformational searching. Additionally, the industrially derived stochastic random search algorithm AESOP was used to ensure a thorough search of the conformational space. Molecular databases were prepared in Sybyl formats.

Pharmacophore alignments were constructed as steric-strain, gas-phase derived conformations compositions employing established comprehensive conformational analysis methods (Marshall, 1995; Opera et al., 1995) with three VGLUT inhibitor ligands, 5,6-fused-quinoline dicarboxylic acid (5,6-QDC) and Congo red fragment (CRF) (for comparative pharmacological properties, (Bartlett, 1999)). Conformational space of the VGLUT inhibitors was comprehensively searched by employing two computational protocols: Randomsearch (Tripos Sybyl) and the stochastic technique AESOP (Masek, 1998). The random search procedure locates energy minima by randomly adjusting the selected bonds and minimizing the energy of the resulting geometry. Chiral centers, ring closure distances, and energy ranges were checked for consistency. This comparison was based on an RMS match between non-hydrogen atoms in the previously found conformers and the current conformer. Two random searches (or more) were performed on each training set ligand and other test cases. Data from the Sybyl random searches were deposited into a molecular database. AESOP is an alternative stochastic derived

program used to search conformational space. It applies high temperature to the molecule (which results in the molecule being torqued and tensed), and was set to capture a conformer snapshot every 5 fs. Temperatures and times were set between 1600 and 1800 K and 60 and 80 fs. Data from the AESOP spreadsheets were deposited in the databases established earlier. Subsequently, all conformers from both search protocols were minimized to zero energy change defining the nearest energy well profile. Conformer database entries were sorted as a function of total energy and cases of degenerate energy profiles were crosschecked as plausible duplicates, based on select distances and angles defined in an exported Molfile spreadsheet. Duplicate or nearly duplicate conformers (e.g., certain rotamers) were eliminated. Some conformations would not have been found only if one conformer search routine had been used.

CHAPTER 3: RESULTS

Section I: Specificity of inhibition elicited by sulfated neuroactive steroids, substituted QDCs, and derivatives of naphthalene sulfonic acids at VGLUT

Introduction

Competitive inhibitors of vesicular glutamate uptake vary widely in their basic structures, from glutamate derivatives, which share obvious similarities with the endogenous substrate, to those of the ergopeptides with less obvious structural commonalities. Among those compounds which are clear homologues of glutamate, *trans*-1-aminocyclopentane-1,3-dicarboxylic acid (*trans*-ACPD) and *erythro*-4-methyl-L-glutamic acid (MGlu) appear to be the most potent inhibitors, with K_i values of 0.44 mM and 0.73 mM, respectively (Winter and Ueda, 1993). It is important to keep in mind that VGLUT exhibits a K_M of 1-3 mM for L-glutamate, unlike that of the high-affinity, Na^+ -dependent transporters, which have K_M values of 5-50 μM . The naphthalene sulfonic acids are much larger molecules that still retain some structural similarities with L-glutamate. Evans blue and Chicago sky blue are the most potent compounds within this class of inhibitors, initially characterized with K_i values of 40 nM and 90 nM, respectively (Roseth et al., 1995). Previous work in our lab described another naphthalene sulfonic acid, Congo red (CR), as a competitive inhibitor with a K_i value of 0.840 μM (Bartlett, 1999).

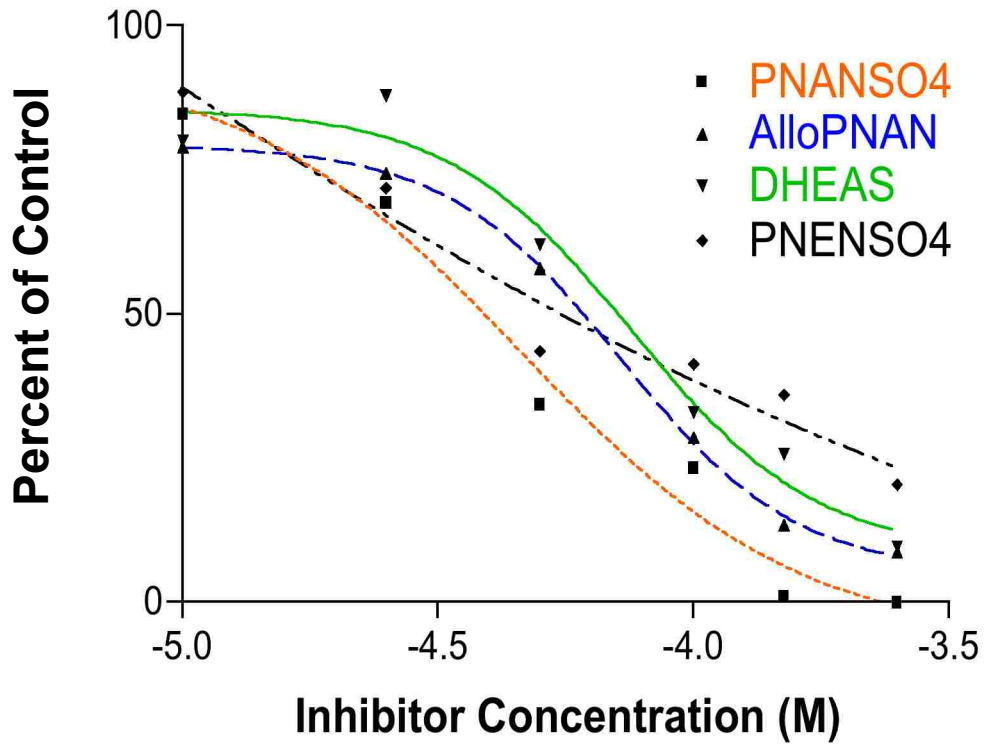
Although the naphthalene sulfonic acids are one of the most potent groups of compounds to date, they are difficult to obtain in sufficient purity and have cross-reactivity with other sites within the glutamatergic system. In conjunction with the laboratory of Charles Thompson (C.N. Carrigan), another inhibitor series has been developed to address these limitations. The utilization of QDC as a template for this inhibitor series was based on three criteria: (1) an embedded glutamate molecule with a coplanar arrangement, (2) a bicyclic aromatic system, and (3) activity at VGLUT (Carrigan et al., 1999). The coplanar arrangement of an embedded glutamate was decided upon based on the desirable properties of the kynurenate analogues. Two of them, 7-Cl-kynurenate and xanthurenate were shown to exhibit K_i values of 0.59 mM and 0.19 mM, respectively (Bartlett et al., 1998). Further, it was noted that compounds containing bicyclic ring system were more effective inhibitors than those with monocyclic ring systems. This observation led to the decision to include bicyclic ring systems into the inhibitor design template. With respect to specificity for VGLUT, the potent kynurenate analogues mentioned previously, displayed little, if any, activity at the EAATs and minimal activity at glutamatergic receptors. Consistent with the criteria used in the design of these molecules, the development and subsequent testing of 6-(4'-biphenyl)-QDC yielded a molecule with an enhanced inhibitory activity ($K_i = 0.041$ mM). This increase in potency was hypothesized to be due to the addition of a lipophilic moiety in the form of an aryl or aryl-linked group at the 6- or 7- position.

Another inhibitor, 5,6-naphthyl-QDC (5,6-QDC), designed from this template, was also shown to have activity at VGLUT uptake (Carrigan, 2000). Interestingly, the structure of

this compound resembled the basic structure of a steroid molecule (Fig. 1.2; Fig. 1.4). Specifically, the bicyclic core and lipophilic addition suggested that certain steroids may be active at VGLUT. Moreover, modeling studies, discussed in section 2 of this work, indicate that neuroactive steroids might also be accommodated in the binding-site. Additional credence for this possibility is found in recent evidence that neuroactive steroids act at distinct sites within the glutamatergic system, i.e. NMDA receptors. These sites have been shown to be responsive to PREGS and $3\alpha,5\beta$ -TH PROG in positive and negative modulatory roles, respectively (Park-Chung et al., 1997). To further explore this observation, a panel of neuroactive steroids that most resemble QDCs was initially tested by Holly Cox, for their ability to block vesicular uptake of glutamate (Table 3.I.1). Interestingly, only the sulfated neuroactive steroids were active inhibitors of vesicular glutamate uptake, as opposed to nonsulfated compounds such as estradiol 3-benzoate, estrone hemisuccinate, PREG-3-acetoxy, and PREG. Neuroactive steroids, which displayed the greatest degree of activity, were then characterized with a dose-response analysis at VGLUT (Figure 3.I.1; Table 3.I.1). Of these compounds (DHEAS, PREGS, $3\alpha,5\alpha$ TH PROGS, and $3\alpha,5\beta$ TH PROGS), $3\alpha,5\beta$ TH PROGS was the most active with an estimated K_i value of 26.2 μ M.

To confirm the specificity of inhibition at the biochemical level, this work presents a more detailed kinetic analysis of PREGS. For comparative purposes, 5,6-QDC was also kinetically characterized in parallel with the PREGS. The results of this work are potentially significant in that the SAR data may provide a link between a synthetically derived compound and a new endogenous ligand. Further, the characterization of these

Figure 3.I.1. Concentration-response analysis of potent sulfated-neuroactive steroids at VGLUT



Dose-response analysis of neuroactive steroid inhibition of VGLUT. Glutamate ($^3\text{H-L-}$) uptake was performed as described in Chapter 2. Neuroactive steroids were tested against vesicular glutamate uptake at six concentrations (10, 25, 50, 100, 250, 500 μM). A variable slope plot was utilized due to poor aqueous solubility of neuroactive steroids. Data courtesy of H. Cox, unpublished results.

Table 3.I.1. Inhibition of VGLUT by sulfated neuroactive steroids

Compound	Percent of Control (250 μ M)	K_i (μ M)
DHEAS	23 \pm 3	54 \pm 5
Pregnenolone	100 \pm 4	
Pregnenolone 3-acetoxy	86 \pm 5	
Pregnenolone Sulfate	31 \pm 3	63 \pm 5
Pregnanolone Sulfate	15 \pm 4	26 \pm 2
Allopregnanolone Sulfate	8 \pm 3	40 \pm 7
Estradiol 3-benzoate	111 \pm 3	
Estrone Sulfate	52 \pm 8	
Estrone hemisuccinate	109 \pm 20	

Pharmacological data for neuroactive steroid inhibition of $^3\text{H-L}$ -glutamate uptake into isolated synaptic vesicles. Data are reported as % of control values and represent the mean \pm SEM ($n \geq 3$). Control values were 1500 ± 110 pmol/min/mg protein. K_i values were calculated using the Cheng-Prusoff equation (GraphPad Prism software) in at least three independent experiments. K_i values were only determined for active compounds. Sulfated neuroactive steroids were shown to be the more potent inhibitors. Unpublished data courtesy of H. Cox.

compounds as competitive inhibitors make them useful in the development and refinement of the VGLUT pharmacophore model.

Results

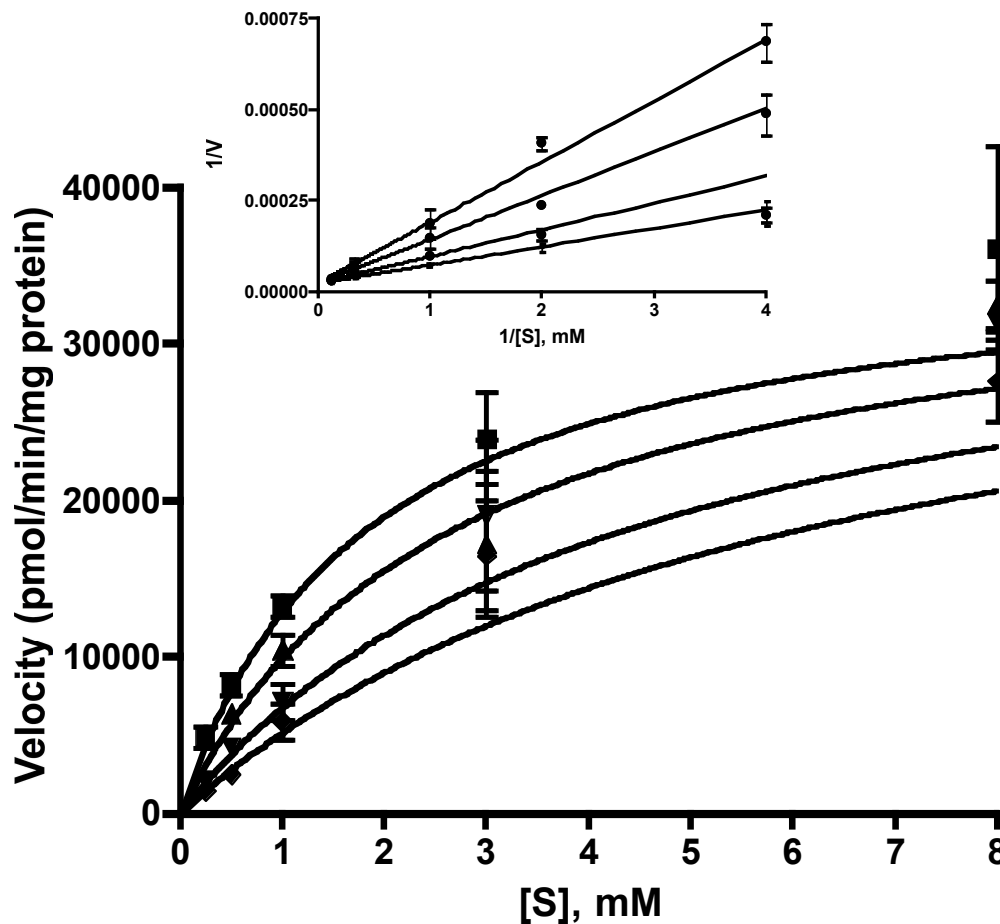
PREGS was assayed at three concentrations (50 μ M, 150 μ M, and 250 μ M) against a range of glutamate concentrations (0.250-8.0 mM). The data was analyzed using GraphPad PRISM Software utilizing a nonlinear regression approach. The results of a replot of data derived from nonlinear regression to the form of a double-reciprocal plot were consistent with PREGS being a competitive inhibitor ($K_i = 107 \mu$ M) that exhibits a K_M and V_{max} of 1.81 ± 0.37 mM and 36.2 ± 4.2 nmol/min/mg, respectively for glutamate uptake (Fig. 3.I.2). A similar analysis was performed with 5,6-QDC at concentrations of 10 μ M, 50 μ M, and 150 μ M. Similar to PREGS, nonlinear regression analysis reveals that 5,6-QDC is a competitive inhibitor ($K_i = 228 \mu$ M) with a $K_M = 1.21 \pm 0.22$ mM and a $V_{max} = 27.6 \pm 2.7$ nmol/min/mg for glutamate uptake (Fig. 3.I.3).

These results suggest that binding of PREGS and 5,6-QDC are mutually exclusive at the substrate-binding site. This does not, however, rule out the possibility that these molecules are binding to the substrate site in different manners. For instance, the differences in overall length of conformations of these competitive inhibitors may result in the occupation of the substrate-binding site in slightly different ways. Thus, VGLUT inhibitors with a longer overall length may occupy subdomains in addition to those required for the binding of L-glutamate. Alternatively, a VGLUT inhibitor may not only

occupy subdomains through which L-glutamate is transported, but also bind to distinct site(s) that disrupt the conformational changes necessary for the transport of L-glutamate. The classification of these compounds as competitive inhibitors designates that [³H]-L-glutamate will not bind to VGLUT while in the presence of the inhibitor.

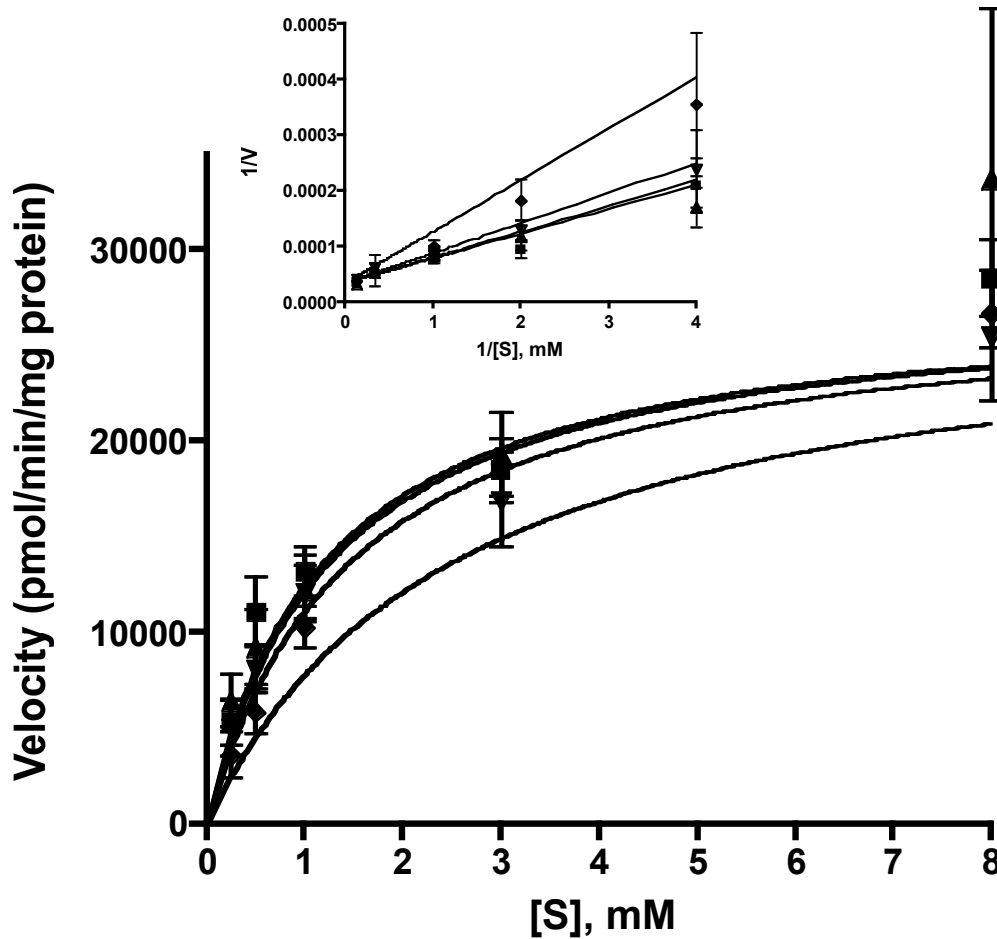
In summary, these results confirm that previously identified structural features (i.e., lipophilic moiety, bicyclic core) that are important for inhibitor activity at VGLUT (Fig. 3.I.4). Moreover, the conclusion that 5,6-QDC is a competitive inhibitor provides further support for selectivity of the QDC template. The classification of PREGS as a competitive inhibitor at VGLUT adds another binding site for neuroactive steroids within the CNS. The K_i values observed for these compounds exhibit a 10-fold higher affinity for VGLUT than the endogenous substrate; whereas, the azo- dyes are 1000-fold more potent than L-glutamate.

Figure 3.I.2. Demonstration of the competitive inhibition of PREGS on ^3H -L-glutamate the uptake into synaptic vesicles.



Nonlinear regression plot ($n = 3$) of the effect PREGS (50, 150, 250 μM) has on the uptake of ^3H -L-glutamate (0.25-8.0 mM) into synaptic vesicles. Nonlinear regression yields a $K_M = 1.81 \pm 0.37$ mM, a $V_{\max} = 36.2 \pm 4.2$ nmol/min/mg for glutamate uptake, and a $K_i = 0.107 \pm 0.021$ mM. Inset shows a replot of the nonlinear regression in the form of a double-reciprocal plot.

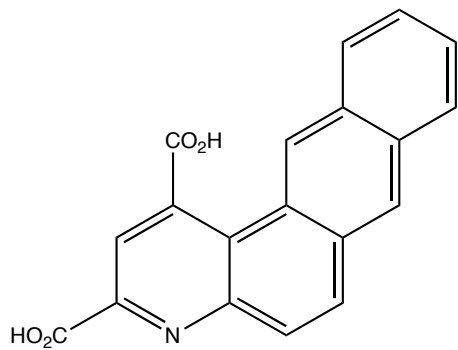
Figure 3.I.3. Demonstration of the competitive inhibition of 5,6-QDC on the uptake of $^3\text{H-L-glutamate}$ into synaptic vesicles.



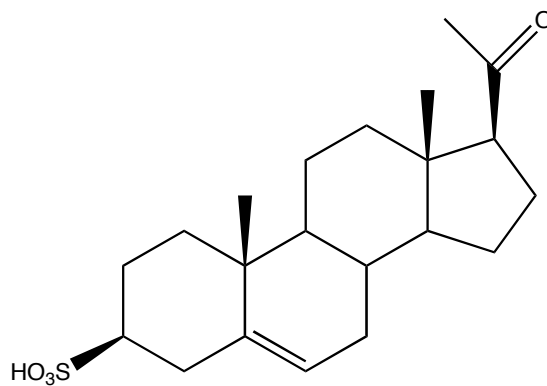
Nonlinear regression plot ($n = 3$) of the effect 5,6-QDC (50, 150, 250 μM) has on the uptake of $^3\text{H-L-glutamate}$ (0.25-8.0 mM) into synaptic vesicles. Nonlinear regression yields a $K_M = 1.21 \pm 0.22$ mM, a $V_{\max} = 27.6 \pm 2.7$ nmol/min/mg, and a $K_i = 0.228 \pm 0.075$ mM for glutamate uptake. Inset shows a replot of the nonlinear regression superimposed on a double-reciprocal graph of the data.

Figure 3.I.4. Structures of identified competitive inhibitors

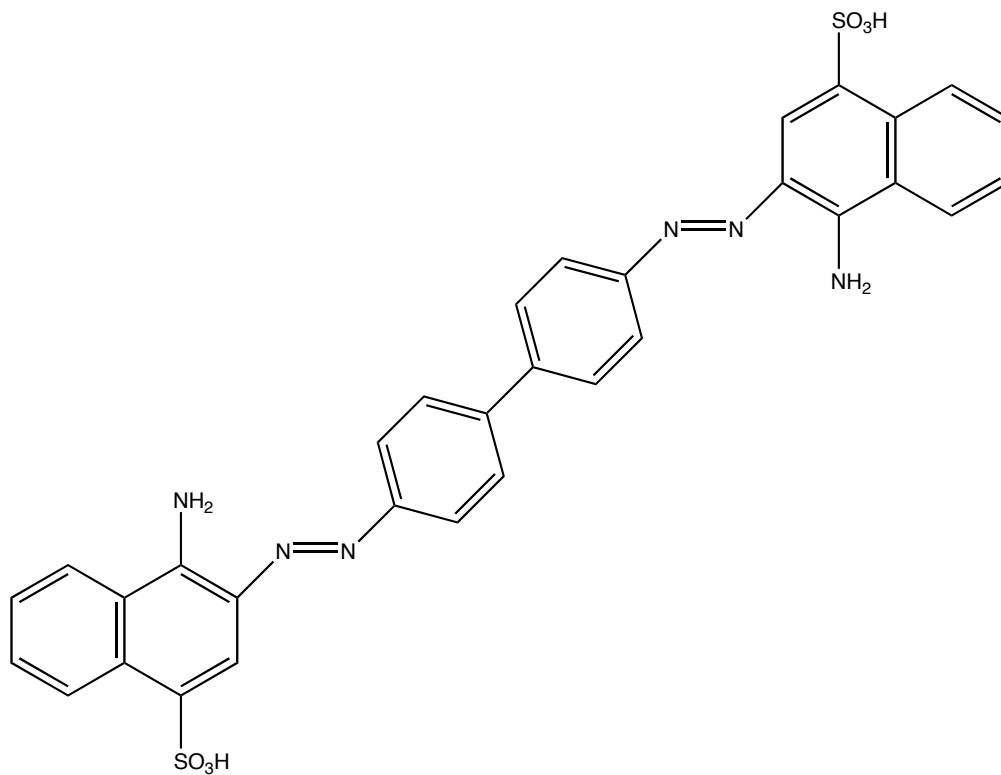
(a)



(b)



(c)



The structures of identified inhibitors: (a) 5,6-naphthyl-QDC, (b) PREGS, and (c) Congo red

Section II: Development of a VGLUT pharmacophore model and alignments with identified, competitive inhibitors

Introduction

As more compounds are characterized as competitive inhibitors of the vesicular glutamate system, it becomes possible to visualize the three-dimensional (3D) space necessary to understand the structural requirements needed for binding. One of the most effective methods to achieve this is through the construction of a 3D, ligand-based pharmacophore model, which essentially defines the structural characteristics of active molecules. As computational power has increased, the development of three-dimensional models is generally more valuable than two-dimensional (2D) ones. The basic assumption underlying the model is that the compounds used to generate the pharmacophore model are binding to the protein in a similar manner; this assumption is consistent with the nature of inhibition elicited by competitive inhibitors (Leach, 2001).

Previous work in our lab initially sought to develop a ligand-based pharmacophore model for VGLUT using a best-fit, three-point analysis of L-glutamate, xanthurenate, and (1R,3S)-ACPD. This analysis was intended to identify the maximum overlap of identified groups. In this instance, the groups selected were α -nitrogens, α -carboxylates, and electron densities of distal carboxylates and aromatic groups. Two models emerged from these efforts; the first of which predicted a high degree of overlap between glutamate and xanthurenate, while the second model predicted a “cupped” conformation of (1R,3S)-ACPD. Interestingly, this “cupped” conformation was proposed as an active

conformation at mGluRs, which could be problematic in the effort to develop inhibitors that are specific for VGLUT and do not crossreact with mGluRs (Bartlett et al., 1998).

This pharmacophore model was subsequently refined, in collaboration with C.M. Thompson and coworkers, through development and characterization of the quinoline dicarboxylic acids QDCs. The QDC template was essentially a composite of structural characteristics from L-glutamate, kynurenate and the naphthalene sulfonic acids, as depicted in Chapter 1 of this work (Fig. 1.3). The resulting SAR data illuminated the structural requirements necessary for activity at VGLUT (Carrigan et al., 2002). First, a bicyclic aromatic core, present in the QDCs and naphthalene sulfonic acids, represented the most basic structural moiety of the model. Secondly, an embedded glutamate structure, present in the previous pharmacophore model and incorporated into this design, was proposed to facilitate binding. This “embedded glutamate” includes the two carboxylic acids and an amine group in a coplanar arrangement, with specificity at VGLUT. Finally, the presence of a lipophilic functional group was included in the QDC template due to associated increases in potency. The lipophilic moiety, present in the form of biphenyl or naphthyl groups, improved K_i values two-fold or greater (200 μM to 100 μM) (Carrigan et al., 2002).

In collaboration with the laboratories of J.M. Gerdes and C.M. Thompson, the most recent iteration of this pharmacophore model was constructed (E. Bolstad, unpublished results) with more advanced computational modeling methods (Esslinger et al., 2005) (Fig. 3.II.1). This pharmacophore model offers a more thorough understanding of the

important functional groups and their relationship in 3D space (Fig. 3.II.2). This model was created by the superposition of a diverse set of three molecules chosen based on structural diversity and potency (K_i in the micromolar range). The three molecules chosen, Chicago sky blue monomer (CSB), bromocriptine (BCT), and 6-(4'-biphenyl) QDC (6-(4')-QDC), underwent conformational analysis to elucidate common binding moieties. Conformationally-constricted molecules are particularly valuable in this type of analysis. To begin with, conformational constraints limit the number of conformers reasonably obtainable by the analogues. One analogue, by itself, is not especially problematic; however, among the three molecules used to generate the conformer, 2806 conformers were found. Conformer groups, used in the analysis of the molecules employed in the pharmacophore model, totaled 419,475,368 (Table 3.II.1). Also, these molecules define conformational space in a known manner, which aids in the orientation of these molecules when aligned amongst each other. Four regions and 6 measures were determined for the refined pharmacophore model. Two aryl ring moieties, designated by ring 1 and 2, are similar to the bicyclic core and lipophilic moiety present in the previous pharmacophore model (Fig. 3.II.2). Two regions of electronegativity/electron density, designated as region 1 and 2, correspond to the (γ)-distal carboxylate isosteres also present in the preliminary pharmacophore model (Fig. 3.II.2). These measures represent the averages (represented in Fig. 3.II.2)

Based on its structural qualities, pregnenolone sulfate (PREGS) was chosen as novel inhibitor to verify this pharmacophore model using a "leave-one-out" procedure (in collaboration with E. Bolstad, unpublished results).

Figure 3.II.1. Illustration of the superposition of CSB, BCT, and 6-(4')-QDC

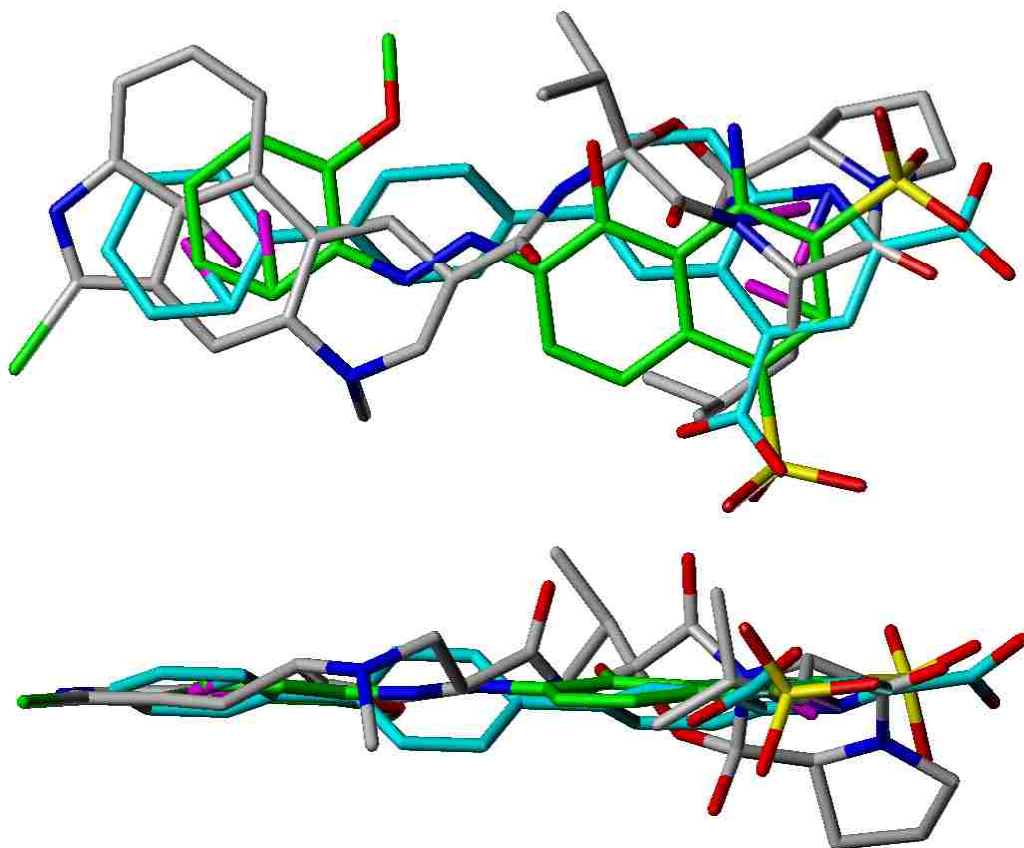
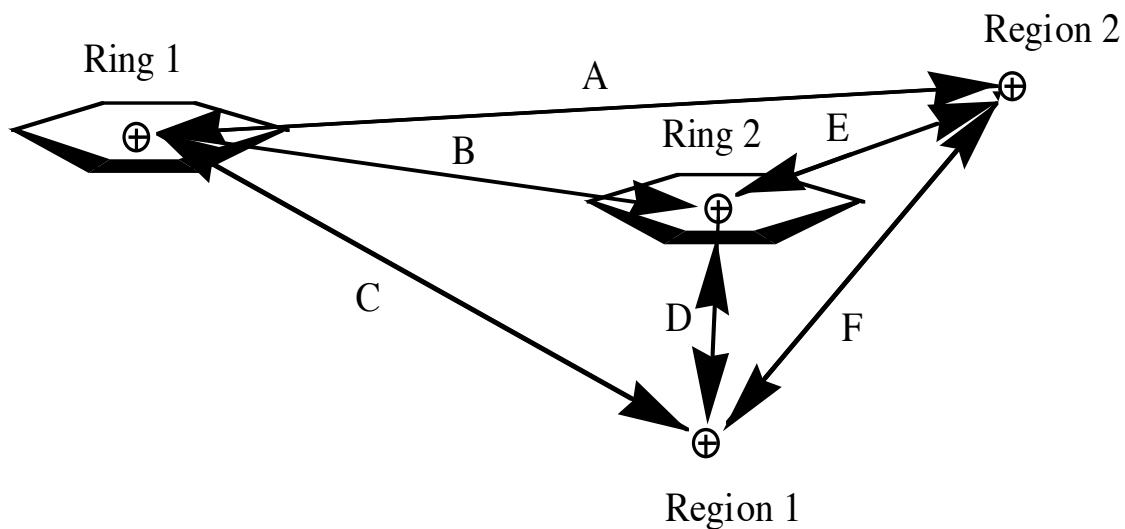


Image depicting VGLUT pharmacophore model shows the superposition of 6-(4')-QDC (aqua blue), Bromocriptine (grey), and Chicago sky blue Monomer (green). Electronegative regions are distinguished by the oxygen groups (marked in red). The centroids of identified rings are represented by pink (E. Bolstad, unpublished results). The training set molecular conformations were brought together with a 1 cal spring constant. Top panel shows common ring lipophilic regions and correlated electronegative groups (top panel, right). The bottom panel emphasizes the planar quality of the superposition pharmacophore model.

Figure 3.II.2. Identified regions and intraregion measures of the VGLUT Pharmacophore model

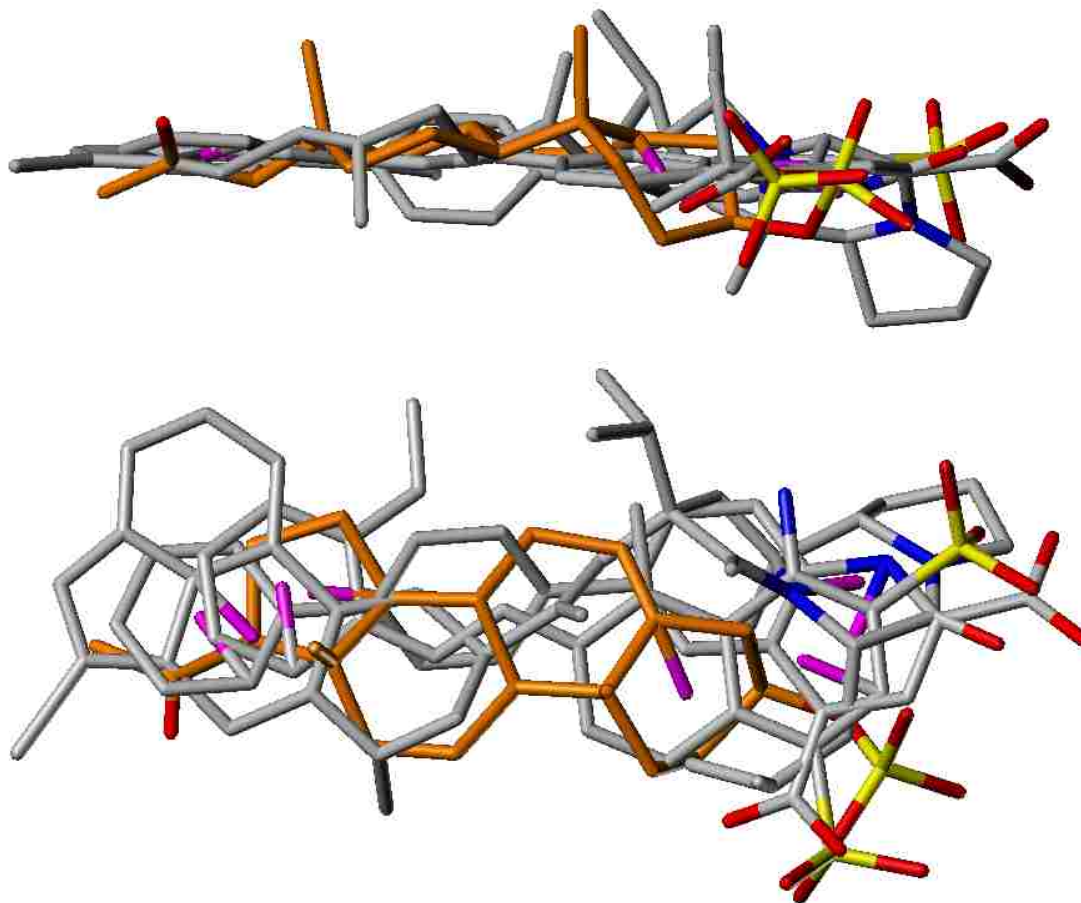


Measurements of the VGLUT pharmacophore model. Four regions and six measures were determined for the refined pharmacophore. Two aryl ring moieties, designated by ring 1 and 2, are similar to the aryl ring and bicyclic core present in the previous pharmacophore. Two regions of electronegativity/electron density, designated as region 1 and 2, correspond to the (γ)-distal carboxylate isosteres also present in the preliminary pharmacophore. The measurements compared are as follows: A. 12.3 Å; B. 9.8 Å; C. 9.7 Å; D. 3.3 Å; E. 2.9 Å; F. 4.9 Å (E. Bolstad, unpublished results)

This protocol, which also provided my initial training in modeling, is a method for validation of the pharmacophore model, in which a potent competitive inhibitor is not included in the model construction training molecular set. Ideally, the test molecule chosen exhibits certain distinct characteristics, which makes it valuable as a test case, i.e. a planar conformation with select functional groups, to clearly challenge the model fit qualities. The alignment of a PREGS conformation, with a minimized conformer energy of 22.54 Kcal/mol, produced a good fit using an all-combinational analysis technique (Fig. 3.II.3). The neuroactive steroid (orange) was easily superpositioned within the pharmacophore model (silver), thereby demonstrating the model's robust qualities. The centroids of the aryl ring moieties of each molecule are colored pink. Electronegative regions are shown in yellow (sulfur), and silver (carbon) with red (oxygen) ends. The VGLUT pharmacophore model predicts that competitive inhibitors would have a planar structure with two electronegative areas and a lipophilic moiety.

The model conformer energies (Table 3.II.1) were often higher than of the global minima conformer energy (lowest energy listed in the strain energy range). A conformer energy, which is higher than the conformer energy minima, can be explained since the most energetically favored conformations do not always represent the biologically active ones. This energy difference can be explained by the energy involved in ligand-receptor interactions (Rupp et al., 1994). The neuroactive steroid selected was PREGS which then was pharmacologically characterized at VGLUT, amongst other proteins as described in the previous section of this dissertation.

Figure 3.II.3. Alignment of VGLUT pharmacophore model with PREGS

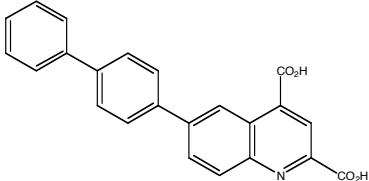
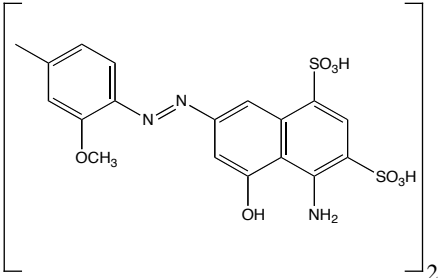
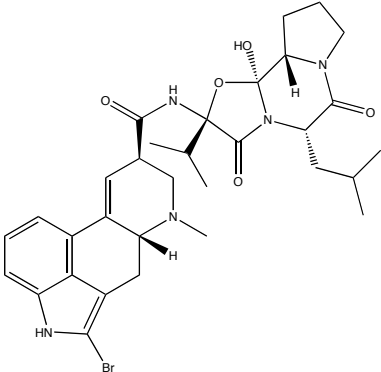


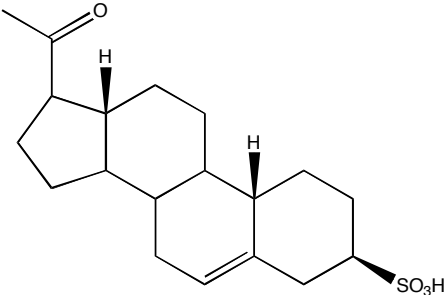
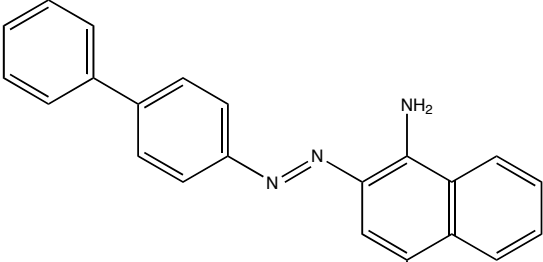
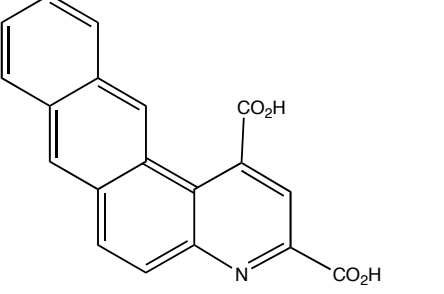
Alignment of the VGLUT pharmacophore model and PREGS (orange) performed as described in the text. Conformational space searching resulted in 78 conformers. The strain energy range of the conformers was 21.78-41.65 (Kcal/mol). The strain energy of the conformer used in the alignment was 22.54 (Kcal/mol) (E. Bolstad, unpublished results). The conformers are brought together with a minimal 1 cal spring constant. The planar qualities of PREGS are shown in the top panel. The bottom panel reveals the overlap of the PREGS 3-position sulfonate group with one of the model electronegative groups (lower right).

At the time the VGLUT pharmacophore model began, we decided to select one sulfonated neuroactive steroid as a representative example of the molecular class. The neurosteroid selected was PREGS, which then was pharmacologically characterized at VGLUT, amongst other proteins as described in other sections of this dissertation.

To further utilize the pharmacophore model, the alignments of identified competitive inhibitors, 5,6-QDC and Congo red, were also performed. These molecules were not used in a leave-one-out protocol, due to the potential bias that compounds from the same inhibitor classes (6-[4'-biphenyl]-QDC, QDCs; Chicago sky blue, naphthalene sulfonic acids) being used in the development of the pharmacophore model. In combination, these approaches can serve to synergistically increase the visual understanding of the VGLUT binding domain by providing rigorous computational models that are verified and refined through kinetic analysis.

Table 3.II.1. Training set ligands used in the generation and testing of the VGLUT pharmacophore model and related test cases.

VGLUT Ligand	K_i (VGLUT)	Total Number of Conformers	Strain energy range of conformer set (Kcal/mol)	Model conformer energy (Kcal/mol)	Structures
6-[4']-QDC	95 μ M	274	7.88-10.9	7.91	
Chicago sky blue (Monomer)	190 nM	1,534	30.3-35.1	30.3	
Bromocriptine	22 μ M	998	37.7-58.4	46.9	

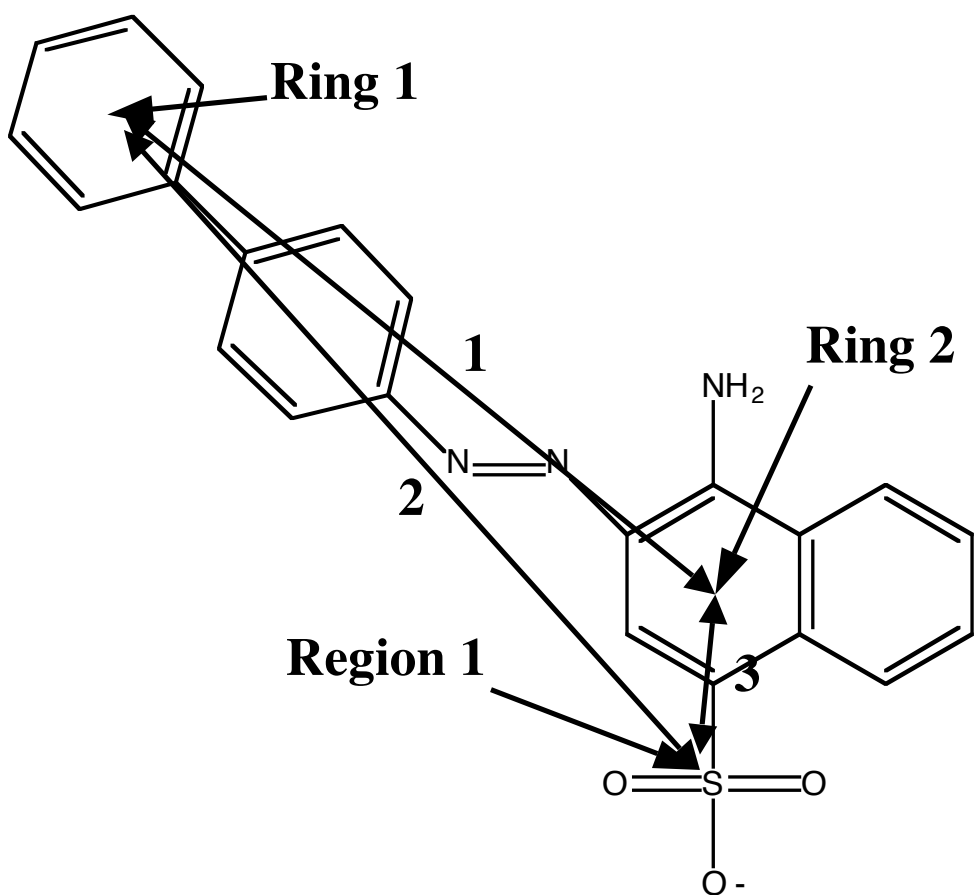
PREGS	107 μM	78	21.78-41.65	22.54	
Congo red (Fragment)	27 μM^*	243	10.96-12.95	11.88 (A1) and 11.84 (A2)	
5,6-QDC	228 μM	17	10.36-12.92	11.18	

Ligands used in the generation and testing of the VGLUT pharmacophore model demonstrate the structural diversity of these molecules. One criterion of this data set is the selection of molecules with a K_i for VGLUT in the micromolar range.

Results

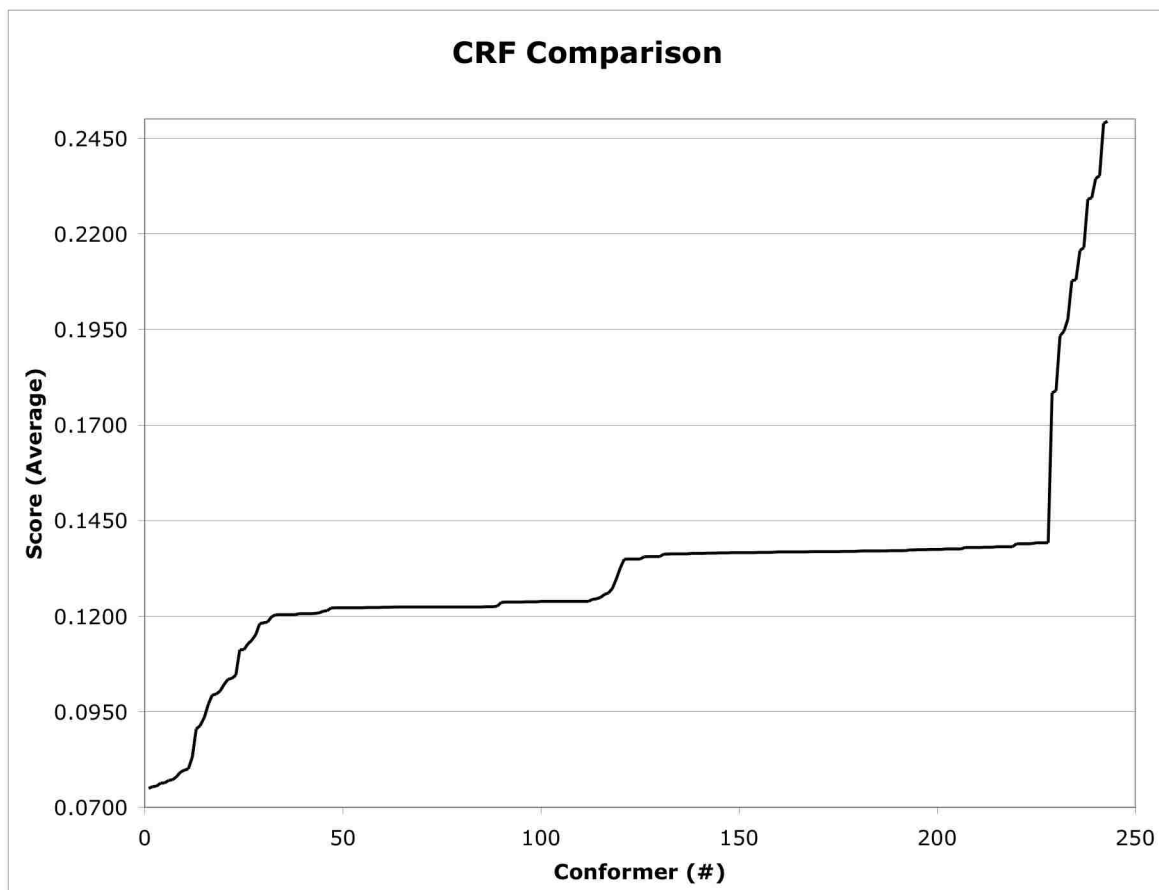
To generate an alignment with Congo red fragment (CRF), the distance between the defined groups of the pharmacophore model and corresponding defined groups of the conformers were measured and recorded. An average of the differences of these measures was plotted against an arbitrarily assigned conformer group number. Although a lower score is generally indicative of a better 3D alignment, a range of alignments with the lowest scores was examined for a realistic superposition, as they may vary somewhat. As the molecular modeling software only aligns designated points, it is possible for a ligand superposition with a low score to have a variable pharmacophore model fit. A group of conformers with a score in the lower range of the scale was chosen and visually inspected. For example, one alignment showed a grossly out-of-plane aromatic ring and azo-linker (Fig. 3.II.6). The sulfonate group on CRF was aligned with Region 1 of the defined pharmacophore model regions (Fig. 3.II.4). The conformer used in this alignment had an energy of 11.88 Kcal/mol and had a strain energy range of 10.96-12.95 Kcal/mol. The alignment graph (Fig. 3.II.5) demonstrates various plateaus in the fit scored differences between the superposition possibilities. Conformers from the lower plateaus were chosen for visual inspections. To further explore alignment possibilities, another point-oriented fit was generated. In this alignment the sulfonate group of CRF was aligned with Region 2 of the pharmacophore model (Fig. 3.II.7). The second alignment (conformer energy of 11.84 Kcal/mol) yields a more consistent overall superposition fit across all the ligand conformers (Fig. 3.II.9). The relative alignment

Figure 3.II.4. Diagram of CRF alignment with VGLUT pharmacophore model (A1)



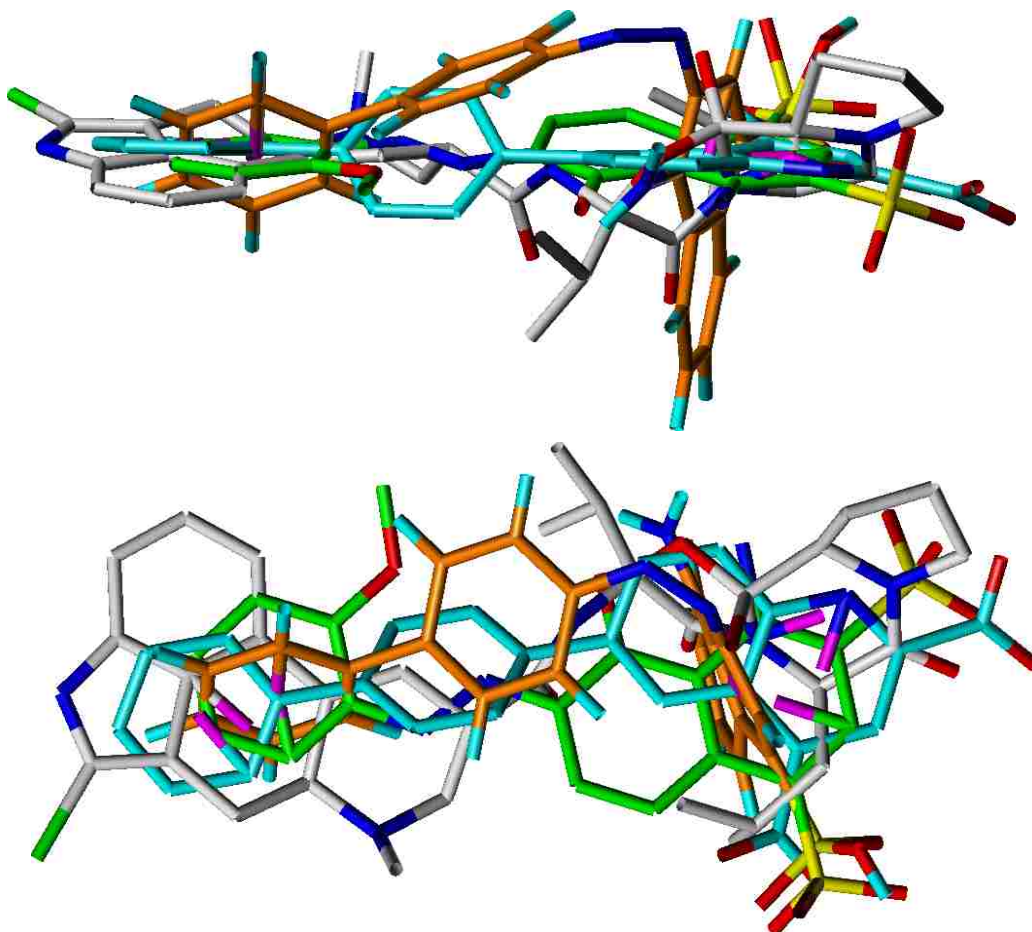
CRF was superpositioned on the VGLUT pharmacophore model. The sulfonate group of CRF was aligned with Region 1 of the pharmacophore model shown in Fig. 3.II.2.

Figure 3.II.5. Demonstration of pharmacophore model alignment (A1) *versus* conformer number



The alignment (A1) of CRF was described in section 2. This graph depicts the score of the alignment *versus* an arbitrarily assigned conformer number. The score is the average of the relative difference measured distances of defined points of CRF from the defined points of the training set pharmacophore model.

Figure 3.II.6. Alignment 1 (A1) VGLUT pharmacophore model with CRF

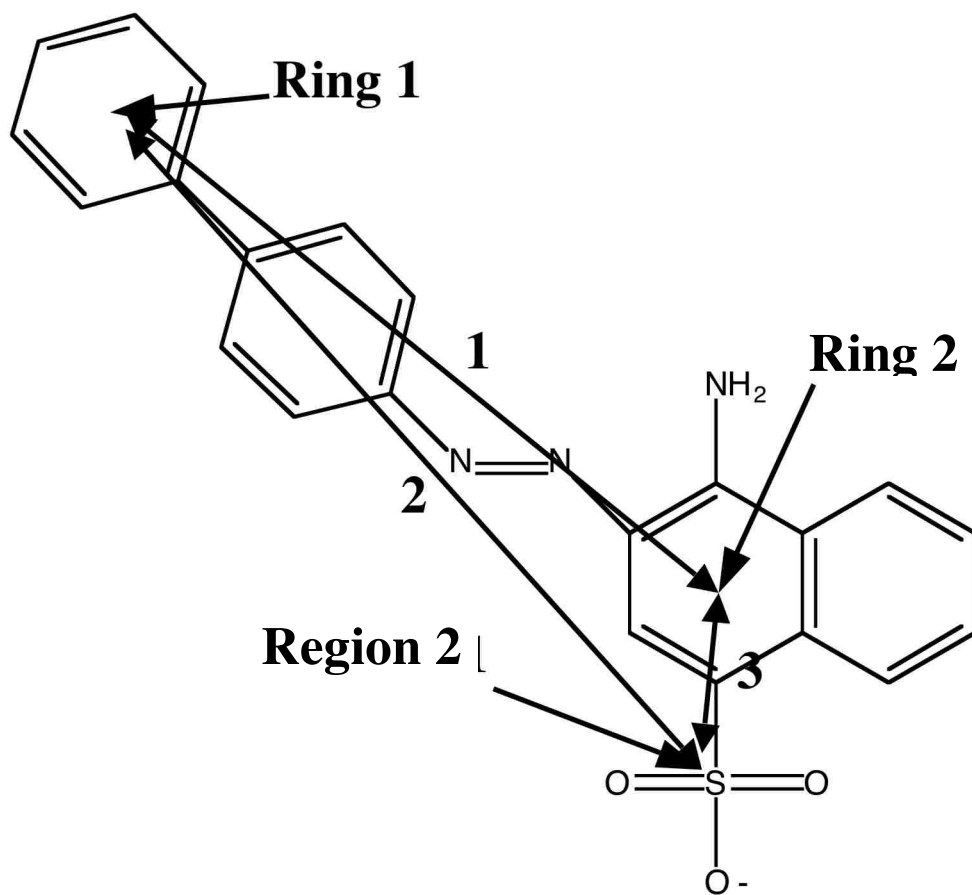


Alignment 1 (A1) of VGLUT pharmacophore model and CRF (orange) performed as described in the text. Conformational space searching resulted in 243 CRF conformers. The strain energy range of conformers was 10.96-12.95 Kcal/mol. The strain energy of the conformer used in the alignment was 11.88 Kcal/mol. The top view emphasizes the overall planar quality of the model. The bottom view reveals the common alignment of the electronegative group (lower right). Ligand conformers were brought together using a 1 cal spring constant. Certain alignments, such as this one, can result in an unfavorable fit.

scores were much lower on average in the second alignment (A2) than the first alignment (A1). The QDC, 5,6-QDC, much like that of PREGS exists in primarily a planar conformation (Fig. 3.II.11). The fit of 5,6-QDC appears similar to PREGS. However, the arrangement of the bicyclic core and naphthyl groups of 5,6-QDC makes it appear shorter in overall length than that of PREGS (Fig. 3.II.11). This may explain the slight difference in K_i values of 107.1 μM and 203.8 μM for PREG and 5,6-QDC, respectively. 5,6-QDC had a narrow energy strain range of 10.36-12.92 Kcal/mole, much like that of 6-4'-QDC due to the conformational constriction inherent to its molecular structure. The energy of the conformer used in the alignment was 11.18 Kcal/mole.

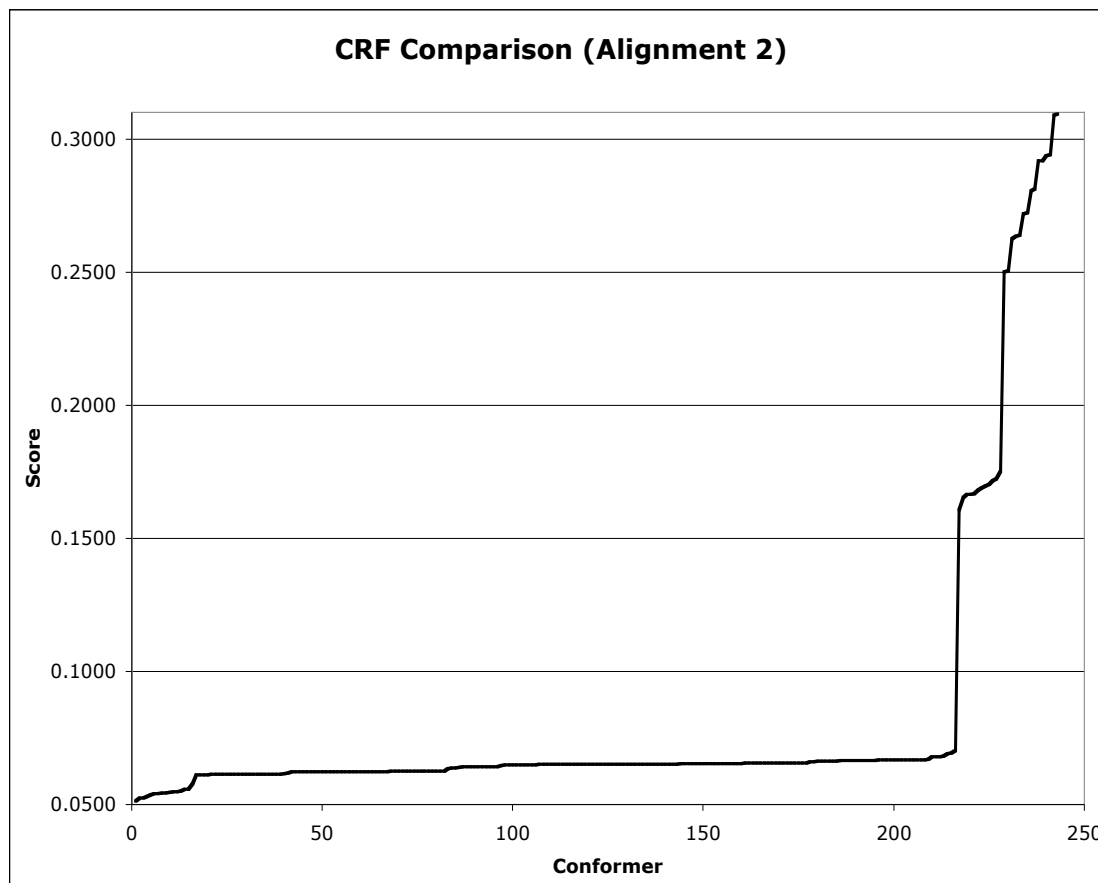
In summary, a correlation between kinetic results and pharmacophore model fits are indicative that the Figure 3.II.3 model displays consistent superposition properties. Most of the potent compounds contain a bicyclic core, electronegative region(s), and a lipophilic substituent. While the fit of 5,6-QDC and CRF, albeit good, are potentially biased due to the inclusion of analogues from their respective classes, PREGS offers validation of the pharmacophore model derived with the training set ligands. Structurally, PREGS contains all of the groups identified by earlier design efforts further confirming the effectiveness of the QDC template. While these results are encouraging, much more work utilizing the pharmacophore model is planned. Future docking experiments with protein models based upon crystal structures such as Gouaux's structure of the glutamate transporter homologue from *P. horikoshii* (Yernool et al., 2004) are underway and promise insights along with interesting debates (Yernool et al., 2004)

Figure 3.II.7. Diagram of CRF alignment with VGLUT pharmacophore model (A2)



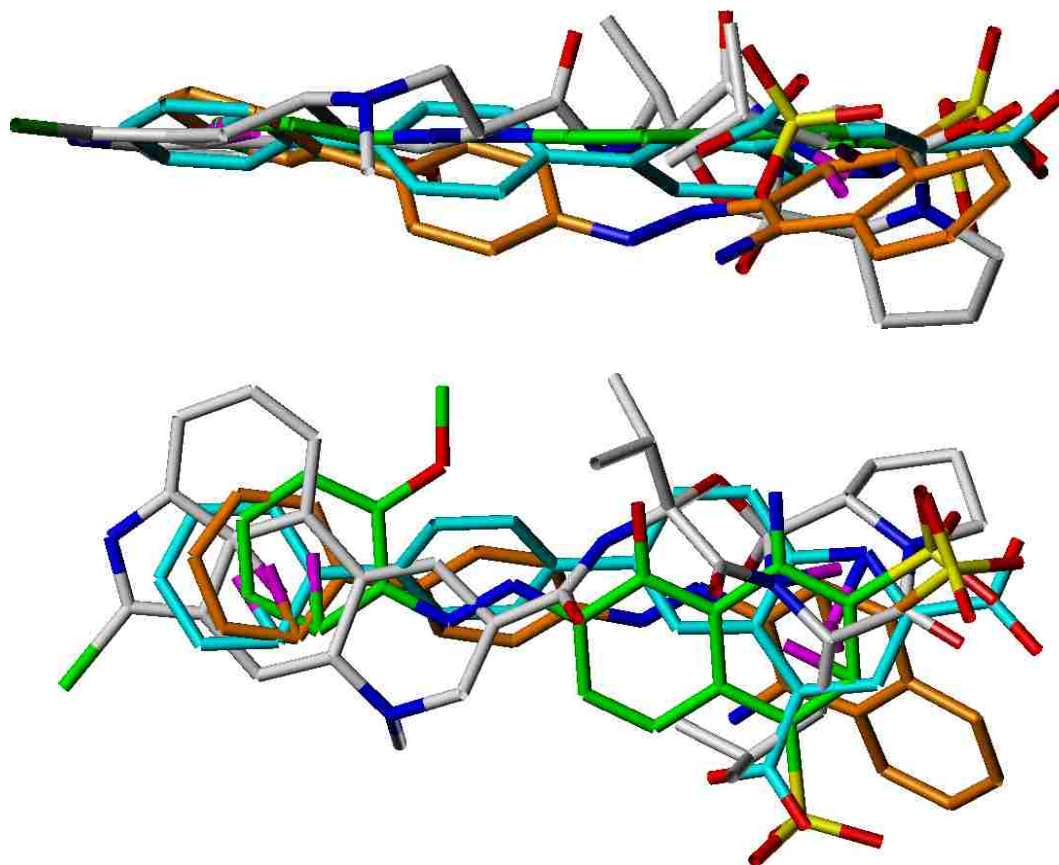
CRF was superpositioned on the VGLUT pharmacophore model. The amino group of CRF was aligned with Region 1 of the pharmacophore model. The numbers 1,2, and 3 correspond with the measures used in the alignment against the training set pharmacophore model shown in Fig. 3.II.3.

Figure 3.II.8. Demonstration of 3D similarity for (A2) *versus* the conformer group number



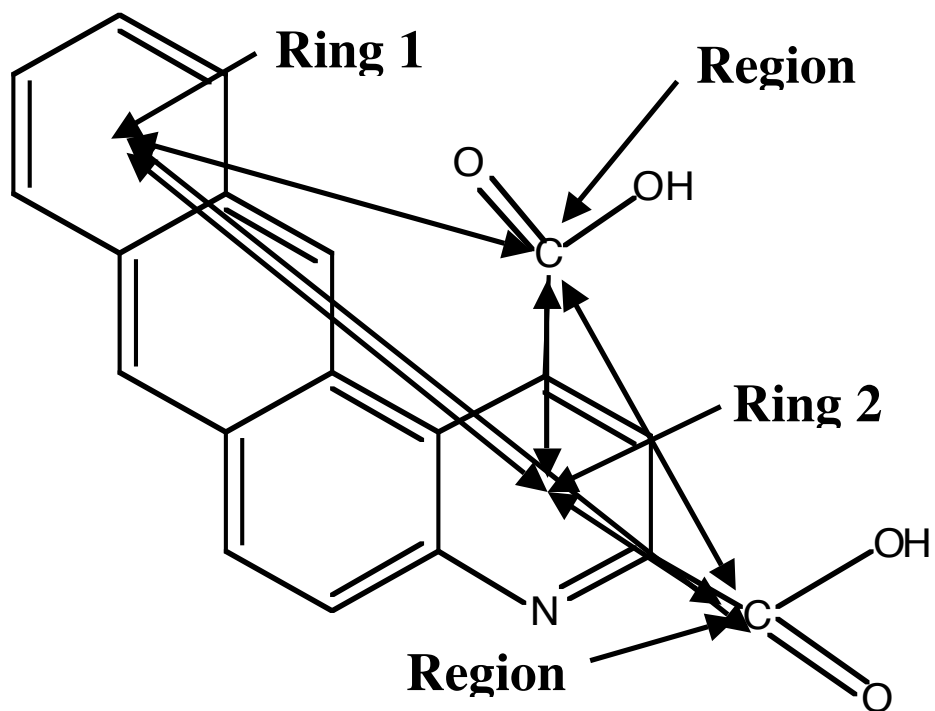
The alignment (A2) of CRF was described in section 2. This graph depicts the score of the alignment *versus* an arbitrarily assigned conformer number. The score is the average distance of defined points on CRF from the defined points of the pharmacophore model.

Figure 3.II.9. Alignment (A2) of the pharmacophore model with CRF



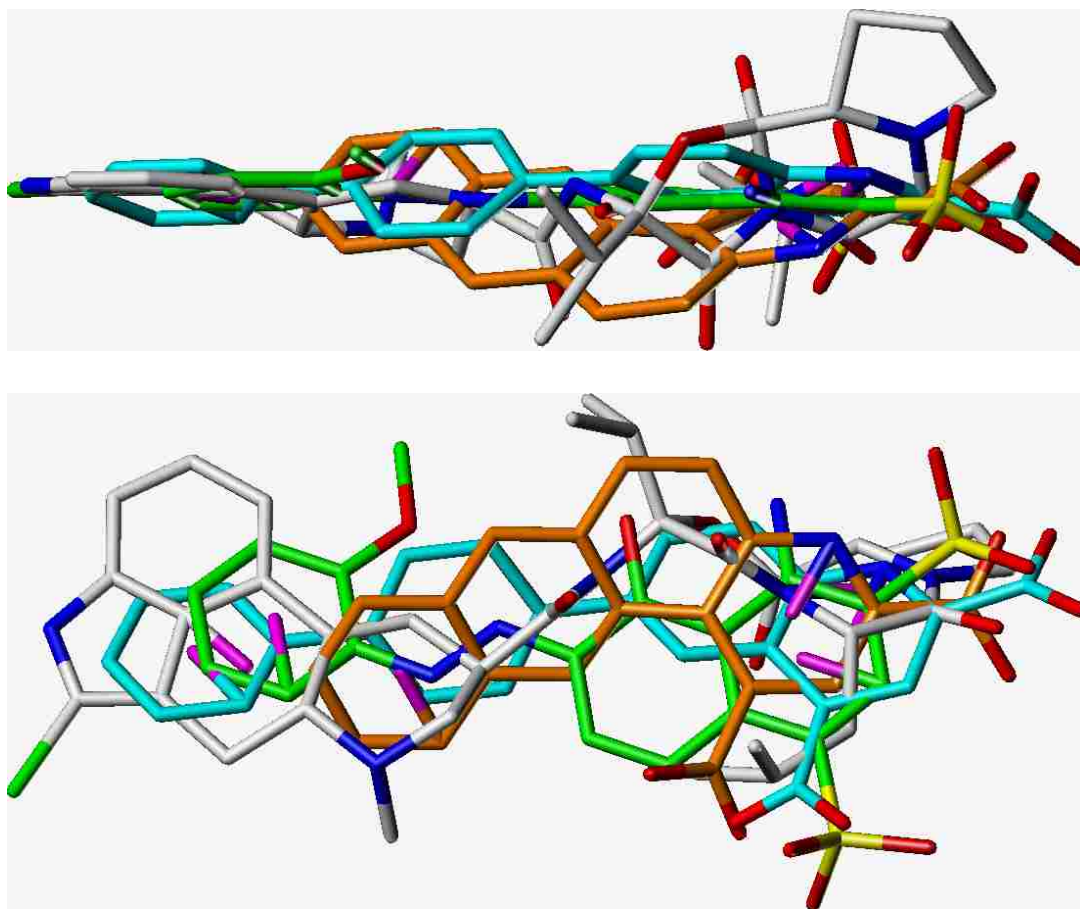
Alignment of the VGLUT pharmacophore model and CRF (orange) performed as described in the text. Conformational space searching resulted in 243 CRF conformers. The strain energy range of CRF conformers was 10.96-12.95 Kcal/mol. The strain energy of the conformer used in the alignment was 11.837 Kcal/mol. The ligand conformers were superpositioned with a 1 cal spring constant. Differences between this CRF A2 alignment may be compared to the A1 alignment shown in Fig. 3.II.6.

Figure 3.II.10. Alignment of 5,6-QDC with pharmacophore model



A schematic depicting how 5,6-QDC was aligned to the pharmacophore model. Alignment of 5,6-QDC was straightforward with all four identified areas corresponding with defined regions of the pharmacophore model shown in Fig 3.II.3.

Figure 3.II.11. Alignment of VGLUT pharmacophore model with 5,6-QDC



Alignment of VGLUT pharmacophore model and 5,6-QDC (orange) performed as described in the text. Conformational space searching resulted in 17 5,6-QDC conformers. The strain energy range of conformer was 10.36-12.92 Kcal/mol. The strain energy of the conformer used in the alignment was 11.18 Kcal/mol. The ligand conformers were superpositioned with a 1 cal spring constant.

With respect to ligand-binding interactions, the development of a substrate-binding pharmacophore model may be helpful in discerning structural elements necessary for transport. A larger set of diverse known substrates is needed before the development of a substrate pharmacophore model may be implemented.

Section III: Influence of neuroactive steroids and related compounds on ³H-L-glutamate efflux from synaptic vesicles

Introduction

Synaptic vesicles isolated by variable speed centrifugation and gel filtration contained lower levels of L-glutamate than would be expected in an organelle involved in classical Ca²⁺-dependent neurotransmitter presynaptic release (De Belleruche and Bradford, 1973). While these low levels of glutamate observed led to the suggestion that the amino acid could be released from cytosolic stores, it was not appreciated at the time that the low levels actually represented loss of glutamate from synaptic vesicles. The issue of whether glutamate was released from synaptic vesicles or cytosolic pools was resolved when transmission electron microscopy (TEM) images showing immunolabeled L-glutamate in synaptic vesicles were reported (Storm-Mathisen et al., 1983). Further, numerous studies had shown that the accumulation of glutamate into synaptic vesicles occurred in the presence of ATP (Maycox et al., 1988; Naito and Ueda, 1983; Naito and Ueda, 1985). As previously discussed, ATP is necessary to generate the electrochemical gradient which promotes the accumulation of glutamate into synaptic vesicles. The electrochemical gradient established by ATP for the uptake of glutamate may also be necessary for the retention of glutamate in the synaptic vesicles, thus the lack of ATP in the synaptic vesicle isolations proved to be the reason for the low levels of glutamate. Consistent with this conclusion, the addition of ATP to synaptic vesicle isolation buffer prevented the loss of the amino acid. The same effect could be achieved by the addition

of N-ethylmaleimide (NEM)(Burger et al., 1989), presumably by interfering with a sulfhydryl group on the protein.

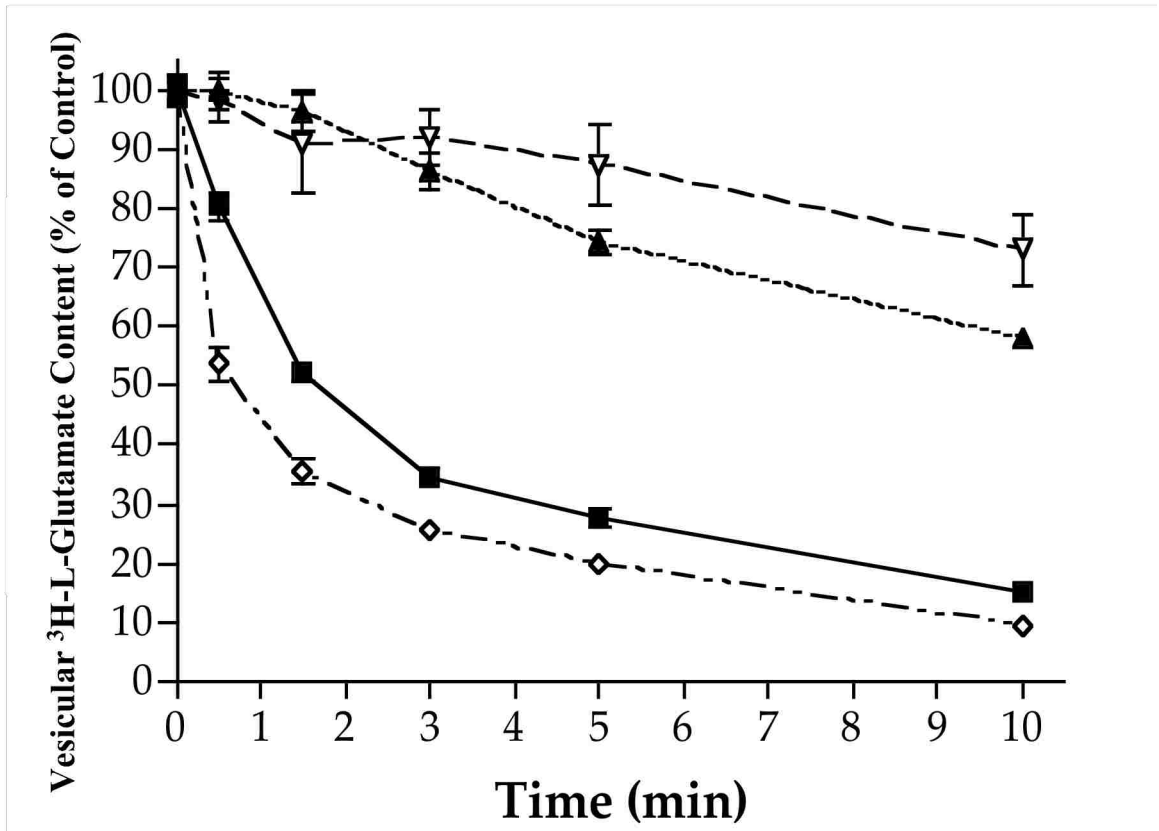
In addition to the dependence on the electrochemical gradient, vesicular glutamate uptake is also affected by the concentration gradient between the intra- and extravesicular space. When synaptic vesicles equilibrated with ^3H -L-glutamate are diluted into a volume large enough to prevent reuptake of the radiolabel to an insignificant level, a net efflux of the tritiated amino acid was observed (Carlson and Ueda, 1990; Wang and Floor, 1994). This net efflux was presumed to be transporter mediated, because it could be attenuated by either low temperature or the addition of NEM. If the assumption that both uptake and efflux occur through the same transporter in a bidirectional manner is in fact true, it is possible that the presence of nonradiolabeled L-glutamate in the dilution buffer could result in an apparent increase in the amounts of glutamate exiting the vesicles via the process of *trans*-stimulation. The phenomena of *trans*-stimulation has been previously shown to occur in other transport systems, including synaptic vesicles loaded with [^3H]dopamine (DA) (Christensen, 1975). *Trans*-stimulation is a process (to be more thoroughly explained later in the discussion), which involves the exchange of substrates, rather than the net movement in one direction.

Previous work in our lab suggested that a similar effect might also be observed with glutamatergic synaptic vesicles (Fig. 3.III.1). The addition of 20 mM L-glutamate (at $10\times K_M$) to synaptic vesicles previously equilibrated with ^3H -L-glutamate increased the rate of efflux beyond the levels that occur in the absence of added glutamate, indicating

the occurrence of *trans*-stimulation. It is possible to block efflux by including CR (previously identified as a non-substrate inhibitor by R. Bartlett, (Bartlett, 1999)) at $10 \times K_i$ with 20 mM glutamate. Efflux of $^3\text{H-L-glutamate}$ was also blocked at 0°C , consistent with a carrier-mediated event. Given these two effects, this assay can serve to rapidly screen competitive inhibitors for their activity as either alternative substrates or nonsubstrate inhibitors. Thus, nonsubstrate inhibitors bind to the transporter, lock the "alternative access" binding site in the external position and prevent efflux. On the other hand, alternative substrates still allow efflux to occur, albeit at possible slower rates than observed with L-glutamate. Compounds to be evaluated in this manner are added at a concentration that is 10 times the K_i value at VGLUT to ensure at least 90% occupancy of the transporter binding-site.

The findings reported in the previous two chapters indicate that PREGS, and 5,6-QDC are both competitive inhibitors. Assuming that these compounds bind as is typical of competitive inhibitors, raises the possibility that the analogues may also act as alternative substrates of VGLUT. To address this possibility, these compounds were tested for their effect on the efflux of $^3\text{H-L-glutamate}$ from synaptic vesicles. A time-course of [^3H]-L-glutamate efflux, in the presence and absence of 3α , 5β -TH PROGS, was also conducted to more thoroughly characterize the effects of this molecule on efflux over time. Additionally, a mathematical model of efflux based on Michaelis-Menten kinetics was developed to aid in distinguishing between nonsubstrate inhibitors and partial substrates.

Figure 3.III.1. Effect of a nonsubstrate inhibitor and demonstration of *trans*-stimulation on vesicular $^3\text{H-L-glutamate}$ efflux



Experiments were carried out by loading synaptic vesicles with $^3\text{H-L-glutamate}$ for 5 min. Loaded vesicles were then diluted 20x with buffer for 5 min, including: 20 μM Congo red and 20 mM L-glutamate (∇), 2 μM Congo red (\blacktriangle), control (\blacksquare), 20 mM L-glutamate (\diamond), and terminated at the indicated times (150 mM KCl). Results represent the mean \pm SEM for $n = 6$ determinations. Total uptake values were determined after the 5 min preloading with $^3\text{H-L-glutamate}$, but prior to dilution. Competitive inhibitors are included in dilution buffer at 10x K_i (when indicated) to insure similar levels of binding occupancy at the transporter. Results from R. Bartlett (Bartlett, 1999).

Results

In addition to PREGS and 5,6-QDC, other potent neuroactive steroids were included in the dilution assay to test for their ability to act as alternative substrates at VGLUT. As previously described for uptake, synaptic vesicles were pre-incubated for 5 min for temperature equilibration. Subsequently, ^3H -L-glutamate [250 μM] was added to the vesicular mixture and uptake was allowed to proceed for 5 minutes prior to a 20-fold (0.100 ml: 2.000 ml) dilution in assay buffer. Where indicated, an identified competitive inhibitor was included in the dilution with the assay buffer at a concentration 10x its estimated K_i value. This was done to ensure a similar level of binding occupancy at about 90%. The assay was terminated 5 minutes later, after which the radiolabel remaining in the vesicles was determined in the same manner as uptake assays.

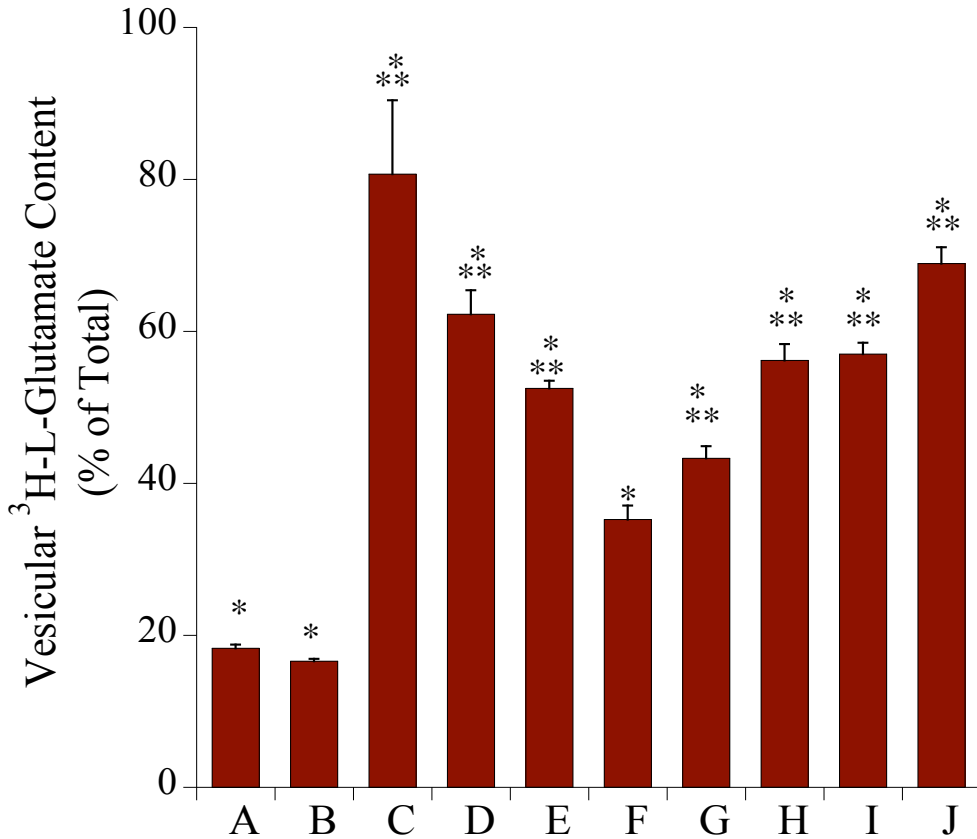
Consistent with the time-course, the inclusion of CR (2 μM) essentially abolished the efflux of [^3H]-L-glutamate from the synaptic vesicles when measured at 3 min (Fig. 3.III,1). The amount retained in the synaptic vesicles, in the presence of CR, was not significantly different from the efflux quantified at 0° C (Bartlett, 1999). In contrast, when the known VGLUT substrate, *trans*-ACPD, was included in the dilution buffer, [^3H]-L-glutamate efflux proceeded to a much greater degree, with only 35% of the radiolabel retained in the vesicles after 3 minutes. When the other compounds of interest were tested in this manner, the level of efflux fell between that of Congo red and *trans*-ACPD. More specifically, the amount of radiolabel that remained in vesicles in the presence CSB, DHEAS, PREGS, pregnanolone sulfate ($3\alpha,5\beta$ -TH PROGS), and 5,6-

QDC was 62.3%, 68.9%, 57.0%, 56.2%, and 43.3% respectively (Fig. 3.III.2). Interestingly, levels of radiolabeled L-glutamate, present in vesicles, when 5,6-QDC was being assayed were close to those of *trans*-ACPD. Previous research has directly shown *trans*-ACPD to be a substrate of VGLUT (Winter, 1993). While the structure of 5,6-QDC and that of *trans*-ACPD differ, their similar effects on glutamate efflux would suggest that 5,6-QDC is also a partial substrate.

To further investigate the data generated at a single time point, a more detailed time-course was carried out to examine L-glutamate efflux in the presence of 3 α ,5 β -TH PROGS (Fig. 3.III.3). Over the ten minute time course, 3 α ,5 β -TH PROGS produced an efflux of glutamate that was slower (more [³H]-L-glutamate retained in the vesicles) than in the absence of the inhibitor, but still faster than levels of efflux observed in the presence of a nonsubstrate inhibitor or at 0° C. Examination of the time course revealed that the efflux was not linear and that the difference between CR and 3 α ,5 β -TH PROGS was greater at the 1.5, 3 and 5 min time points. An additional analysis was also made based upon the rate of efflux during the first 30 sec, with the expectation that this might best represent the initial rate of efflux. The rates of CR and 3 α ,5 β -TH PROGS were, however, not significantly different, potentially due dilution artifacts at this time point (e.g., broken vesicles).

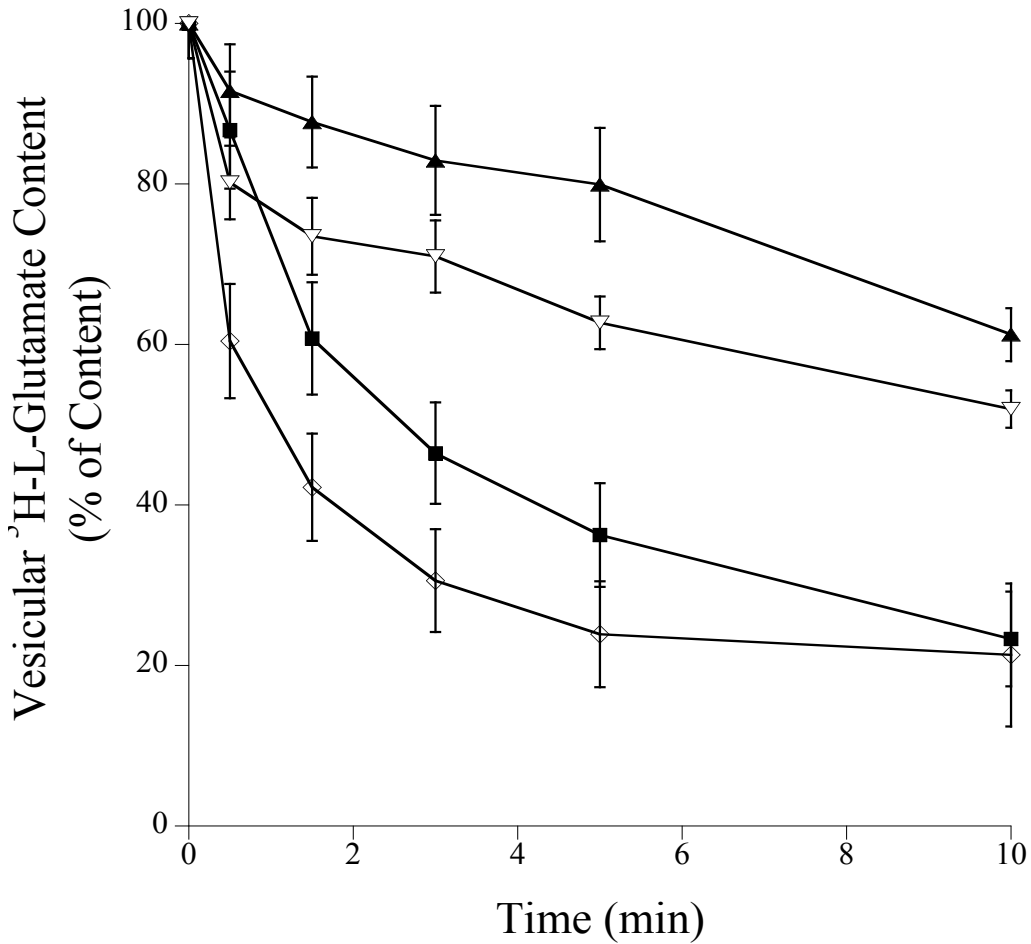
To further analyze this data, a simulation, based on Michaelis-Menten kinetics, was conducted in collaboration with Dr. Emily Stone (Fig. 3.III.4). This simulation was based on a fit describing the curve of ³H-L-glutamate efflux over time.

Figure 3.III.2. Demonstration of the effect of VGLUT inhibitors on ³H-L-glutamate efflux from synaptic vesicles



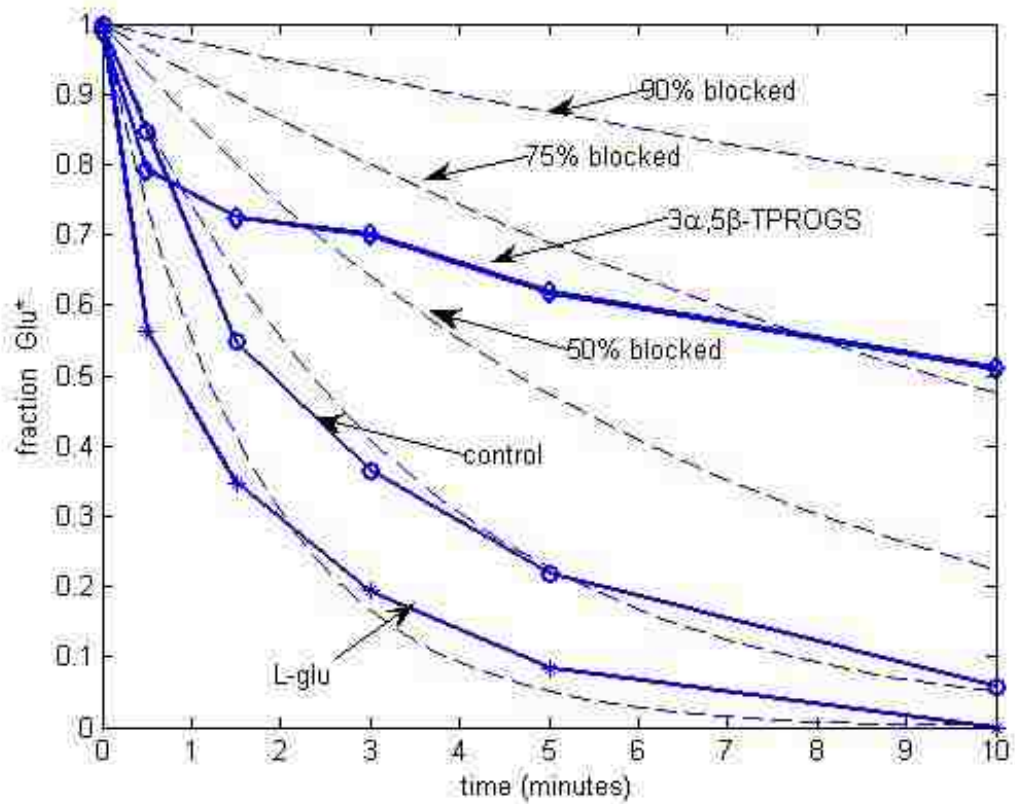
Efflux levels may be indicative of substrate activity (A) Control; (B) 20 mM L-glutamate; (C) 5 μ M Congo red; (D) 2 μ M Chicago sky blue (CSB); (E) 2 mM xanthurenic acid; (F) 5 mM *trans*-ACPD; (G) 670 μ M 5,6-naphthyl-QDC; (H) 262 μ M pregnanolone sulfate; (I) 627 μ M pregnenolone sulfate; (J) 540 μ M DHEAS. Results represent the mean \pm SEM for $n = 3$ determinations. Total uptake values (7.34 ± 0.08) were determined after 5 min of preloading, but before dilution. Efflux was terminated at 3 min. Statistical tests were performed with a one-way ANOVA followed by Tukey's multiple comparison. * and ** represent $p < 0.05$ for differences from total uptake and control, respectively.

Figure 3.III.3. Effect of a partial substrate on vesicular $^3\text{H-L-glutamate}$ efflux



Experiments were carried out by loading synaptic vesicles with $^3\text{H-L-glutamate}$ for 5 min. Loaded vesicles were then diluted 20x with buffer for 5 min, including: 262 μM 3 α , 5 β -TH PROGS (∇), 2 μM Congo red (\blacktriangle), control (\blacksquare), 20 mM L-glutamate (\diamond), and terminated at the indicated times (150 mM KCl). Results represent the mean \pm SEM for $n = 6$ determinations. Total uptake values (3.73 ± 0.2) nmol/mg protein) were determined after the 5 min preloading with $^3\text{H-L-glutamate}$, but prior to dilution. Competitive inhibitors are included in dilution buffer at 10x K_i (when indicated) to insure similar levels of binding occupancy at the transporter.

Figure 3.III.4. Mathematical simulation of L-glutamate efflux from synaptic vesicles



A simulation of L-glutamate efflux from synaptic vesicles was developed utilizing Michaelis-Menten kinetics in collaboration with Dr. E. Stone. Rate constants were approximated as K_{ON} , $10^7 \text{ sec}^{-1} \text{ M}^{-1}$, K_{OFF} , 2000 sec^{-1} , and transport, 2000 sec^{-1} . It was assumed that there were 2000 molecules of glutamate per transporter.

Hypothetical microconstants of the simulation were as follows: K_{ON} , $10^7 \text{ sec}^{-1} \text{ M}^{-1}$; K_{OFF} , 2000 sec^{-1} ; transport, 2000 sec^{-1} ; transporter: glutamate, 1:2000. As these values are not known for glutamate, K_{ON} , K_{OFF} , and transport numbers were estimated from EAAT3 calculated constants (M. Kavanaugh, personal communication). Similarly, the ratio of transporter to glutamate molecule was estimated assuming one transporter per vesicle and a vesicular content of approximately 2000 glutamate molecules (Daniels et al., 2006). The simulated curves were similar to experimentally derived ones. A curve generated to theoretically replicate efflux with 90% of available transporters blocked was also similar to the experimentally derived curve in the presence of CR (Fig 3.III.3). Curves simulating a block of 25% and 50% of available transporters were also generated. A compound, which influences efflux in such a way that the resulting vesicular content is lower than the simulation (with 90% of the transporters are blocked), would be presumed to be a partial substrate. The curve with $3\alpha,5\beta$ -TH PROGS was different than predicted of a straight-forward nonsubstrate inhibitor, and consistent with the uptake of this compound.

While this simulation suggests that $3\alpha,5\beta$ -TH PROGS and similar compounds can act as partial substrates at VGLUT, it remains to be directly confirmed. Utilizing radiolabeled compounds is the gold standard for this type of analysis; however, it is cost- and time-intensive. This exchange protocol, however, provides an efficient initial screen for potential alternative substrates. Upon identification of alternative substrates, compounds would be confirmed through direct tests, i.e. radiolabeled compounds. Furthering our understanding of the characteristics necessary for transport through the VGLUTs holds

particular allure, because of the potential to identify molecules that could then be delivered to receptors via presynaptic release. This may be useful for both experimental protocols and for therapeutic use in a clinic. Similarly, the presynaptic release of a neuroactive steroid may describe the endogenous mode of delivery for these molecules.

Section IV: Specificity of sulfated neuroactive steroids and related compounds at other sites on the synaptic vesicle

Introduction

Standard kinetic assays of PREGS, CR and 5,6-QDC have revealed that these compounds inhibit vesicular glutamate uptake in a manner consistent with a competitive mechanism. To be more exact, the results demonstrate that binding of the competitive inhibitor and L-glutamate is mutually exclusive, i.e., that only one can be bound at any one time. Moreover, models depicting the fits of PREGS, CR, and 5,6-QDC are consistent with the conclusion that these molecules, like L-glutamate, fit within the VGLUT pharmacophore. Finally, exchange studies suggest that PREGS and 5,6-QDC are partial substrates, which would only be expected of competitive inhibitors, i.e. compounds, which bind at the substrate binding-domains. Taken together, these studies provide evidence that the compounds block VGLUT uptake by binding to the substrate binding domains. Even if this is the case, it seemed prudent to investigate whether or not these compounds may have a second site of action.

As previously discussed, vesicular glutamate uptake is driven by an electrochemical gradient generated by the hydrolysis of ATP. The enzyme that catalyzes this hydrolysis, V-ATPase, is specific to synaptic vesicles. The V-ATPase can be distinguished from other ATPases, i.e. F₀/F₁-ATPase, E₀/E₁-ATPase, by its sensitivity to N-ethylmaleimide (NEM) and insensitivity to Oligomycin B and vanadate (Cidon and Sihra, 1989). The transport of protons into the vesicular lumen by the V-ATPase serves to establish a pH

gradient (ΔpH) between the vesicle lumen ($\sim\text{pH } 6.8$) and the extravesicular space ($\sim\text{pH } 7.4$). Likewise, the proton transport establishes an electrical gradient ($\Delta\Psi$) across the vesicular membrane with an inside positive and outside negative.

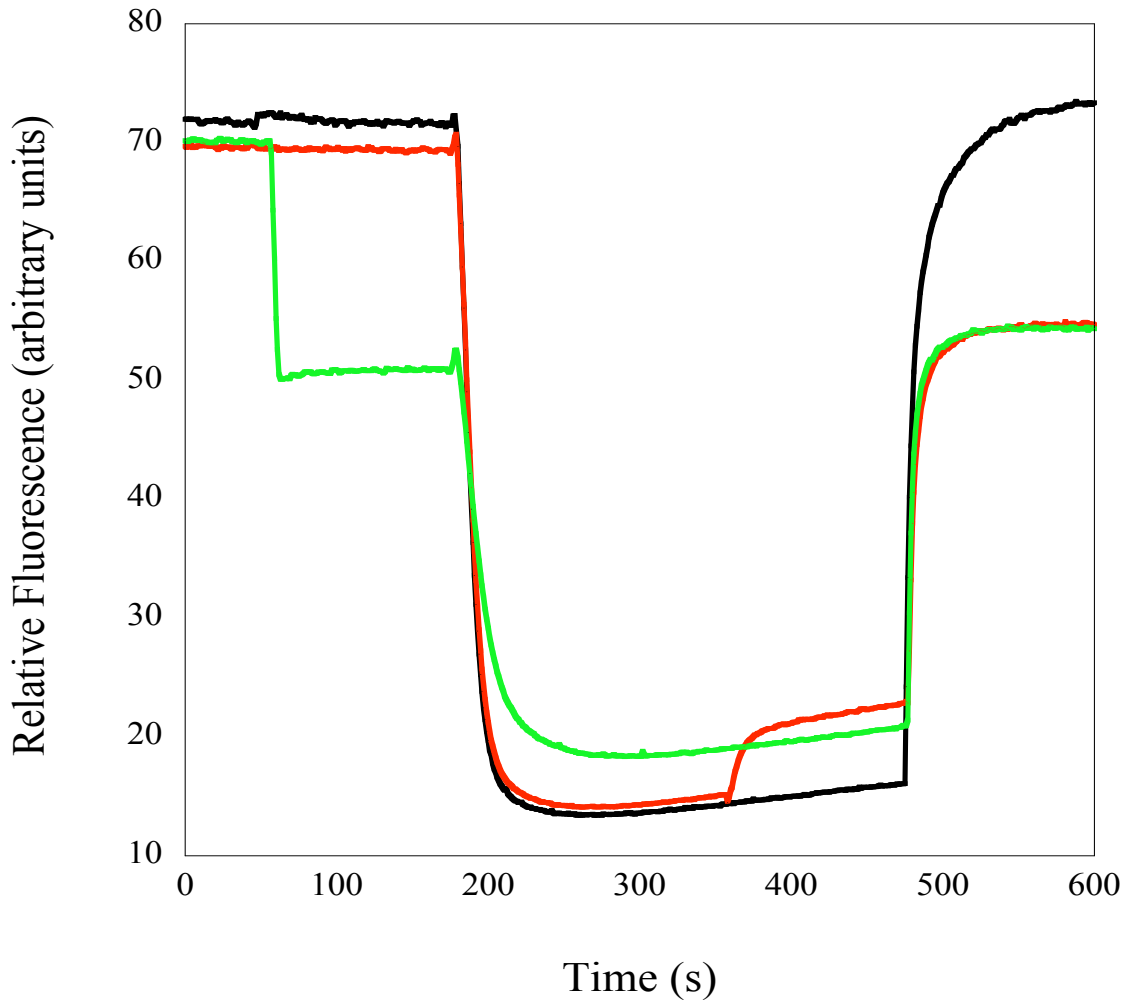
The driving forces necessary for sequestration of neurotransmitter into synaptic vesicles are favorable due to one or both of the electrical or chemical gradients. The uptake of ACh and monoamines is dependent primarily on the pH gradient, resulting from the antiport of two protons for one molecule of substrate (Parsons, 2000). GABA and glycine uptake are dependent on the pH gradient and the electrical component, as well as the antiport of one proton per GABA molecule. Additional studies indicate that uptake of GABA into synaptic vesicles is inhibited by 50% if either the ΔpH or $\Delta\Psi$ is inhibited (McIntire et al., 1997). On the other hand, the primary driving force of glutamate sequestration into synaptic vesicles is presumed to be the $\Delta\Psi$ (Maycox et al., 1988). Clearly, alterations of either the membrane potential or proton gradient could potentially affect glutamate uptake. For this reason, the compounds were assayed for their effect on the electrochemical gradient.

Experiments were conducted with fluorescent dyes capable of measuring $\Delta\Psi$. The voltage-sensitive dye oxonol V (OXV) was used to measure any changes in the electrical gradient established by the V-ATPase. Similarly, acridine orange (AO) was used to measure changes in the pH gradient. The addition of ATP causes a quenching in the baseline fluorescence of the indicator dye (i.e., AO, OXV) as the $\Delta\mu_{\text{H}^+}$ is generated. Any changes in the quenching of the dye would be consistent with a change in the $\Delta\Psi$.

Results

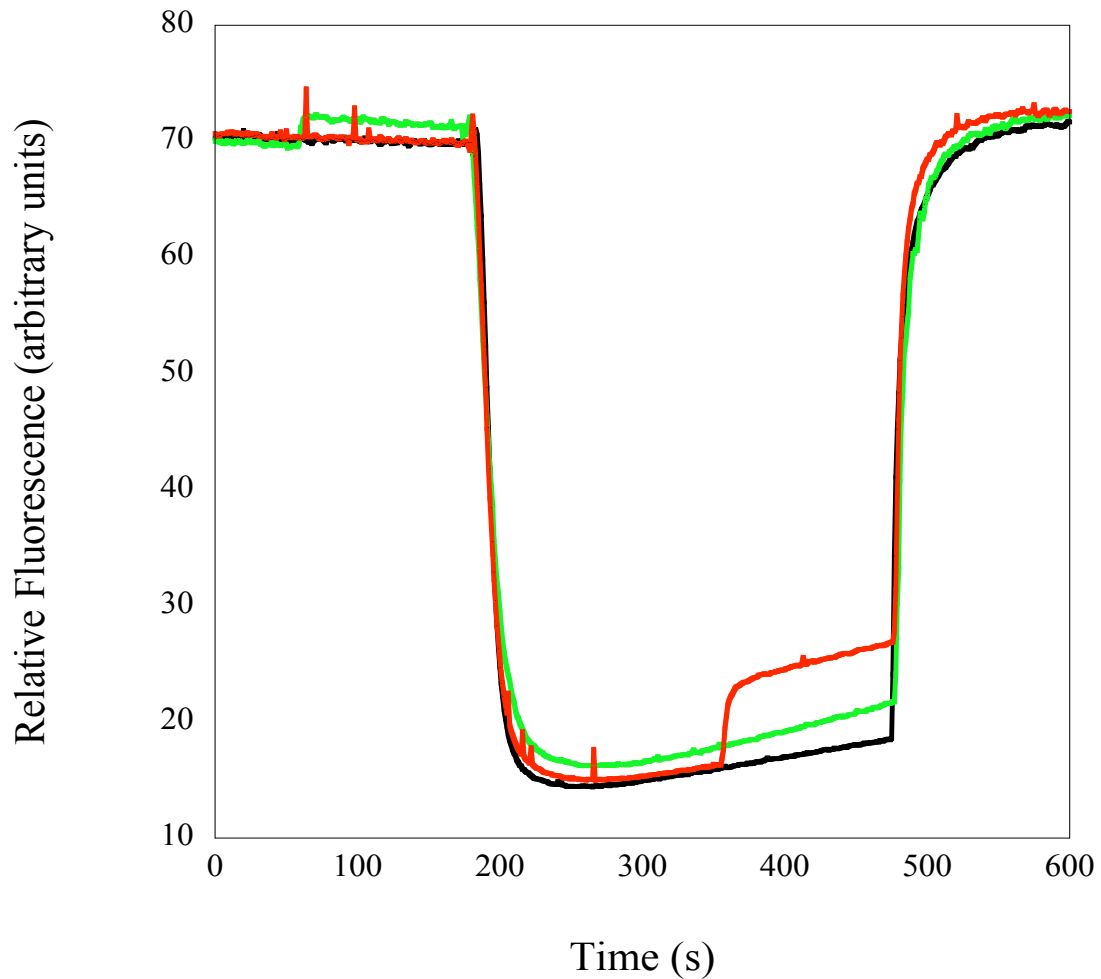
The proton gradient was measured by monitoring the changes of acridine orange fluorescence at an excitation wavelength of 492 nm and an emission wavelength of 520 nm. Thirty microliters of protein (100-150 μg) were added to 2 mL of KCl assay buffer (10 mM HEPES/KOH (pH 7.4), 4 mM KCl, 4 mM MgSO_4) and 2 μL of acridine orange (10 μM). This mixture was allowed to preincubate for 5 minutes at 37°C while stirring. After five minutes of preincubation, fluorescence measurements were started. The generation of the proton gradient was initiated by adding 25 μL of ATP (2 mM) directly into the cuvette. The generation of the proton gradient produces a rapid quenching of acridine orange fluorescence. Compounds of interest were added at either 60 sec or 360 sec. Only a slight reduction of fluorescence was evident after the addition of 5,6-QDC to the cuvette (Fig. 3.IV.1). Part of the reduction in fluorescence was most likely due to a direct interaction of 5,6-QDC and acridine. Thus, when the absorption, emission, and excitation spectra of acridine orange were assessed, in the presence and absence of 5,6-QDC, a direct interaction was evident (data not shown). PREGS demonstrated little if no effect to the pH gradient when added at 60 sec (Fig. 3.IV.2). Addition at 360 sec with PREGS produced a slight decrease in fluorescence quench (Fig. 3.IV.2). Overall, these results indicate only a slight affect of 5,6-QDC and PREGS on the pH gradient, and this suggests that these compounds did not interfere with [^3H]-L-glutamate uptake as a consequence of disrupting the pH gradient. While evidence suggests that CR is a competitive inhibitor, it should be noted that similar experiments were not reported due to a significant quench of the fluorescence signal as the result of an interaction between CR

Figure 3.IV.1. Effect of 5,6-QDC on the proton gradient generated by a V-ATPase in synaptic vesicles.



An overlay of a control trace (black line) with a 5,6-QDC added at 60 sec (green line) and 360 sec (red line) from three representative trials. Each trace was performed $n \geq 3$. The proton gradient was measured with acridine orange at an excitation wavelength of 492 nm and an emission wavelength of 520 nm. Fluorescence intensity was measured for 10 minutes. The ATP was added at 180 sec. Generation of the membrane potential was terminated with the addition of a protonophore (CCCP) at 480 sec.

Figure 3.IV.2. Effect of PREGS on the proton gradient generated by a V-ATPase in synaptic vesicles.



An overlay of a control trace (black line) with a PREGS added at 60 sec (green line) and 360 sec (red) from three representative trials. Each trace was performed $n \geq 3$. The pH gradient was measured with acridine orange at an excitation wavelength of 617 nm and an emission wavelength of 643 nm. Fluorescence intensity was measured for 10 minutes. The ATP was added at 180 sec. Generation of the membrane potential was terminated with the addition of a protonophore (CCCP) at 480 sec.

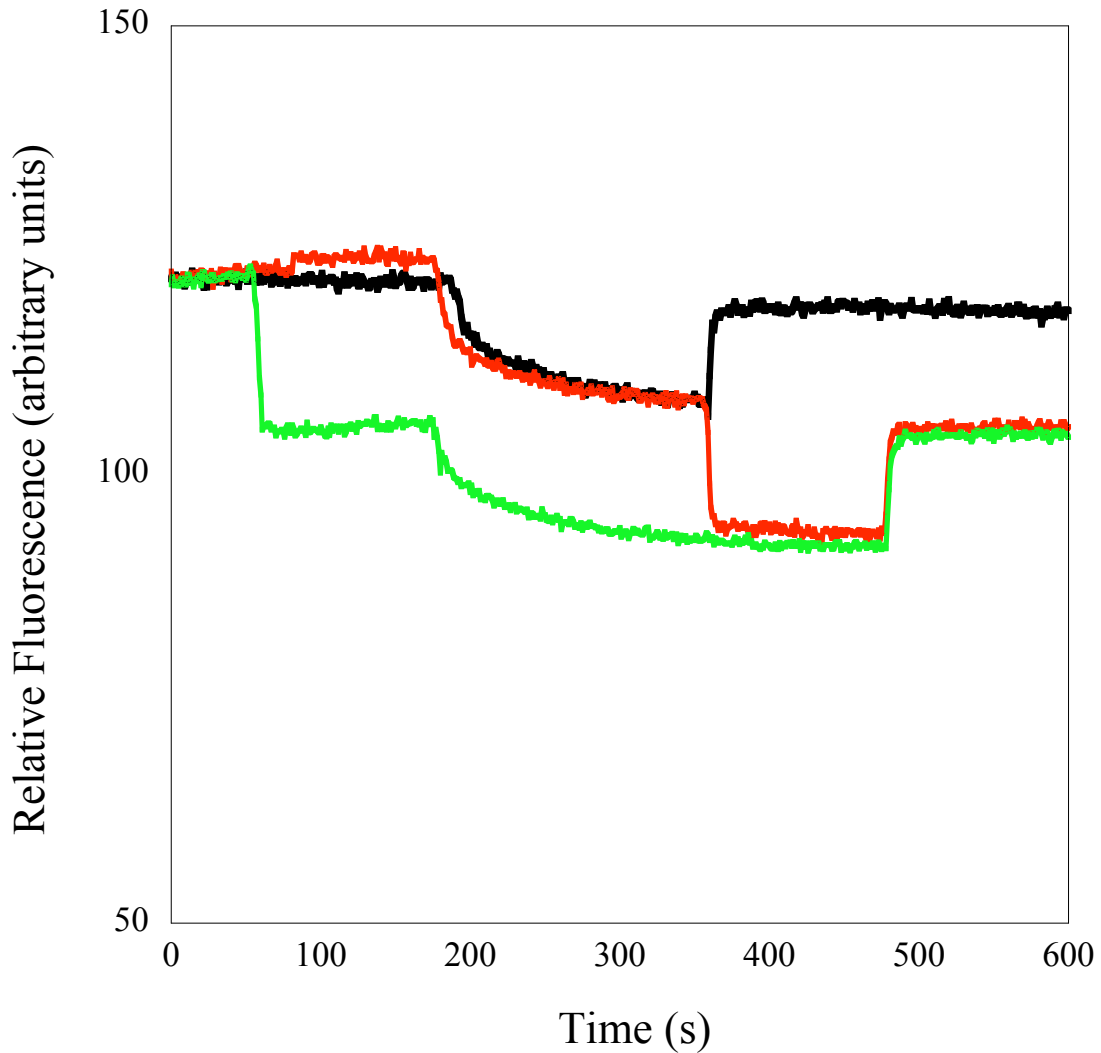
acridine orange.

A similar series of experiments were conducted to measure the membrane potential in the presence and absence of 5,6-QDC and PREGS. The addition of 5,6-QDC produced an immediate quench of fluorescence of about 25 units. However, upon the addition of ATP, a similar relative amount of quench was observed to occur as in the control (Fig. 3.IV.3). A similar effect of 5,6-QDC could be seen if it was added at 360 sec. The protonophore, CCCP, was added to disrupt the membrane potential and terminate individual experiments. Interestingly, the source of additional quench was not revealed in parallel studies in which 5,6-QDC was tested on the spectra of oxonol V.

In contrast to a quench, the addition of PREGS produced an increase in fluorescence. Once again, quench of the signal occurred, rapidly following the addition of ATP. The increase in fluorescence was also observed when PREGS was added at 360 sec. Addition of PREGS at 60 sec reveals a slight loss in membrane potential fluorescence signal in the range examined (550-750 nm). When the disturbances to these signals are subtracted, there seems to be only a minor effect on the maintenance of the membrane potential, in the case of PREGS (Fig 3.IV.4). An absorbance spectrum of oxonol V was included to illustrate that the dye was not defective (Fig. 3.IV.5).

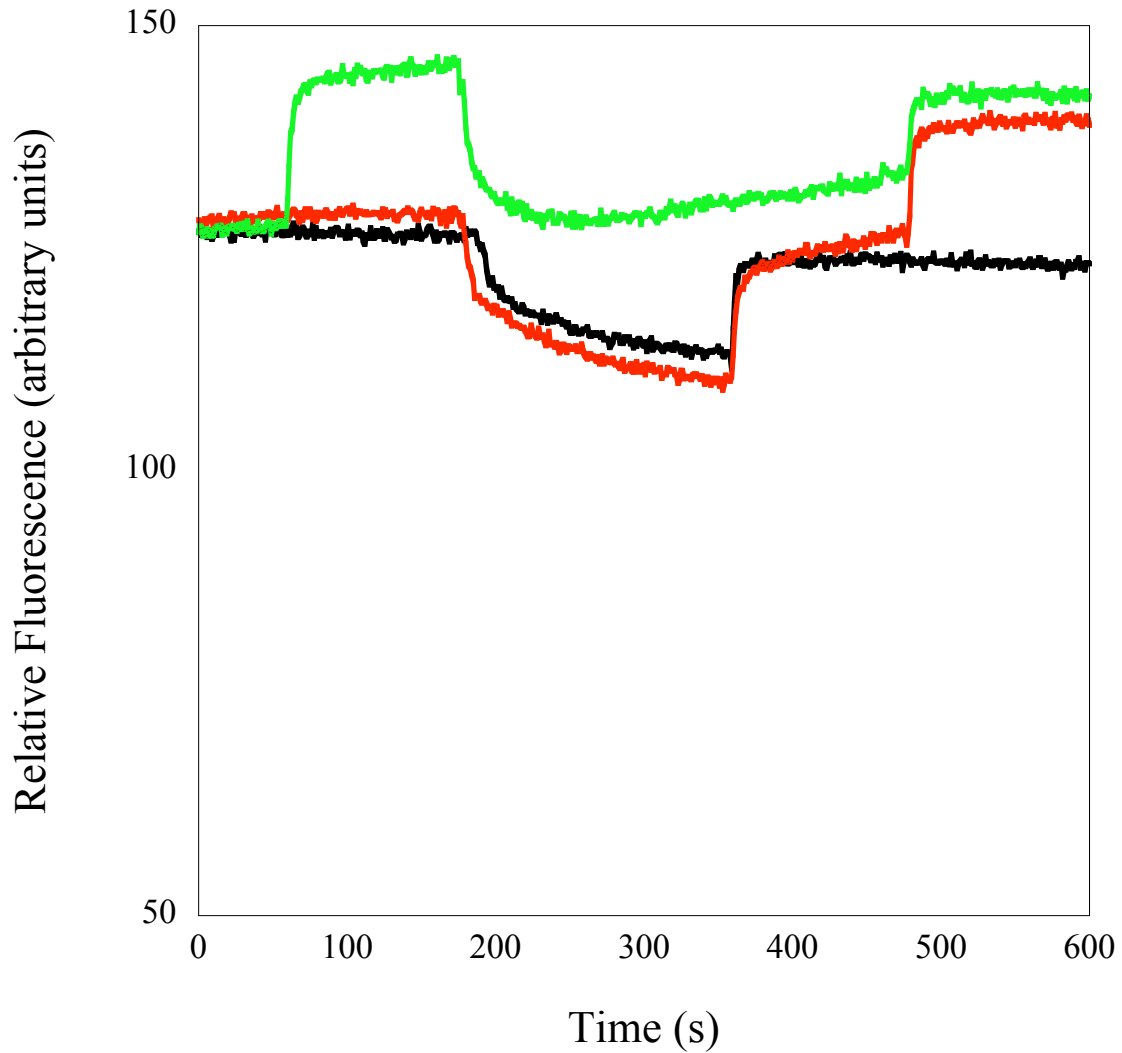
These results indicate that at the concentration tested, PREGS and 5,6-QDC had little effect on the membrane potential and proton gradient. In the instance of PREGS, this compound was included at a concentration of 90 μM , which was roughly equivalent to its

Figure 3.IV.3. Effect of 5,6-QDC on the membrane potential generated by a V-ATPase on synaptic vesicles.



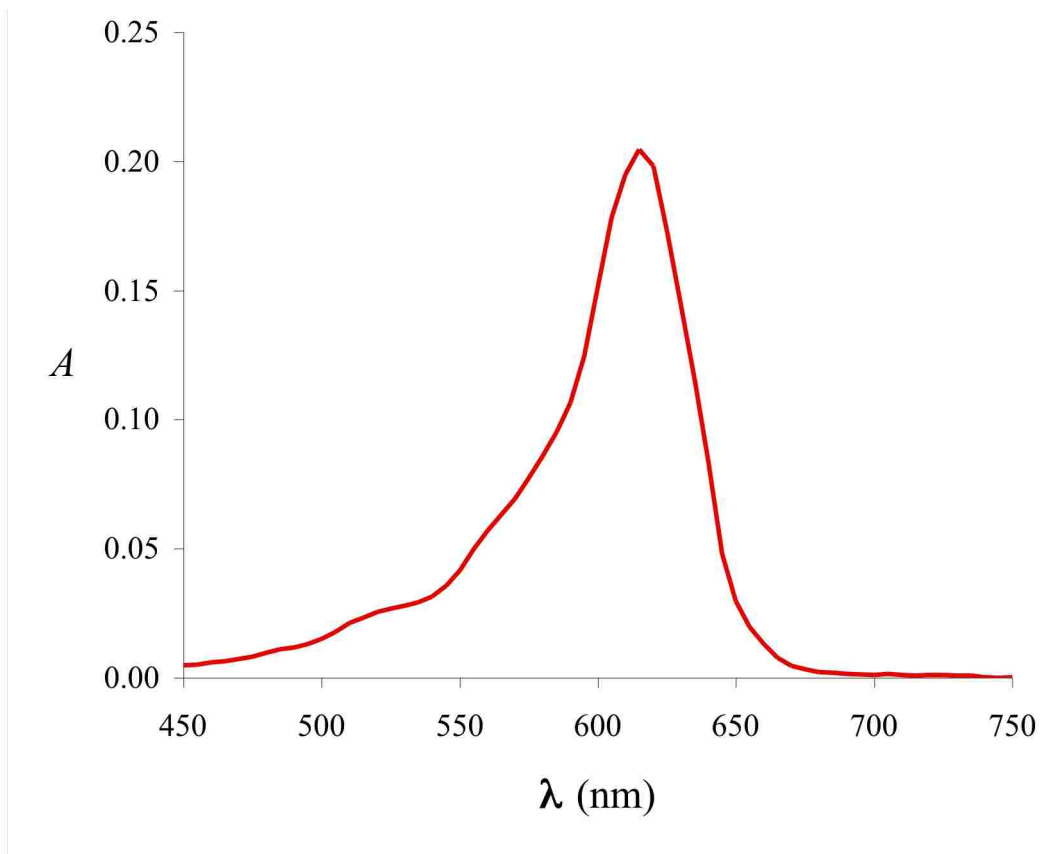
An overlay of a control trace (black line) with a 5,6-QDC added at 60 sec (green line) and 360 sec (red line) from three representative trials. Each trace was performed $n \geq 3$. Membrane potential was measured with oxonol V at an excitation wavelength of 617 nm and an emission wavelength of 643 nm. Fluorescence intensity was measured for 10 minutes. The ATP was added at 180 sec. Generation of the membrane potential was terminated with the addition of a protonophore (CCCP) at 480 sec.

Figure 3.IV.4. Effect of PREGS on the membrane potential generated by a V-ATPase on synaptic vesicles.



An overlay of a control trace (black line) with a PREGS added at 60 sec (green line) and 360 sec (red line) from three representative trials. Each trace was performed $n \geq 3$. Membrane potential was measured with oxonol V at an excitation wavelength of 617 nm and an emission wavelength of 643 nm. Fluorescence intensity was measured for 10 minutes. The ATP was added at 180 sec. Generation of the membrane potential was terminated with the addition of a protonophore (CCCP) at 480 sec.

Figure 3.IV.5. Absorbance spectrum of Oxonol V



The absorbance spectrum of oxonol V (10 μ M) in assay buffer (0.320 mM Sucrose, 10 mM HEPES/KOH (pH 7.4), 4 mM KCl, 4 mM MgSO₄) reveals a λ_{\max} at 615 nm.

predicted K_i value. Likewise, the K_i of 5,6-QDC was included at 70 μM , again roughly equivalent to its respective K_i . Although it would be prudent to evaluate the effects of PREGS and 5,6-QDC at a high concentration, such experiments may be problematic, due to the direct influence on the fluorescence properties of the included compounds on the electrochemical gradient. Despite this potential complication, they are still considered VGLUT inhibitors. Another complexity of the measurement is the heterogeneity of the vesicle preparation, thereby making it difficult to definitively assess the affect of these compounds on the electrochemical gradient selectively on the glutamate containing vesicles. Establishing a method to either isolate VGLUT vesicles or reconstituting functional vesicles with VGLUT would provide a more reliable system.

Section V: Specificity of sulfated neuroactive steroids and related compounds at other vesicular transporters (i.e. VMAT, VGAT)

Introduction

Each neurotransmitter in the CNS has an associated transporter that mediates its uptake into synaptic vesicles, i.e. vesicular GABA transporter (VGAT), vesicular acetylcholine transporter (VAChT), vesicular monoamine transporter (VMAT), etc. These transporters exhibit distinct specificities and have kinetic properties that generally correlate with the intracellular concentrations of the respective ligand. For instance, VGAT and VGLUT have K_M values in the millimolar range, corresponding with the demonstrated intracellular concentrations of glutamate and GABA (Schousboe, 1981). Likewise, the vesicular monoamine transporter (VMAT), which transports serotonin, dopamine, and norepinephrine, has a K_M value in the nanomolar range to facilitate effective sequestration of low intracellular concentrations of monoamines (Squire et al., 2002).

VGLUT and VGAT tend to be specific for endogenous substrates, particularly when compared to the plasma membrane transporter counterparts. For example, the glutamate plasma membrane transporters (i.e. EAATs), which have a K_M value in the micromolar range, translocate L-glutamate, D- and L-aspartate; whereas, VGLUT translocates L-glutamate, but neither D- nor L-aspartate. VMAT, on the other hand, appears to be less specific. VMAT is able to transport a number of biogenic amines, including tyramine, tryptamine and amphetamines. The specificity of the neurotransmitter transported into monoaminergic vesicles apparently conferred by at least two characteristics: the contents

of vesicle and the presence of specific synthetic enzymes (i.e., Tyrosine hydroxylase, aromatic L-amino acid decarboxylase, etc.). Serotonin (5HT) vesicles differ from catecholaminergic (CA) vesicles in that CA vesicles contain ATP, and 5HT vesicles contain serotonin-binding protein (SBP). Serotonin-binding protein binds to serotonin with high-affinity and specificity, serving to retain serotonin in synaptic vesicles. In contrast, dopamine- β -hydroxylase is present in noradrenergic vesicles (Coyle and Kuhar, 1974).

As previously discussed, Congo red, PREGS, and 5,6-QDC have been shown to be competitive inhibitors, as well as their activity at other sites of VGLUT. The structural diversity of these compounds prompted us to investigate the activity of these compounds at other vesicular transporters. Assessing the specificity of these compounds may resolve a number of issues relevant to each class of inhibitors. For example, the QDCs represent one of the more potent classes of VGLUT inhibitors to result from a rational design effort. Assessing the possible activity at other vesicular transporters offers an opportunity for further characterization of specific VGLUT inhibitors that may be utilized as pharmacological probes physiological preparations. As for the neuroactive steroids, the elucidation of their physiological roles in the overall functioning of the CNS is still being investigated. Understanding which neuroactive steroids are active at what vesicular transporters may add new information to this newly emerging area of research. To begin to understand the specificity of the neuroactive steroids on vesicular uptake, a panel of compounds was tested against uptake by VMAT and VGAT.

Results

A number of neuroactive steroids and related compounds were tested for their ability to inhibit uptake into synaptic vesicles using the same protocol employed for the VGLUT studies. Synaptic vesicles were prepared from rat forebrain and assayed for the uptake of either 5-[³H]-hydroxytryptamine (serotonin) or γ -[³H]-aminobutyric acid (GABA). Tritiated substrate and ATP were incubated, with vesicles for 1.5 min, in the presence and absence of potential inhibitors following a 5 min temperature preincubation. The transport of tritiated substrate was terminated by the addition of ice-cold 150 mM potassium chloride (3x) onto filter paper under vacuum filtration and compounds were included at the indicated concentrations. Data is reported as percent of control (Table 3.V.1); thus, the lower the number, the greater the inhibition. Among the compounds tested, CR exhibited the highest degree of selectivity with respect to VGLUT, with approximately 100-fold greater activity at the L-glu transport system, than that of the other systems. When tested at 250 μ M, 5,6-QDC and 6-(4'-biphenyl)-QDC, appeared to be moderately selective for VGLUT (2-fold) in relation to the other vesicular transporters. Among the neuroactive steroids tested, 3 α ,5 β -TH PROGS showed the most activity at all three transporters, while DHEAS was most selective for VGLUT. To examine the activity in greater detail, the neuroactive steroids were also evaluated at 50 μ M (Table 3.V.1). At these lower concentrations, DHEAS appeared to have the greatest specificity for VGLUT with percent of control values of 57.1, 94.1, and 98.0 at VGLUT, VMAT, and VGAT, respectively. The least specific neuroactive steroids, 3 α ,5 α -TH

PROGS, exhibited similar levels of inhibition, e.g., 65.3, 61.9, and 70.8 at VGLUT, VMAT, and VGAT, respectively.

However, because these three vesicular transporters have K_M values that vary over a large range (mM vs. μ M), concentration-response analyses were carried out with PREGS, $3\alpha,5\alpha$ -TH PROGS, $3\alpha,5\beta$ -TH PROGS, and DHEAS at VMAT and VGAT over a range of concentrations that spanned the predicted K_i values (Fig. 3.V.1; Fig. 3.V.2). The IC_{50} values were determined and K_i values were estimated using the Cheng-Prusoff relationship (Cheng, 1973). Among the neuroactive steroids, the most potent inhibitor at VGLUT was $3\alpha,5\beta$ -TH PROGS with an estimated K_i value of 26.0 μ M (Table 3.V.2). On the contrary, PREGS was the least potent inhibitor with a K_i value of 107.4 (Table 3.V.2). Of particular note, the estimated K_i value of DHEAS was 54.0 μ M at VGLUT; whereas, the estimated K_i values for VMAT and VGAT were 2.74 mM and 1.29 mM, respectively (Table 3.V.2). Other neuroactive steroids had estimated K_i values that ranged from 26.0-162 μ M. Allopregnanolone sulfate had the greatest activity at VMAT, with an estimated K_i value of 28.0 μ M. The most potent compound identified for VGAT was $3\alpha,5\beta$ -TH PROGS with an estimated K_i value of 48.7 μ M. Kinetic values for the activity of PREGS at VGAT could not be determined due to the solubility limits of PREGS.

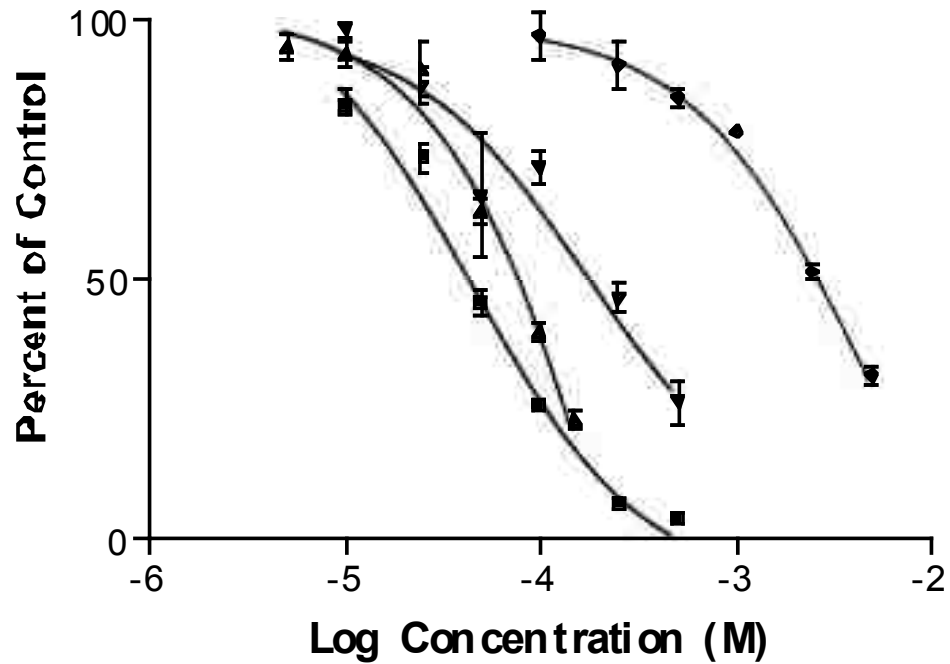
These experiments clearly demonstrate a variable degree of selectivity among the neuroactive steroids as vesicular transport inhibitors. The marked selectivity of DHEAS for VGLUT is interesting, considering the role of glutamate in excitotoxicity, and the

Table 3.V.1. Pharmacological specificity of neuroactive steroids.

Compound	VGLUT	VMAT	VGAT
PREG (250 μ M)	100 \pm 3.5	79.4(6) \pm 7.0	69.9(6) \pm 10.0
PREG (50 μ M)	100 \pm 11.1	106 \pm 11.4	99.3 \pm 8.2
PREGAc (250 μ M)	85.7 \pm 5.0	76.3	88.9 \pm 3.23
PREGS (250 μ M)	53.2 \pm 8.2	68.5(6) \pm 7.5	77.5(6) \pm 7.0
PREGS (50 μ M)	52.6 \pm 11.3	86.9 \pm 8.5	91.1 \pm 12.7
DHEAS (250 μ M)	23.2 \pm 3.2	63.7 \pm 5.1	84.6(2) \pm 22.3
DHEAS (50 μ M)	57.1 \pm 12.6	94.1 \pm 7.4	98.0 \pm 10.1
3 α ,5 β -TH PROGS (250 μ M)	14.6 \pm 3.8	20.7 \pm 2.1	22.3 \pm 4.3
3 α ,5 β -TH PROGS (50 μ M)	72.8 \pm 11.1	63.6 \pm 15.7	58.3 \pm 13.0
3 α ,5 α -TH PROGS (50 μ M)	65.3 \pm 17.1	94.1 \pm 7.4	70.8 \pm 10.9
5,6-QDC (100 μ M)	42*	79.8 \pm 11.0	69.9 \pm 10.0
6-[4']-QDC (100 μ M)	43*	68.1 \pm 7.7	79.4 \pm 3.9
QDC (100 μ M)	38.4 \pm 4.0	91.7 \pm 6.8	81.4 \pm 0.3
Congo Red (100 μ M)	0.55*	69.9 \pm 11.0	55.2 \pm 1.6

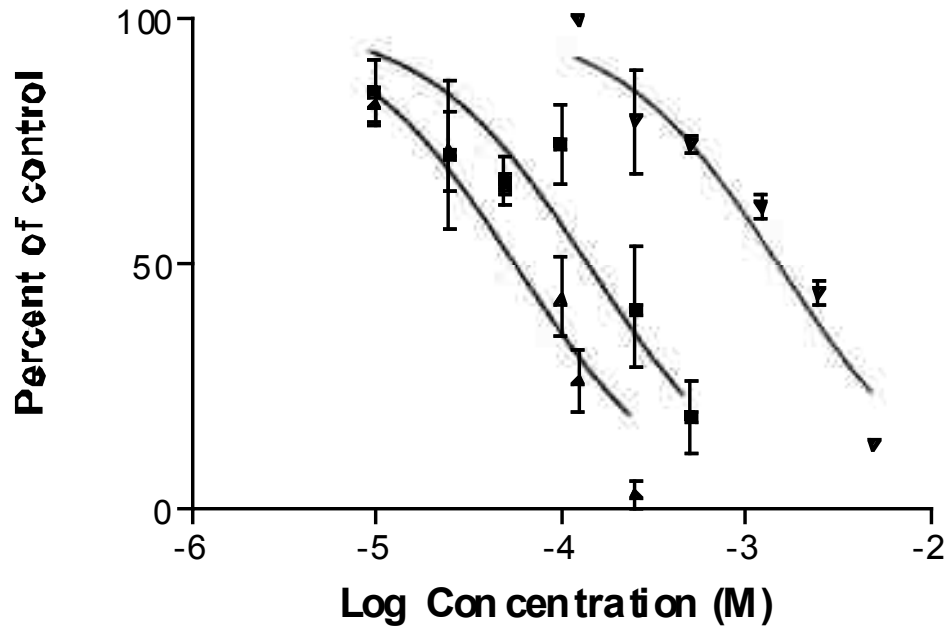
Percent of control values for active VGLUT inhibitors tested against VGAT and VMAT uptake. All data represents 3 experiments and is reported as percent of control \pm standard deviation. VMAT uptake was tested with 100 nM 5-hydroxy-[3 H]-tryptamine. Control uptake for VMAT was \sim 13 pmol/min/mg protein. VGAT uptake was tested with γ -[2,3- 3 H(N)]-aminobutyric acid with control uptake values of \sim 550 pmol/min/mg protein. * indicates estimated values.

Figure 3.V.1. Concentration-response analysis of PREGS, DHEAS, 3 α ,5 β -TH PROGS, and 3 α ,5 α -TH PROGS against vesicular ^3H -5HT uptake



Uptake of ^3H -5HT was performed as described in Chapter 2. Sulfated-neuroactive steroids were tested included in the assays over a range of concentrations. Data points represent mean \pm SEM for 3-4 experiments. Control values for ^3H -5HT uptake were 114.74 ± 25.31 pmol/min/mg protein for $n = 16$. Neuroactive steroids are represented by: 3 α ,5 α -TH PROGS, ■; 3 α ,5 β -TH PROGS, ▲; PREGS, ▼; and DHEAS, ◆.

Figure 3.V.2. Concentration-response analysis of DHEAS, 3 α ,5 β -TH PROGS, and 3 α ,5 α -TH PROGS for vesicular uptake of ^3H -GABA.



Uptake of ^3H -GABA was performed as described in Chapter 2. Sulfated-neuroactive steroids were tested included in the assays over a range of concentrations. Data points represent mean \pm SEM for 3-4 experiments. Control values for ^3H -GABA uptake were 459.49 ± 42.21 pmol/min/mg protein for $n = 12$. Neuroactive steroids are represented by: 3 α ,5 α -TH PROGS, ■; 3 α ,5 β -TH PROGS, ▲; and DHEAS, ◆.

Table 3.V.2. Pharmacological specificity of sulfated-neuroactive steroids as inhibitors of VGLUT, VMAT and VGAT

Compound	IC ₅₀ (nM)	K _i (nM)
VGLUT		
PREGS	159.1 ± 9.8	107.1 ± 21.5
DHEAS	60.8 ± 5.6	54.0 ± 5.0
3 α ,5 α THPROG S	29.3 ± 2.3	26.0 ± 2.0
3 α ,5 β THPROGS	45.0 ± 7.9	40.0 ± 7.0
VMAT		
PREGS	180.4 ± 17.7	108.2 ± 10.6
DHEAS	4573.0 ± 209.4	2744.0 ± 125.7
3 α ,5 α THPROG S	269.4 ± 29.1	161.6 ± 17.5
3 α ,5 β THPROGS	46.7 ± 1.5	28.0 ± 1.0
VGAT		
PREGS	n.d.*	n.d.*
DHEAS	1600.0 ± 41.6	1280 ± 33.3
3 α ,5 α THPROG S	60.9 ± 1.2	48.7 ± 1.0
3 α ,5 β THPROGS	150.9 ± 4.1	120.7 ± 3.3

The transport of [³H]-L-glutamate (250 μ M), [³H]-5HT (100 nM), and [³H]-GABA (250 μ M) into synaptic vesicles was performed as described in Chapter 2. IC₅₀ values were generated on GraphPad Prizm Software with nonlinear curve fitting, assuming a one-site binding model. K_i values (\pm SEM) were calculated utilizing the Cheng-Prusoff equation in at least three independent experiments. Control values for ³H-5HT uptake were 114.74 \pm 25.31 pmol/min/mg protein for *n* = 16. Control values for ³H-GABA uptake were 459.49 \pm 42.21 pmol/min/mg protein for *n* = 12. K_i values were only determined for active compounds. *PREGS inhibitory values could not be tested at VGAT due to poor solubility.

purported role of DHEAS limiting excitotoxic damage (Lapchak et al., 2000). The other neuroactive steroids examined do not seem to exhibit a high degree of specificity. In light of previously mentioned distinctions between excitatory (e.g., DHEAS and PREGS), and inhibitory neuroactive steroids (e.g., $3\alpha,5\beta$ -TH PROGS and $3\alpha,5\alpha$ -TH PROGS), it is interesting that these compounds display such remarkably similar estimated K_i values at these transporters. The lack of differential activity among the neuroactive steroids and the possibility of $3\alpha,5\beta$ -TH PROGS transport into vesicles via VGLUT suggests that vesicles may represent a synaptic delivery system which extends beyond classic neurotransmitters.

CHAPTER 4: DISCUSSION

From the perspective of the neurotransmitter, synaptic transmission can be divided into two major temporal components that occur during the signaling process. The first is the presynaptic release of neurotransmitter, with the second being the binding of neurotransmitter to postsynaptic receptors. Following receptor activation, the postsynaptic neuron is affected in a number of ways, ranging from a change in membrane potential (e.g., depolarization or hyperpolarization) to the activation or inhibition of a second messenger system. Historically, pharmacological research on psychiatric and neurological diseases has generally targeted the interactions between neurotransmitters and postsynaptic receptors. While valuable drugs have been developed with this approach, it can also present certain disadvantages. For example, the constant presence of a receptor antagonist can prevent normal function, as well as potentially induce pathology. On the other hand, by modulating synaptic transmission at the presynaptic level, it is conceivable that potential therapies might only act during pathological events. For example, epilepsy is generally thought of as a state involving reduced inhibitory GABAergic activity. However, recent evidence suggests increased VGLUT1 expression may account for some types of increased epileptiform activity which follows hypoxic-ischemic insult (Kim et al., 2005). The modulation of VGLUT transport activity may attenuate the epileptiform neurological activity by reducing glutamate levels during times of excessive stimulation, but not affect glutamate levels during normal functioning.

If it is discovered that the specific modulation of glutamate uptake into synaptic vesicles can indeed affect presynaptic release, it represents a new level of modulation of excitatory transmission. In this manner, the development and characterization of specific VGLUT uptake inhibitors may not only provide a better understanding of the role of VGLUT in presynaptic release of glutamate, but also result in new therapeutic strategies. Beyond this, the elucidation of structural characteristics necessary for transport of glutamate may allow the design of molecules, active at post-synaptic receptors, that can be delivered to the synapse via exocytosis of the content of the vesicle during synaptic signaling.

While the elucidation of competitive VGLUT inhibitors has developed substantially over the past decade, the development of compounds which are specific to VGLUT are still underway. Efforts of our laboratory, in conjunction with those of C.M. Thompson and J.M. Gerdes, has focused on designing, synthesizing, and testing compounds which are selectively active at VGLUT. The substituted 2,4-quinoline dicarboxylic acids have proven to be one of the more useful groups of VGLUT inhibitors developed through a rational design effort (Bartlett et al., 1998; Carrigan et al., 2002; Carrigan et al., 1999). To date, the substituted QDC, 6-[4'-biphenyl], has been the most potent inhibitor resulting from this effort, with a K_i value of 41 μM (Carrigan et al., 2002). Aryl and aryl-linked substitutions of the 5-,6-,7-,and 8- positions were included in the SAR analysis to explore a hypothesized lipophilic pocket in the transporter binding-domain. One of these compounds, 5,6-naphthyl QDC, displayed good activity, but more importantly, had a

structure which strongly resembled that of a steroid. This resemblance prompted the testing of neuroactive steroids at VGLUT.

In this work, a series of neuroactive steroids have been pharmacologically assessed for their activity as inhibitors of vesicular glutamate uptake. Among those compounds exhibiting inhibitory activity, pregnenolone sulfate (PREGS) was selected for more detailed kinetic characterization. In parallel with PREGS, the structurally related, synthetically derived molecule that prompted the interest in the neuroactive steroids, 5,6-QDC, was also included in these analyses. To assess the specificity of these compounds at VGLUT, the cross-reactivity of the neuroactive steroids with other vesicular transporters was also examined. Additionally, these compounds were tested for potential activity at sites other than VGLUT, specifically at the level of the electrochemical gradient. To better understand the structure-activity relationships (SARs), molecular modeling analyses of PREGS, 5,6-QDC and CR were performed. Lastly, an evaluation of the ability of identified competitive inhibitors to heteroexchange with ^3H -L-glutamate previously equilibrated into vesicles was conducted to gain insights into the SARs that govern substrate translocation. The results of this work have afforded an initial understanding of the ligand structural characteristics necessary for the binding and transport of glutamate via VGLUT.

Are PREGS and 5,6-QDC specific for VGLUT?

As previously mentioned, PREGS emerged as one of the more potent blockers when a series of neuroactive steroids were assayed for their ability to block the uptake of ^3H -L-glutamate into synaptic vesicles. For this reason, PREGS was advanced to more detailed kinetic analysis. When subjected to either Lineweaver-Burk or nonlinear regression analysis, the pattern of inhibition produced by PREGS, as well as 5,6-QDC, was consistent with competitive inhibition. The K_i values generated for these compounds were 228 μM and 107 μM for 5,6-QDC and PREGS, respectively. While of modest potency, these K_i values are an order of magnitude lower than the K_M for VGLUT. These ligands are classified as competitive inhibitors, which is important for two reasons: First, the compounds provided additional SAR data for delineation of the pharmacology of VGLUT. Secondly, these results suggest that neuroactive steroids and/or related compounds may be endogenous regulators of VGLUT.

As exemplified by PREGS, only the sulfated forms of neuroactive steroids were found to be inhibitors of ^3H -L-glutamate uptake into synaptic vesicles. This was concluded since the activity of the sulfated excitatory steroids, PREGS and DHEAS, were considerably more active than the non-sulfated varieties at other sites within the CNS, such as NMDA receptors. Of potential physiological significance, certain sulfated neuroactive steroids, i.e. PREGS, DHEAS, $3\alpha,5\beta$ -TH PROGS, and $3\alpha,5\alpha$ -TH PROGS, were identified as active (K_i values) in the micromolar range at VGLUT at a level 1000-fold less than the K_M of L-glutamate at VGLUT. Consistent with these levels of activity, neuroactive

steroids have been shown to exhibit kinetic values in the micromolar range for glutamatergic receptors. For example, the EC₅₀ values of 3 α ,5 β -TH PROGS and PREGS are in the micromolar range (62 μ M and 57 μ M, respectively) at NMDA receptors (Park-Chung et al., 1994; Wu et al., 1991). This does not, however, address the issue of whether the neuroactive steroids reach their effective concentrations at synaptic vesicles *in vivo*. While reports of neuroactive steroid concentrations in the brain vary, local concentrations may be even more variable, due to the actions of localized synthetic enzymes present in proximity of a particular site of action. This may allow for a transient increase in the intracellular concentration of neuroactive steroids to a level at which VGLUT function is affected. While the sulfation of molecules is typically regarded as a Phase II detoxification process, the sulfate moiety of these compounds could render them compartment bound, as a manner for cells to regulate neuroactive steroid concentrations.

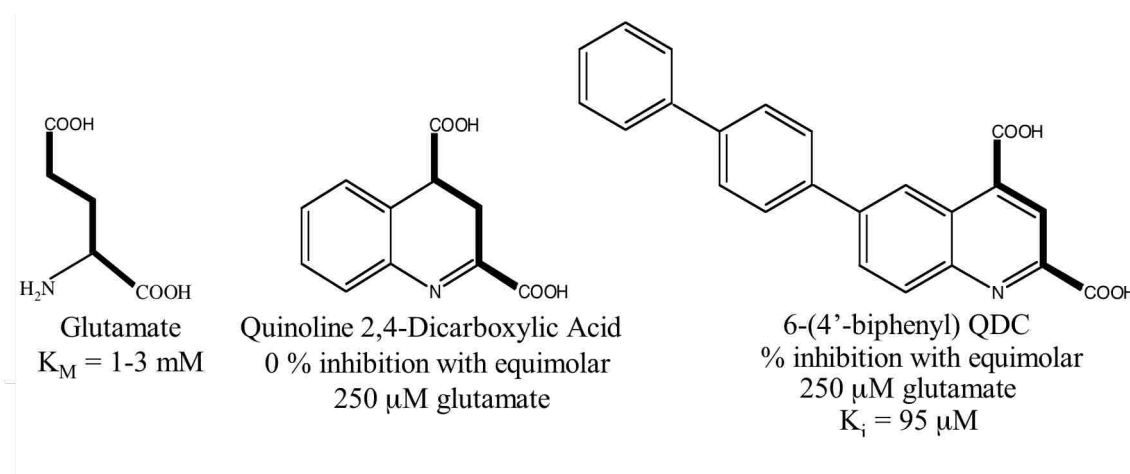
What does this add to SAR?

Of the QDCs tested, 5,6-QDC structurally appears to be the closest steroid mimic and , thus, was included in many of the SAR studies. Both the neuroactive steroid and QDC inhibitory ligands raise interesting points regarding the structural characteristics shared by VGLUT inhibitors, especially related to the planar aspects of their structures. These features are also shared with the naphthalene sulfonic acids that were first characterized as inhibitors by the lab of F. Fonnum (Roseth et al., 1995). Their initial efforts showed Evans blue and Chicago sky blue to have K_i values of 40 nM and 190 nM, respectively (Roseth et al., 1995), which makes them some of the most potent inhibitors yet identified.

In a subsequent study, trypan blue, Evans blue, naphthol blue black, and benzopurpurin 4B were determined to have planar structures with conjugated double bonds throughout the molecule with associated amino and sulfonic acid substitutions (Roseth et al., 1998). The authors concluded that functional groups other than amino and sulfonic acid moieties are necessary for inhibition, based on the finding that naphthylamine sulfonic acids were not potent even at concentrations 100-1000-fold higher than used with the dyes. Naphthylamine sulfonic acids differ from naphthalene sulfonic acids in that naphthylamine sulfonic acids are not dimeric, as are the dyes, and they do not contain a lipophilic side group attached to the naphthalene core (Roseth et al., 1998). Interestingly, these conclusions differ somewhat from the SAR data emerging from the QDC studies in that electronegative regions corresponding to an embedded glutamate were presumed to be important (Fig. 4.1) (Carrigan et al., 2002; Carrigan et al., 1999). In this respect, the work of Fonnum may have overlooked these inconsistencies, because an intermediate length compound was not included in the analysis. The finding that PREGS and 5,6-QDC are competitive inhibitors of VGLUT may address these inconsistencies by illustrating the importance of both lipophilic regions and the electronegative regions (in the form of sulfonates or carboxylates). These particular structural differences will be addressed in more depth in the discussion regarding the VGLUT pharmacophore model.

Pregnenolone sulfate has been shown to have multiple sites of action within the CNS, and more specifically, the glutamatergic system. This raised the possibility that the neuroactive steroids may also have multiple sites of action among the vesicular transporters. Thus, PREGS, 3 α ,5 α -TH PROGS, 3 α ,5 β -TH PROGS, and DHEAS were

Figure 4.1. Development of the QDC template



These VGLUT inhibitors were used in the development of the QDCs. The “embedded” glutamate is the most obvious common structural feature between these molecules. The addition of a bicyclic core, evident in QDC and 6-(4’)-QDC, increases potency. The largest increase in potency has been due to lipophilic additions, such as the biphenyl group in the 6 position on the QDC structure.

tested for their inhibitory activity of the uptake of ^3H -serotonin at VMAT and ^3H -GABA at VGAT. Pregnenolone sulfate, $3\alpha,5\alpha$ -TH PROGS, and $3\alpha,5\beta$ -TH PROGS did show inhibitory activity. However, these compounds did not display a specificity (K_i values) for VGLUT greater than ~ 5 -fold versus VMAT and VGAT. The lack of specificity displayed by these compounds is peculiar given their respective specificity at receptors in the CNS (i.e. for NMDA and GABA_A); this, however, may be due to two possibilities: that their cross-reactivity (1) is a vestigial artifact of evolution, and/or (2) is part of larger neurophysiological mechanisms. The first possibility is partly supported by evidence in the literature. The vesicular monoamine transporter has been classified as a member of the toxin-extruding antiporters (TEXANs) and ABC-type adenosinetriphosphatases (Schuldiner et al., 1995). This class of proteins transports a large range of toxic cations by utilizing proton gradients. VGLUT may represent an anion transporter counterpart; there is one report of VGLUT protecting cells from Evans blue toxicity (Israel et al., 2001).

In contrast, DHEAS exhibited greater specificity for VGLUT relative to the other compounds tested. Thus, its activity at VGLUT was ~ 50 -fold more potent than at VMAT and ~ 20 -fold more potent than at VGAT. While speculative, this activity is of interest in light of the neuroprotective effects of DHEAS. DHEAS has been shown to be neuroprotective against ischemic damage via GABA_A receptors in a spinal cord ischemia model (Lapchak et al., 2000). Additionally, DHEAS was shown to attenuate apoptosis in symapthoadrenal medulla cells by stimulating a variety of antiapoptotic pathways (Charalampopoulos et al., 2004). DHEAS has also been shown to be a neuroprotectant

against excitotoxicity in hippocampal cultures (Kimonides et al., 1998). Given that glutamate, in excess, can trigger excitotoxicity, it is possible that DHEAS may provide an endogenous mechanism for cells to protect against excessive release of glutamate under pathological conditions.

Do the neuroactive steroids block vesicular uptake at other sites?

Prompted by the ability of PREGS and 5,6-QDC to block the uptake of glutamate, additional studies were conducted to examine the effects of these molecules on the electrochemical gradient. Two components (pH gradient and membrane potential) were tested in order to provide a more global understanding of effects potentially elicited by PREGS and 5,6-QDC. Both of these molecules showed only a slight effect on the generation and maintenance of an electrochemical gradient. During experiments measuring the proton gradient, 5,6-QDC appears to have a direct effect on the fluorescence signal of acridine orange. A visual examination of the fluorescence traces in experiments measuring the electrochemical profile demonstrated a marked change in the intensity of the fluorescence signal when either PREGS or 5,6-QDC was added. The interaction between PREGS, 5,6-QDC, and oxonol V were directly assessed, and no direct effects on fluorescence were found. While no direct effects of either compound on oxonol V were detected, the generation of the electrochemical gradient does not appear to be effected. Although beyond the scope of this project, these results must take into account the heterogeneity of the synaptic vesicle preparation utilized. Thus, this

In summary, 5,6-QDC and PREGS have been shown to inhibit VGLUT in a competitive manner. Neuroactive steroids active at VGLUT also display pharmacological effects on VMAT and VGAT. While it seems possible that a nonspecific manner of inhibition would explain the cross-reactivity of the neuroactive steroids, the results from experiments assessing the effect of 5,6-QDC and PREGS on electrochemical gradient suggest otherwise. However, higher concentrations of these compounds may interrupt the electrochemical gradient, as has been shown for other inhibitors (Ogita, 2001; Roseth et al., 1995). Concentration-response experiments of these compounds and their effects on the electrochemical gradient may more thoroughly describe any effects. Additionally, more detailed kinetic analyses of PREGS at VMAT and VGAT should give insights into its manner of inhibition.

Do PREGS, 5,6-QDC, and Congo red align well with the VGLUT pharmacophore model?

As the inventory of potent VGLUT inhibitors increases, a manner to visualize SAR data becomes useful. The development of a ligand-based pharmacophore model is the most practical method to model this SAR data, given the lack of a crystal structure being readily available. A 3D, ligand-based pharmacophore model is a representation of a set of features, common to a group of active compounds, within three-dimensional space. This VGLUT pharmacophore model was generated by Erin Bolstad, with three training set molecules from structurally distinct classes of competitive VGLUT inhibitors. Chicago sky blue, 6-(4'-biphenyl)-QDC, and bromocriptine were conformationally searched, and the conformations of these three molecules were assessed to identify the

most similar alignments in 3D space. The chosen alignment of these three molecules yielded a pharmacophore model, which demonstrates a planar conformation with two electronegative groups, also previously identified in the QDC template. The alignments of PREGS, 5,6-QDC and Congo red fragment (CRF) with this model were convincing, consistent with the suspected mode of binding which would be produced by a competitive inhibitor. The overall length of 5,6-QDC appeared shorter than PREGS in the pharmacophore model fit. The slight difference in K_i values (PREGS = 107 μM vs. 5,6-QDC = 228 μM) might be explained by a better fit of PREGS. Differences between these compounds raise an issue concerning the importance of the electronegative region(s) positioning on the bicyclic core. In contrast to the conclusions of Fonnum's group that the amino and sulfonic groups were unnecessary for binding, two electronegative regions were proposed to be important for potent inhibition of VGLUT during the initial development of the QDCs (Carrigan et al., 2002; Roseth et al., 1998). PREGS may provide a way to address this inconsistency. The increased affinity of PREGS over 5,6-QDC may suggest that only one region of electronegativity is essential for binding. Alternatively, differences in the structure of the lipophilic moiety most distal to the electronegative regions may also explain the difference in affinity between these two compounds. PREGS contains an additional area of electronegativity, in the form of a carbonyl group, attached to the "D" ring of the steroid nucleus. This begins to address an issue raised by (Roseth et al., 1998), which proposed that the difference in binding affinity between Evans blue and Chicago sky blue was due to a methoxy group on the dimethyl-biphenyl linker of Chicago sky blue, as opposed to a methyl in Evans blue (Roseth et al., 1995; Roseth et al., 1998). There may be certain subtle differences in the

structure on the lipophilic region that contribute to relative differences in inhibitory potency. The alignment of CRF further addresses issues regarding the electronegative regions.

Congo red fragment does not contain either of the electronegative groups in the form of the “embedded glutamate”, as may be proposed for trypan blue or Evans blue, i.e. the C3 and C6 or C5 and C7 positions. It does, however, contain a sulfonic group at the C8 position of the naphthalene groups on Evans blue or trypan blue. The sulfonic group of CRF was aligned at each of the electronegative regions identified in the pharmacophore model. In the first alignment (A1), the sulfonic group of CRF was orientated to the electronegative region designated as Region 1. This orientation produced a grossly out-of-plane fit. A second fit was generated to compare to the first one. The second fit consisted of aligning the sulfonic group with Region 2, the distal electronegative region. This alignment exhibited a better fit than the first, revealing a planar conformation of CRF. In the dimeric form, CR is structurally similar to trypan blue, yet displays a K_i value that is 1000-fold less potent than Evans blue as pictured in Chapter 1 of this work (Fig. 1.2). The primary structural differences between these two molecules is the presence of the dimethyl-biphenyl linker and positions of hydroxyl and sulfonate groups. One may conclude that the presence of a dimethyl-biphenyl linker and properly positioned electronegative groups would be most effective for inhibition of glutamate uptake; however, the molecules, mentioned here, also exhibit undesirable levels of cross-reactivity with NMDA receptors (Bartlett, 1999). Multiple iterative refinements for the

pharmacophore model development and additional kinetic data are necessary to address these issues of specificity.

Most recently, an additional VGLUT pharmacophore model was generated utilizing the GASP (Tripos, St. Louis, MO) method (Thomson et al., 2005). The GASP protocol was selected to develop an unbiased, automatically aligned and iterative model. This was achieved by the exploration of superposition orientations, generation of molecular overlays, and identification of pharmacophore model points. The same training set utilized in the development of the initial VGLUT pharmacophore model was used for the GASP analysis. This analysis developed a model which best satisfied five criteria: 1) similar overlap volume, 2) fitness score, 3) the feasibility and number of determined pharmacophore model points, 4) the potential for pharmacophore model regions not determined by GASP, and 5) overall structural alignment. The model which emerged was represented by three points to quantify important interatomic distances. These points, designated as A, B, and C, corresponded with points identified in the previous pharmacophore model, i.e. lipophilic pocket, two electronegative regions (Thomson et al., 2005). The GASP protocol did not identify certain pharmacophore model regions that were identified by the previous pharmacophore model. Thus, while GASP provides a good unbiased approach to initial pharmacophore model generation, the need for rigorous pharmacophore model development is still apparent.

In summary, the VGLUT pharmacophore model has predictive qualities of VGLUT inhibitors as verified by the fit of PREGS. The steroid-like molecule, 5,6-QDC was

aligned to the pharmacophore model in a similar manner as PREGS. The fit of CRF displayed one plausible fit and one that was less favorable. The binding-site of the naphthalene sulfonic dyes may allow for different arrangements of amine and sulfonic substituents, and suggests that Ring 2 (lipophilic moiety) may confer additional binding properties that render the electronegative regions less important. The recent development of a new VGLUT pharmacophore model presents an opportunity to generate alignments, and compare the alignments with previous pharmacophore representations, which may ultimately lead to the development of new inhibitors. Identification of alternative substrates at VGLUT may lead to the development of a pharmacophore model, which describes transport characteristics of VGLUT transport.

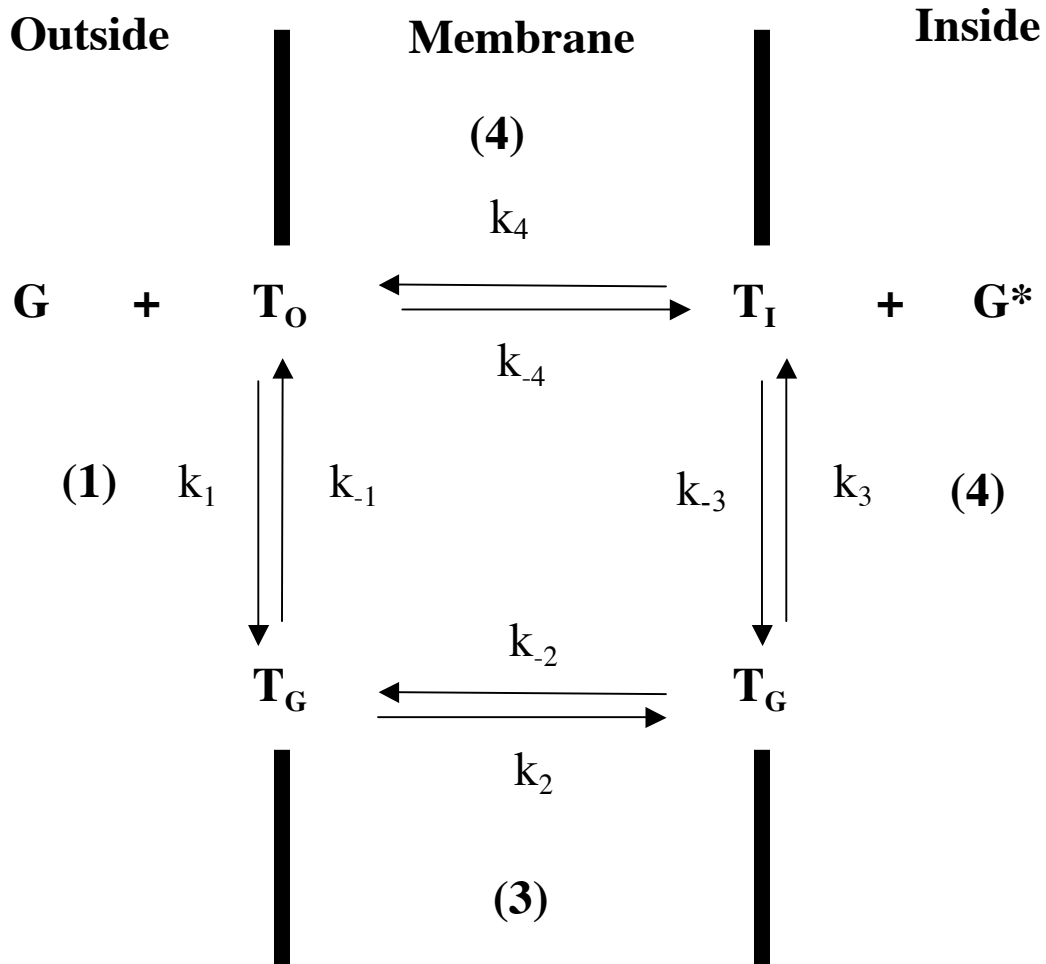
Are these competitive inhibitors also substrates?

Recent studies of various neurotransmitter transporters have begun to distinguish the process of binding and translocation. Thus, while the characterization of competitive inhibitors supports the conclusion that a particular compound can bind to the substrate-site of the transporter, it does not address whether or not the compound can also be transported (i.e., act as an alternative substrate). Studies on the EAATs have led to the development of competitive inhibitors that exhibit substrate activity that ranges from similar to L-glutamate to non-substrate inhibitors. One of the ways to directly address substrate activity is to synthesize a radioactive derivative of the compound or devise an alternative way to measure its concentration in synaptic vesicles. As either process can be expensive and/or labor intensive, we hypothesized that quantifying exchange might

prove to be a way to assess substrate activity. Thus, given an alternative access model, it is often possible to exploit the exchange process to study transports mechanisms.

The process of exchange is most often studied by “preloading” synaptic vesicles with a substrate and measuring its rate of efflux. To produce this efflux, preloaded vesicles are diluted 20-fold into incubation buffer in the absence of ATP. The amount of $^3\text{H-L}$ -glutamate retained in the vesicles is then quantified. This process is presumed to occur via the alternating access, as depicted in Figure 4.2. Normal transporter function occurs when transporter cycles through steps k_1 , k_2 , and k_3 to facilitate the translocation of glutamate from the extravesicular space to the intravesicular compartment. To complete the cycle, the transporter reorients towards the extravesicular space unoccupied by glutamate (k_4). The process of efflux is measuring the movement of $^3\text{H-L}$ -glutamate from the intravesicular space to the extravesicular space. In the absence of inhibitors this will occur via the reverse operation of k_{-3} , k_{-2} , and k_{-1} . In the presence of the appropriate concentration of either externally applied L-glutamate, or an alternative substrate, efflux of $^3\text{H-L}$ -glutamate proceeds through steps k_{-3} , k_{-2} , and k_{-1} , followed by uptake of extravesicular unlabeled glutamate, or alternative substrate via steps k_1 , k_2 , and k_3 . If this process is faster than efflux in the absence of external substrate, it is referred to as *trans-stimulation*. For VGLUT, our data suggests that the unoccupied transporter reorients at a rate slightly slower than when occupied after transport of a glutamate. In contrast to substrate, the addition of a non-substrate inhibitor would be expected to “trap” the binding-site on the extravesicular side and prevent reorientation. In our studies, the

Figure 4.2. Model of VGLUT alternate access transport process



G - unlabeled L-glutamate

G^* - 3H -L-glutamate

T_O - unoccupied transporter site on extra-vesicular surface

T_I - unoccupied transporter site on intra-vesicular surface

inclusion of a nonsubstrate inhibitor resulted in a reduction of efflux equal to a level at observed at 4° C. In experiments performed at 4° C, efflux was virtually nonexistent. Congo red, previously identified as a non-substrate inhibitor, is able to block the efflux of ³H-L-glutamate to the same degree as when these experiments are performed at 4°C, because CR essentially traps the binding-site on one side and prevents the cycling necessary for significant efflux.

Presumably, an effective substrate (*trans*-ACPD) would increase levels of efflux, whereas, a non-substrate inhibitor (CR) would decrease efflux levels. A number of compounds were screened for their effect on ³H-L-glutamate efflux. The majority of the compounds examined reduced efflux of ³H-L-glutamate to a level which fell between that of a L-glutamate and a nonsubstrate inhibitor, raising the possibility that the compounds are active as a partial substrate, i.e., they can be transported, but less efficiently than L-glutamate. Interestingly, 5,6-QDC exhibited characteristics most consistent with that of *trans*-ACPD. Some of the sulfated neuroactive steroids tested (PREGS and 3 α ,5 β -TH PROGS) demonstrated a similar activity to that of 5,6-QDC. The shorter overall length of 5,6-QDC, when aligned in the pharmacophore model, and lack of electronegative group in the distal lipophilic region as compared to PREGS may confer some increases in substrate characteristics.

While the identification of good substrates at VGLUT is rather straightforward, it is more difficult to characterize compounds that act as partial substrates, with intermediate characteristics between that of glutamate and non-substrate inhibitors. We have attempted

to address this issue in two manners: (1) to include compounds tested at a concentration that achieves a theoretical substrate-binding site occupancy of ~90%, and (2) to mathematically examine the effect that various types of inhibitors (i.e., nonsubstrate inhibitor, alternative substrates) would have on efflux; a curve, based on Michaelis-Menten kinetics, was compared with the control level of efflux for demonstration of a representative model. Based on this equation, a curve describing the amount of efflux which would occur if 90% of the transporter binding-sites were removed, was generated. Any level of efflux greater than the level represented by the simulation of 90% transporter removal should signify that a compound has some substrate characteristics. While this is a preliminary model, it may provide some insight into the process of efflux. The data from the experiments ($n \geq 3$) recording the amount of ^3H -L-glutamate efflux in the presence of $3\alpha,5\beta$ -TH PROGS over ten minutes was superimposed over the theoretical curves. This level of efflux was greater than levels expected with 90% transporter removed. The increased level of efflux, despite a binding-site occupancy of 90% occupancy of transporters, suggests that $3\alpha,5\beta$ -TH PROGS is being translocated into synaptic vesicles. This rate is slower than that of L-glutamate, but suggests translocation of $3\alpha,5\beta$ -TH PROGS, nonetheless. These results suggest that a subset of compounds which range from amino acid analogues to naphthalene sulfonic dyes display characteristics of a partial substrate. As previously discussed, this may, in part, be due to the evolution of VGLUT. The VGLUTs are a member of the SLC17/type I phosphate transporter family (Reimer and Edwards, 2004). This transporter family involves many organic anion transporters, present on organelles such as lysosomes. VGLUT may represent a class of proteins similar to that of the TEXANs (of which VMAT belongs),

but rather than transporting organic cations, this putative group of proteins transports organic anions.

Inhibition of uptake by an alternative substrate may result in both reduced amounts of glutamate, and increased amounts of alternative substrate being accumulated in the synaptic vesicle and possibly released presynaptically. On the other hand, the reduction of sequestration into synaptic vesicle by a nonsubstrate alternative would simply result in a decreased amount of neurotransmitter molecules being released presynaptically. These possibilities present some potentially interesting roles that DHEAS may play in neurotransmission.

Particular to DHEAS, research indicates that this neuroactive steroid can stimulate LTP in a dose-dependent manner (Yoo et al., 1996). The finding that DHEAS inhibits uptake of glutamate into synaptic vesicles, but stimulates LTP in the dentate gyrus of *R. norvegicus* presents an inconsistency. While the effect of DHEAS on presynaptic release has not been characterized, it would seem that a reduction in the uptake of glutamate into synaptic vesicles would result in a lower amount released presynaptically. Studies conducted in synaptosomes demonstrate the inclusion of rose bengal, noncompetitive inhibitor of glutamate uptake, can reduce the amount of glutamate released (Ogita, 2001). Alternatively, if DHEAS is translocated into synaptic vesicles as suggested by the analysis of $3\alpha,5\beta$ -TH PROGS, then this may prove to be a manner of presynaptic delivery of the neuroactive substrate to the postsynaptic GABA_A receptors; while concurrently reducing the amount of glutamate released. It is possible that DHEAS could

elicit its effects on LTP by modulating GABA_A receptors, as GABA can inhibit LTP (Majewska, 1992; Opera et al., 1995; Scharfman and Sarvey, 1985), and potentiating sigma and NMDA receptors (Chen et al., 2006; Maurice et al., 1997). Current evidence suggests that DHEAS may also have partial substrate characteristics. An examination of efflux over time is necessary to better characterize this effect. None of these studies have addressed the manner in which DHEAS is introduced into the synapse when its exerted effects are believed to be receptor-mediated. These results indicate the neuroprotective qualities elicited by DHEAS may be partly mediated by the inhibition of glutamate uptake into synaptic vesicles. Consistent with this evidence, DHEA has been shown to decrease glutamate release in synaptosomes of rats under the age of 12 months (Lhullier et al., 2004).

To conclude, this work is the continuation of an effort to better characterize the efflux of ³H-L-glutamate from synaptic vesicles and delineate between alternative substrates and nonsubstrate inhibitors. While none of these molecules, other than *trans*-ACPD, have been directly shown to be alternative substrates, the ability to exchange suggests that 3 α ,5 β -TH PROGS may indeed be a alternative partial substrate. The ability of compounds to be alternative substrates present some interesting possibilities. In the case of the neuroactive steroids, this may represent a manner in which these compounds are delivered to the synapse. Ultimately, this may be a potential mode for presynaptic delivery of therapeutic agents.

Conclusions

The structurally similar molecules, 5,6-QDC, and PREGS, have been identified as competitive inhibitors of vesicular glutamate uptake. PREGS and 5,6-QDC have minimal effect on the electrochemical gradient generated by the V-ATPase. This effect was expected given their characterization as competitive inhibitors. The minimal effects on the electrochemical gradient do not rule out the possibility that they would produce a greater disruption at higher concentrations. Most neuroactive steroids identified as potent, competitive inhibitors of VGLUT were also active at VMAT and VGAT. The one exception, DHEAS, was much more potent at VGLUT than either VMAT or VGAT. DHEAS may play unique roles in synaptic neurotransmission. The VGLUT inhibitors, 5,6-QDC and CRF, also appeared to fit the pharmacophore model in a convincing manner, consistent with kinetic data. Experiments conducted to examine the effect of identified VGLUT inhibitors on the efflux of $^3\text{H-L-glutamate}$ suggest that certain inhibitors display partial substrate characteristics. The translocation of these compounds into the synaptic vesicles suggests that they could potentially be released exocytotically into the synapse. This possibility carries with it many implications given the well-recognized effect of neuroactive steroids on both GABA and glutamate receptors.

Bibliography

- Aihara Y, Mashima H, Onda H, Hisano S, Kasuya H, Hori T, Yamada S, Tomura H, Yamada Y, Inoue I, Kojima I and Takeda J (2000) Molecular cloning of a novel brain-type Na(+)-dependent inorganic phosphate cotransporter. *J Neurochem* **74**(6):2622-2625.
- Balazas R, Bridges RJ and Cotman CW (2005) *Excitatory Amino Acid Transmission in Health and Disease*. Oxford University Press, New York.
- Barrett-Conner E and Edelstein SL (1994) A prospective study of dehydroepiandrosterone sulfate and cognitive function in an older population: the Rancho Bernardo Study. *J Am Geriatr Soc* **42**(4):420-423.
- Bartlett RD (1999) Identification and characterization of L-glutamate transport into rat brain synaptic vesicles, in *Pharmaceutical Sciences* pp 1-96, University of Missoula, Missoula.
- Bartlett RD, Esslinger CS, Thompson CM and Bridges RJ (1998) Sustituted quinolines as inhibitors of L-glutamate transport into synaptic vesicles. *Neuropharmacol* **37**(7):839-846.

Baulieu EE (1981) Steroid hormones in the brain: several mechanisms., in *Steroid Hormone regulation of the brain* (Fuxe K, Gustafson, J.A., Wetterberg, L. ed) pp 3-14, Pergamon, Elmsford, NY.

Baulieu EE (1998) Neurosteroids: a novel function of the brain.
Psychoneuroendocrinology **23**(8):963-987.

Baulieu EE, Robel P and Schumacher M (1999) *Neurosteroids: A new regulatory function in the Nervous System*. Humana Press, Totowa, New Jersey.

Burger PM, Mehl E, Cameron PL, Baumert M, Lottspeich F, De Camilli P and Jahn R (1989) Synaptic vesicles immunisolated from rat cerebral cortex contain high level of glutamate. *Neuron* **3**(6):715-720.

Carlson MD, Kish PE and Ueda T (1989) Glutamate uptake into synaptic vesicles: competitive inhibition by bromocriptine. *J Neurochem* **53**(6):1889-1894.

Carlson MD and Ueda T (1990) Accumulated glutamate levels in the synaptic vesicle are not maintained in the absence of active transport. *Neurosci Lett* **110**(3):325-330.

Carrigan CN (2000) Part one. Synthesis of phosphorous-containing amino acid analogues derived from *trans*-4-hydroxyproline and the study of their bioactivity

in the glutamate excitatory neurotransmitter system. Part two. Synthesis, structural modifications and in vitro pharmacology of quinoline-2,4-

dicarboxylic acids as proposed inhibitors of the glutamate vesicular transporter, p 308, University of Montana, Missoula.

Carrigan CN, Bartelett RD, Esslinger CS, Cybulski KA, Tongcharoensirikul P, Bridges RJ and M. TC (2002) Synthesis and *in vitro* pharmacology of substituted quinolone-2,4 dicarboxylic as inhibitors of vesicular glutamate transport (VGLUT). *J Med Chem* **45**(11):2260-2276.

Carrigan CN, Esslinger CS, Bartelett RD, Bridges RJ and Thompson CM (1999) Quinoline-2,4-dicarboxylic acids: synthesis and evaluation as inhibitors of the glutamate vesicular transport system. *Bioorg Med Chem Lett*, **9**:2607-2612.

Charalampopoulos I, Tsatsanis C, Dermitzaki E, Alexaki VI, Castanas E, Margioris AN and Gravanis A (2004) Dehydroepiandrosterone and allopregnanolone protect sympathoadrenal medulla cells against apoptosis via antiapoptotic Bcl-2 proteins. *Proc Nat Acad Sci USA* **101**(21):8209-8214.

Chen L, Miyamoto Y, Furuya K, Dai XN, Mori N and Sokabe M (2006) Chronic DHEAS administration facilitates hippocampal long-term potentiation via an

amplification of Src-dependent NMDA receptor signaling. *Neuropharmacology* **51**(3):659-670.

Chen W, Aoki C, Mahadomrongkul V, Gruber CE, Wang GJ and Blitzbau R (2002) Expression of a variant form of the glutamate transporter GLT1 in neuronal cultures and in neurons and astrocytes in the rat brain. *J Neurosci* **22**(6):2142-2152.

Cheney DL, Uzunov D and Guidotti A (1995) Pregnenolone sulfate antagonizes dizocilpine amnesia: role for allopregnanolone. *Neuroreport* **6**(12):1697-1700.

Christensen HN (1975) *Biological Transport*. W.A. Benjamin, Inc., Reading, MA.

Cidon S and Sihra TS (1989) Characterization of H⁺-ATPase in rat brain synaptic vesicles. Coupling to L-glutamate transport. *J Biol Chem* **264**(14):8281-8288.

Collingridge G (1987) Synaptic plasticity. The role of NMDA receptors in learning and memory. *Nature* **330**(6149):604-605.

Colliver TL, Pryott SJ, Achalabun M and Ewing AG (2000) VMAT-Mediated changes in quantal size and vesicular volume. *J Neurosci* **20**(14):5276-5782.

- Conn JP and Pin JP (1997) Pharmacology and functions of metabotropic glutamate receptors. *Annu Rev Pharmacol Toxicol* **37**:205-237.
- Corpechot C, Robel P, Axelson M, Sjovall J and Baulieu EE (1981) Characterization and measurement of dehydroepiandrosterone sulfate in rat brain. *Proc Nat Acad Sci USA* **78**(8):4704-4707.
- Corpechot C, Synguelakis M, Talha S, Axelson M, Sjovall J, Vihko R, Baulieu EE and Robel P (1983) Pregnenolone and its sulfate ester in the rat brain. *Brain Res* **270**(1):119-125.
- Corpechot C, Young J, Clavel M, Wehrey C, Veltz JN, Touyer G, Mouren M, Prasad V, Banner C and Sjovall J (1993) Neurosteroids: 3 alpha-hydroxy-5 alpha-pregnan-20-one and its precursors in the brain, plasma, and steroidegenic glands of male and female rats. *Endocrinology* **133**(3):1003-1009.
- Coyle JT and Kuhar MJ (1974) Subcellular localization of dopamine beta-hydroxylase and endogenous norepinephrine in the rat hypothalamus. *Brain Res* **65**(3):475-487.
- Daniels RW, Collins CA, Chen K, Gelfand MV, Featherstone DE and DiAntonio A (2006) A single vesicular glutamate transporter is sufficient to fill a synaptic vesicle. *Neuron* **49**(1):11-16.

- De Belleruche JS and Bradford HF (1973) Amino acids in synaptic vesicles from mammalian cerebral cortex: A reappraisal. *J Neurochem* **21**(2):441-451.
- Eliasof S, Arriza JL, Leighton BH, Kavanaugh MP and Amara SG (1998) Excitatory amino acid transporters of the salamander retina: identification, localization, and function. *J Neurosci Res* **18**(2):698-712.
- Esslinger CS, Agarwal S, Gerdes J, Wilson PA, Davis ES, Awes AN, O'Brien E, Mavencamp T, Koch HP, Poulsen DJ, Rhoderick JF, Chamberlin AR, Kavanaugh MP and Bridges RJ (2005) The substituted aspartate analogue L-beta-threo-benzyl-aspartate preferentially inhibits the neuronal excitatory amino acid transporter EAAT3. *Neuropharm* **49**(6):850-861.
- Freneau Jr. RT, Burman J, Quresh T, Tran CH, Proctor J, Johnson J, Zhang H, Sulzer D, Copenhagen DR, Storm-Mathisen J, Reimer RJ, Chaudrey FA and Edwards RH (2002) The identification of vesicular glutamate transporter 3 suggests novel modes of signaling by glutamate. *Proc Nat Acad Sci USA* **99**(22):14488-14493.
- Freneau Jr. RT, Kam K, Qureshi T, Johnson J, Copenhagen DR, Storm-Mathisen J, Chaudhry FA, Nicoll RA and Edwards RH (2004) Vesicular glutamate transporters 1 and 2 target to functionally distinct synaptic release sites. *Science* **304**(5678):1750-1752.

Freneau Jr. RT, Troyer MD, Pahner I, Nygaard GO, Tran CH, Reimer RJ, Bellocchio EE, Fortin D, Storm-Mathisen J and Edwards RH (2001) The expression of vesicular glutamate transporters defines two classes of excitatory synapses. *Neuron* **31**(2):247-260.

Furuta A, Martin LJ, Lin CL, Dykes-Hoberg M and Rothstein JD (1997) Cellular and synaptic localization of the neuronal glutamate transporters: excitatory amino acid transporter 3 and 4. *Neuroscience* **81**(8):1031-1042.

Fykse EM and Fonnum F (1991) Transport of gamma-aminobutyrate and L-glutamate into synaptic vesicles. *Biochem J* **276**(Pt 2):363-367.

Fykse EM, Iversen EG and Fonnum F (1992) Inhibition of L-glutamate uptake into synaptic vesicles. *Neurosci Lett* **135**(1):125-128.

Gegelashvili G and Schousboe A (1998) Cellular distribution and kinetic properties of high-affinity glutamate transporters. *Brain Res Bull* **45**(3):233-238.

Gong LW, Hafez I, Alvarez de Toledo G and Lindau M (2003) Secretory vesicles membrane area is regulated in tandem with quantal size in chromaffin cells. *J Neuroscience* **23**(21):7917-7921.

- Gras C, Herzog E, Bellenchi GC, Bernard V, Ravassard P, Pohl M, Gasnier B, Giros B and El Mestikawy S (2002) A third vesicular glutamate transporter expressed by cholinergic and serotonergic neurons. *J Neurosci Res* **22**(13):5442-5451.
- Guarneri P, Russo D, Cascio C, Leo GD, Piccoli T, Sciuto V, Piccoli F and Guarneri R (1998) Pregnenolone sulfate modulates NMDA receptors, inducing and potentiating acute excitotoxicity in isolated retina. *J Neurosci Res* **54**(6):787-797.
- Hagiwara A, Fukazawa Y, Deguchi-Tawarada M, Ohtsuka T and Shigemoto R (2005) Differential distribution of release-related proteins in the hippocampal CA3 area as revealed by freeze-fracture replica labeling. *J Comp Neurol* **489**(2):195-216.
- Harrison NL, Majewska MD, Harrington JW and Barker JL (1987) Structure-activity relationships for steroid interaction with the γ -aminobutyric acid_A receptor complex. *J Pharmacol Exp Ther* **241**(1):346-353.
- Harrison NL and Simmonds MA (1984) Modulation of the GABA receptor complex by a steroid anaesthetic. *Brain Res* **323**(2):287-292.
- Hartinger J and Jahn R (1993) An anion binding site that regulates the glutamate transporter of synaptic vesicles. *J Biol Chem* **268**(31):23122-23127.

Hell JW and Jahn R (1998) Bioenergetic characterization of gamma-aminobutyric acid transporter of synaptic vesicles, in *Methods Enzymol* pp 116-124.

Herzog E, Gilchrist J, Gras C, Muzerelle A, Ravassard P, Giros B, Gaspar P and El Mestikawy S (2004) Localization of VGLUT3, the vesicular glutamate transporter type 3, in the rat brain. *Neuroscience* **123**(4):983-1002.

Ikemoto A, Bole DG and Ueda T (2003) Glycolysis and glutamate accumulation into synaptic vesicles. Role of glyceraldehyde phosphate dehydrogenase and 3-phosphoglycerate. *J Biol Chem* **278**(8):5929-5940.

Israel M, Tomasi M, Bostel M and Meunier F-M (2001) Cellular resistance to Evans Blue toxicity involves an upregulation of a phosphate transporter implicated in glutamate storage. *J Neurochem* **78**:658-663.

Kim DS, Kwak SE, Kim JE, Won MH, Choi HC, Song HK, Kwon OS, Kim YI, Choi SY and Kang TC (2005) Bilateral enhancement of excitation via up-regulation of vesicular glutamate transporter subtype 1, not subtype 2, immunoreactivity in the unilateral hypoxic epilepsy model. *Brain Res* **1055**(1-2):122-130.

Kimonides VG, H. KN, Svendsen CN, Sofroniew MV and Herbert J (1998) Dehydroepiandrosterone (DHEA) and DHEA-sulfate (DHEAS) protect

hippocampal neurons against excitatory amino acid-induced excitotoxicity. *Proc Nat Acad Sci USA* **95**(4):1852-1857.

Kish PE and Ueda T (1989) Glutamate accumulation into synaptic vesicles, in *Methods Enzymol* pp 9-25.

Koch HP, Kavanaugh MP, Esslinger CS, Zerangue N, Humphrey JM, Amara SG, Chamberlin AR and Bridges RJ (1999) Differentiation of substrate and nonsubstrate inhibitors of the high affinity, sodium-dependent glutamate transporters. *Mol Pharmacol* **56**(6):1095-1104.

Lacroix C, Fiet J, Benais JP, Gueux B, Bonete R, Villette JM, Gourmel B and Dreux C (1987) Simultaneous radioimmunoassay of progesterone, androst-4-enedione, pregnenolone, dehydroepiandrosterone and 17-hydroxyprogesterone in specific regions of human brain. *J Steroid Biochem* **28**(3):317-325.

Lanthier A and Patwardhan VV (1986) Sex steroids and 5-en-3 beta hydroxysteroids in specific regions of the human brain and cranial nerves. *J Steroid Biochem* **25**(3):445-449.

Lapchak PA and Araujo DM (2001) Preclinical development of neurosteroids as neuroprotective agents for the treatment of neurodegenerative diseases. *Int Rev Neurobiol* **46**:379-397.

Lapchak PA, Chapman DF, Nunez SY and Zivin JA (2000) Dehydroepiandrosterone sulfate is neuroprotective in a reversible spinal cord ischemia model: possible involvement of GABA(A) receptors. *Stroke* **31**(8):1953-1956.

Leach A (2001) *Molecular Modeling: Principles and Applications 2nd ed.* Pearson Education Pub. Co., London.

Leblhuber F, Windhager E, Reisecker F, Steinparz FX and Dienstl E (1990) Dehydroepiandrosterone sulphate in Alzheimer's disease. *Lancet* **336**:187-195.

Lhullier FL, Riera NG, Nicolaidis R, Junqueira D, Dahm KC, Cipriani F, Brusque AM and Souza DO (2004) Effect of DHEA glutamate release from synaptosomes of rats at different ages. *Neurochem Res* **29**(2):335-339.

Lin CL, Tzingounis AV, Jin L, Furuta A, Kavanaugh MP and Rothstein JD (1998) Molecular cloning and expression of the rat EAAT4 glutamate transporter subtype. *Brain Res Mol Brain Res* **63**(1):174-179.

Majewska MD (1992) Neurosteroids: endogenous bimodal modulators of the GABAA receptor. Mechanism of action and physiological significance. *Prog Neurobiol* **38**(4):379-395.

Majewska MD, Mienville JM and Vicini S (1988) Neurosteroid pregnenolone sulfate antagonizes electrophysiological responses to GABA in neurons. *Neurosci Lett* **90**(3):279-284.

Marshall GR (ed) (1995) *Molecular modeling in drug design*. Wiley, New York.

Masek BB (1998) The molecular mechanics program, AESOP, was developed by B.B. Masek, of Zeneca, Inc. (Wilmington, DE) derived, in part, from BIGSTERN-3 and MM2/MM3 parameters.

Mattson MP (2003) Excitotoxic and excitoprotective mechanisms: abundant targets for the prevention and treatment of neurodegenerative disorders. *Neuromolecular Med* **3**(2):65-94.

Maurice T, Junien JL and Privat A (1997) Dehydroepiandrosterone sulfate attenuates dizoclopine learning impairment in mice via sigma-1 receptors. *Behav Brain Res* **83**(1-2):159-164.

Maycox PR, Deckerth T, Hell JW and Jahn R (1988) Glutamate uptake by brain synaptic vesicles. Energy dependence of transport and functional reconstitution in proteoliposomes. *J Biol Chem* **263**(30):15423-15428.

- McIntire SL, Reimer RJ, Schuske K, Edwards RH and Jorgensen EM (1997) Identification and characterization of the vesicular GABA transporter. *Nature* **389**:870-876.
- Monnet FP and Maurice T (2006) The sigma 1 protein as a target for the non-genomic effects of neuro(active)steroids: molecular, physiological, and behavioral aspects. *J Pharmacol Sci* **100**(2):93-118.
- Naito S and Ueda T (1983) Adenosine triphosphate-dependent uptake of glutamate into protein I-associated synaptic vesicles. *J Biol Chem* **258**(2):696-699.
- Naito S and Ueda T (1985) Characterization of glutamate uptake into synaptic vesicles. *J Neurochem* **44**(1):99-109.
- Nasman B, Olsson T, Backstrom T, Eriksson S, Grankvist K, Viitanen M and Bucht G (1991) Serum Dehydroepiandrosterone sulfate in Alzheimer's disease and multi-infarct dementia. *Biol Psychiatry* **30**:684-690.
- Ni B, Rosteck Jr. PR, Nadi NS and Paul SM (1994) Cloning and expression of a cDNA encoding a brain-specific Na⁺-dependent inorganic phosphate cotransporter. *Proc Nat Acad Sci USA* **91**:5607-5611.

- Ogita K (2001) Inhibition of vesicular glutamate storage and exocytotic release by rose bengal. *J Neurochem* **77**:34-42.
- Olney JW (2003) Excitotoxicity, apoptosis and neuropsychiatric disorders. *Curr Opin Pharmacol* **3**(1):101-109.
- Opera TI, Ho CMW and Marshall GR (eds) (1995) *De novo design: ligand construction and prediction of affinity*. American Chemical Society, Washington, D.C.
- Ozkan ED, Lee FS and Ueda T (1997) A protein factor that inhibits ATP-dependent glutamate and gamma-aminobutyric acid accumulation into synaptic vesicles: purification and initial characterization. *Proc Nat Acad Sci USA* **94**(8):4137-4142.
- Park-Chung M, Wu F and Farb DH (1994) 3 α -Hydroxy-5 β -pregnan-20-one sulfate: a negative modulator of the NMDA-induced current in cultured neurons. *Mol Pharmacol* **46**:146-150.
- Park-Chung M, Wu F, Purdy RH, Malayev AA, Gibbs TT and Farb DH (1997) Distinct sites for inverse modulation of n-methyl-d-aspartate receptors by sulfated steroids. *Mol Pharmacol* **52**:1113-1123.
- Parsons SM (2000) Transport mechanisms in acetylcholine and monoamine storage. *FASEB J* **14**(15):2423-2434.

Purdy RH, Morrow AL, Moore Jr. PH and Paul SM (1991) Stress-induced elevations of gamma-amino butyric acid type A receptor-active steroids in the rat brain. *Proc Nat Acad Sci USA* **88**(10):4553-4557.

Reimer RJ and Edwards RH (2004) Organic anion transport is the primary function of the SLC17\ Type I phosphate transporter family. *Pflugers Arch* **447**(5):629-635.

Rosenmund C, Stern-Bach Y and Stevens CF (1998) The tetrameric structure of a glutamate receptor channel. *Science* **280**(5369):1596-1599.

Roseth S, Fykse EM and Fonnum F (1995) Uptake of L-glutamate into rat brain synaptic vesicles: effects of inhibitors that bind specifically to the glutamate transporter. *J Neurochem* **65**(1):96-103.

Roseth S, Fykse EM and Fonnum F (1998) Uptake of L-glutamate into Synaptic Vesicles: Competitive inhibition by Dyes with Biphenyl Groups and Amino- and Sulphonic Acid-substituted naphthyl groups. *Biochem Pharmacol* **56**:1243-1249.

Rupp A, Kovar KA, Beuerie G, Ruf C and Folkers G (1994) A new pharmacophoric model for 5-HT reuptake-inhibitors: differentiation of amphetamine analogues. *Pharm Acta Helv* **68**(4):235-244.

- Schafer MK, Varoqui H, Defamie N, Weihe E and Erickson JD (2002) Molecular cloning and functional identification of mouse vesicular glutamate transporter 3 and its expression in subsets of novel excitatory neurons. *J Biol Chem* **277**(50):734-738.
- Scharfman HE and Sarvey JM (1985) Postsynaptic firing during repetitive stimulation is required for long-term potentiation in hippocampus. *Brain Res* **331**(2):264-274.
- Schmitt A, Asan E, Lesch KP and Kugler P (2002) A splice variant of glutamate transporter GLT1/EAAT2 expressed in neurons, cloning and localization in the rat nervous system. *Neuroscience* **109**:45-61.
- Schoepp DD (2001) Unveiling the functions of the presynaptic metabotropic glutamate receptors in the central nervous system. *J Pharmacol Exp Ther* **299**(1):12-20.
- Schoepp DD, Johnson BG, Wright RA, Salhoff CR and Monn JA (1998) Potent, stereo selective, and brain region selective modulation of second messengers in the rat brain by (+)LY354740, a novel group II metabotropic glutamate receptor agonist. *Naunyn Schmiedsberg Arch Pharmacol* **358**(2):175-180.
- Schousboe A (1981) Transport and metabolism of glutamate and GABA in neurons and glial cells. *Int Rev Neurobiol* **22**(1):1-45.

- Schuldiner S, Shirvan A and Linial M (1995) Vesicular neurotransmitter transporters: from bacteria to humans. *Physiol Rev* **75**(2):369-392.
- Selye H (1941) The anesthetic effect of steroid hormones. *Proc Soc Exp Biol Med* **46**:116-121.
- Sepkuty JP, Cohen AS, Eccles C, Rafiq A, Behar K, Ganel R, Coulter DA and Rothstein JD (2002) A neuronal glutamate transporter contributes to neurotransmitter GABA release and epilepsy. *J Neurosci* **22**(15):6372-6379.
- Sliwinski A, Monnet FP, Schumacher M and Morin-Surun MP (2004) Pregnenolone sulfate enhances long-term potentiation in CA1 in rat hippocampus slices through the modulation of N-methyl-D-aspartate receptors. *J Neurosci Res* **78**(5):691-701.
- Smith PK, Krohn RI, Hermanson GT, Mallia AK, Gartner FH, Provenzano MD, Fujimoto EK, Goeke NM, Olson BJ and Klenk BC (1985) Measurement of protein using bicinchoninic acid. *Anal Biochem* **150**(1):76-85.
- Song H, Ming G, Fon E, Bellocchio E, Edwards RH and Poo M (1997) Expression of a putative acetylcholine transporter facilitates quantal transmitter packaging. *Neuron* **18**(5):815-826.

Squire LR, Roberts JL, Spitzer NC, Zigmond MJ, McConnell SK and Bloom FE (eds)
(2002) *Fundamental Neuroscience*. Academic Press, San Diego, CA.

Storm-Mathisen J, Leknes AK, Bore AT, Vaaland JL, Edminson P, Haug FM and
Otterson OP (1983) First visualization of glutamate and GABA in neurones by
immunocytochemistry. *Nature* **301**(5900):517-520.

Tabb JS, Kish PE, Van Dyke R and Ueda T (1992) Glutamate transport into synaptic
vesicles. Roles of membrane potential, pH gradient, and intravesicular pH. *J Biol
Chem* **267**(22):15412-15418.

Tabb JS and Ueda T (1991) Phylogenetic studies on the synaptic vesicle glutamate
transport system. *J Neurosci* **11**(6):1822-1828.

Takamori (2006) VGLUTs: 'exciting' times for glutamatergic research? *Neurochem Res*
55(4):343-351.

Takamori S, Rhee JS and Rosenmund C (2000) Identification of a vesicular glutamate
transporter that defines a glutamatergic phenotype in neurons. *Nature* **407**:189-
193.

- Thomspon CM, Davis E, Carrigan CN, Cox HD, Bridges RJ and Gerdes JM (2005)
Inhibitor of the glutamate vesicular transporter (VGLUT). *Curr Med Chem*
12(18):2041-2056.
- Urani A, Privat A and T. M (1998) The modulation by neurosteroids of the scopolamine-
induced learning impairment in mice involves an interaction with sigma 1
receptors. *Brain Res* **799**(1):64-77.
- Vallee M, Mayo W and Le Moal M (2001) Role of pregnenolone,
dehydroepiandrosterone and their sulfate esters on learning and memory in
cognitive aging. *Brain Res Brain Res Rev* **37**(1-3):301-312.
- Varoqui H, Schafer MK-H, Zhu H, Weihe E and Erickson JD (2002) Identification of the
differentiation-associated Na⁺/Pi transporter expressed in a distinct set of
glutamatergic synapses. *J Neuroscience* **22**:142-155.
- Wang Y and Floor E (1994) Dynamic storage of glutamate in rat brain synaptic vesicles.
Neurosci Lett **180**(2):175-178.
- Winter H and Ueda T (1993) Glutamate uptake system in the presynaptic vesicle:
glutamic acid analogs as inhibitors and alternate substrates. *Neurochem Res*
18(1):79-85.

Winter S, Brunk I, Walther DJ, Holtje M, Jiang M, Peter J, Takamori S, Jahn R, Birnbaumer L and Ahnert-Hilger G (2005) $G\alpha_{o2}$ regulates vesicular glutamate transporter activity by changing its chloride dependence. *J Neuroscience* **25**(18):4672-4680.

Wojcik SM, Rhee JS, Herzog E, Sigler A, Jahn R, Takamori S, Borse N and Rosenmund C (2004) An essential role for vesicular glutamate transporter 1 (VGLUT1) in postnatal development and control of quantal size. *Proc Nat Acad Sci USA* **101**(18):7158-7163.

Wu F, Gibbs TT and Farb DH (1991) Pregnenolone sulfate; a positive allosteric modulator at the NMDA receptor. *Mol Pharmacol* **40**:333-336.

Yernool D, Boudker O, Jin Y and Gouaux E (2004) Structure of glutamate transporter homologue from *Pyrococcus horikoshii*. *Nature* **431**(7010):811-818.

Yoo A, Harris J and Dubrovsky B (1996) Dose-response study of dehydroepiandrosterone sulfate on dentate gyrus long-term potentiation. *Exp Neurol* **137**(1):151-156.